

UNIVERSITÉ DE NICE – SOPHIA ANTIPOLIS
ÉCOLE DOCTORALE DES SCIENCES POUR L'INGÉNIEUR

THÈSE

PRÉSENTÉE POUR OBTENIR LE TITRE DE

DOCTEUR EN SCIENCES

DISCIPLINE : INFORMATIQUE

PAR

Konstantin TCHOUMATCHENKO

MODÉLISATION DE RÉSEAUX DE COMMUNICATION PAR LA GÉOMÉTRIE STOCHASTIQUE

SOUTENU LE 15 DÉCEMBRE 1999 DEVANT LE JURY COMPOSÉ DE:

Y. KUTOYANTS	PRÉSIDENT
P. BRÉMAUD	RAPPORTEUR
I. NORROS	RAPPORTEUR
V. SCHMIDT	RAPPORTEUR
F. BACCELLI	DIRECTEUR
S. ZUYEV	CO-DIRECTEUR
M. LEBOURGES	EXAMINATEUR

Konstantin TCHOUMATCHENKO

**MODELING OF COMMUNICATION
NETWORKS USING STOCHASTIC
GEOMETRY**

Remerciements

J'aimerais exprimer ma reconnaissance à deux personnes qui ont dirigé ma thèse et qui ont contribué à ma formation dans le sens large du terme. François Baccelli savait toujours m'ouvrir des perspectives avec ses conseils. Sergei Zuyev me servait d'exemple d'attitude ouverte et inventive vis-à-vis de la recherche.

Je remercie Pierre Brémaud, Volker Schmidt et Ilkka Norros pour avoir accepté la tâche d'évaluation des résultats de ce travail. Merci à Youri Kutoyants qui a bien voulu présider le jury de soutenance.

Ma gratitude va aussi à Sergei Foss, grâce à qui j'ai découvert le monde fascinant des probabilités, et qui m'avait suivi et encouragé du début jusqu'à la fin de cette thèse.

Merci à Marc Lebourges et tous mes collègues du CNET. Ses questions et remarques pointues m'ont toujours incité à remettre en cause l'utilité pratique des résultats que j'obtenais.

Merci à tous les collègues du projet Mistral à l'INRIA et à l'ENS pour l'environnement stimulant et chaleureux de travail. Merci aux assistantes de recherche pour leur efficacité et l'ambiance qu'elles créaient autour de nous.

Finalement, je fais un clin-d'œil à tous les (ex-)doctorants du projet qui m'ont aidé à surmonter la barrière de la langue et grâce à qui le temps passé en dehors du bureau ne manquait pas de diversité.

K.T.

Contents

1	Introduction	11
1.1	Wired and Wireless Telephone Networks	11
1.1.1	Static Telephone Network	11
1.1.2	Wireless Networks with Mobile Users	13
1.1.3	Mobile Wireless Networks	14
1.1.4	Routing in Packet Switched Networks	16
1.2	Stochastic Geometry Network Models	18
1.2.1	Model Design Principles	19
1.2.2	Basic Cell Model	20
1.2.3	Hierarchical Model	21
1.2.4	Wireless Communications Model	23
1.3	Analytic Results for Stochastic Geometry Models	25
1.4	Contribution of This Thesis	36
1.4.1	Short Paths and Routing Algorithms.	36
1.4.2	Aggregate Tessellations in Network Models	37
2	Markov Paths on the Poisson–Delaunay Graph	41
2.1	Paths Approximating the Euclidean Distance	42
2.2	The Markov Path Algorithm	43
2.3	Markov Property of the Path	45
2.4	Ergodic Properties and Stationary Distribution	51
2.5	Path Length	55
2.6	Convergence of Transition Probabilities	60
2.7	Other Short Paths on the Delaunay Graph	66
2.8	Routing Algorithms for Mobile Communication Networks	71
3	Aggregate and Fractal Tessellations	73
3.1	Operation of Aggregation on Tessellations	74
3.2	Coverage Probability	77

3.3	Evolution of the Aggregate Cells	81
3.4	Existence of the Limit Tessellation	91
3.5	Asymptotics of the Spherical Contact Distribution Function .	97
3.6	Properties of the Fractal Cell Boundary	100
3.7	Modeling Radio Cells of a Wireless Network	102
A	Point Processes and Related Objects	105
A.1	Point Processes: Definitions and Basic Properties	105
A.1.1	Random Point Patterns	105
A.1.2	Palm Probability	108
A.1.3	Poisson Process	109
A.2	Voronoi Diagram and Delaunay Graph	110
B	Résumé	113
	Bibliography	122

Theory attracts practice as the magnet attracts iron.

Karl Friedrich Gauss (1777-1855)

Preface

The demand for efficient technology for information exchange is constantly growing all around the world. The design and operation of communication networks requires a wide range of problems to be solved, relating both to engineering and economics. Analysis of mathematical models of real-world systems often helps to handle these challenges successfully and opens new perspectives for the evolution of communication tools.

Usually, the study of a communication network has to be based on incomplete or unpredictable information on many factors that influence its behavior. Common examples of *a priori* unknown environmental factors are the time, the location, and the amount of user demand for the service. Also, a complete description of network architecture—the locations and connection scheme of all of its components—is not always available. Probability theory can deal with such uncertainty, making it possible to incorporate hypotheses on the external environment, on the configuration, and on the behavior of the system into the model.

The principal function of a network is to transfer information, so there is obviously a link between the effectiveness of the system on one side and the spatial distribution of network elements and user demand on the other. The statistical information about the network is often available only in the form of aggregate data, which is not sufficient for performance analysis. For example, from the total amount of offered load and rejected calls, it is not possible to identify the part of the network that creates bottlenecks. A macroscopic network model must therefore account for the *spatial factor*,

i.e. provide a description of the architecture and distinguish between the individual network elements in space.

Stochastic geometry provides a notion of a random object in space [40], and therefore turns out to be particularly suitable for macroscopic modeling purposes. The idea of the new modeling approach developed in [4] is to represent the components of a network (subscribers, nodes, service zones, link and transportation infrastructure) as a family of random objects (point patterns, graphs, tessellations), i.e. as realizations of stochastic processes with distribution parameters that can be estimated by measurements and observations.

Why use a stochastic description instead of the more traditional combinatorial one? The reason is that spatial distribution laws provide a much more compact representation for the locations of network elements than collections of individual coordinates. The network characteristics expressed as functionals of stochastic processes depend only on a limited number of distribution parameters. As a consequence, for really large networks, probabilistic representations are easier to treat well by analytical methods.

This thesis is a contribution to the analysis of network performance using methods from stochastic geometry. It is organized around two problems: the evaluation of the effectiveness of a routing mechanism, and the analysis of the spatial distribution of service zones in hierarchical networks.

The aim of Chapter 1 is to explain what types of networks can so far be modeled with such an approach and how these models are constructed. This chapter also presents a survey of problems that can be treated and discusses the results of this thesis in the context of network applications.

It should be noted that the analysis of stochastic spatial network models is based on *general* methods of stochastic geometry, of the theory of point processes, of spatial statistics, and of graph theory. New methods developed for studying the geometry of random graphs and tessellations and for the calculation and optimization of functionals of point processes expand the scope of the approach and are important in their own right.

Chapter 2 is devoted to the issues of routing, i.e. of finding a path for delivering information from the source to the destination. In some situations, finding the shortest path turns out to be a high-cost operation. We consider a simple ray-shoot algorithm for finding *short* paths and test its performance on a random graph representing the communication network. For this, we study the class of paths generated by this algorithm. The segments of paths

from this class form a Markov chain. We look at its ergodic properties and derive the stationary distribution. This is the central result of this part, and it allows us to find the mean relative length of a short path with respect to the Euclidean distance between its end-points. Comparing this value with the length of the shortest path (obtained by simulation) we get an idea of the effectiveness of the considered path-finding procedure. Using these results, we sketch a routing algorithm in which the routing decisions are based on local views of a network rather than on the knowledge of the state of all of its links.

Chapter 3 is the study of partitions of space into areas corresponding to the individual stations of a multi-level, hierarchically organized network (for instance, a telephone network). Assume that each level of stations is represented by a stationary point process. The space is divided between the stations into service zones, hence the stations can be viewed as nuclei of the cells, which form a tessellation. Consider a situation in which each station of level n controls the stations of level $n + 1$ located in its cell. Iterating this scheme, we obtain a branching process. We now look at a group of stations of level n that have a common ancestor at the top level. Our aim is to describe the geometry of the area assigned to such stations, i.e. of the union of the corresponding cells of the n -level tessellation. For each n , such areas form an *aggregate tessellation* (AT), which we study in this part of the thesis.

We trace the evolution of the shape of a typical aggregate cell as n grows, and find a closed-form expression for the coverage probability, which may be explicitly evaluated for network models based on Poisson–Voronoi tessellations. The main result of this part is a general condition for the existence of the limit tessellation as $n \rightarrow \infty$. We also look into the properties of its boundary in the special case when this tessellation is a fractal. Finally, we discuss potential applications of AT-based models to the modeling of cellular structures in wireless networks.

The results presented in this thesis were published as [6] and [59].

Chapter 1

Introduction

1.1 Wired and Wireless Telephone Networks

We begin with short overviews of the communication networks to which the models considered in this thesis are related. The goal of this section is to bring forward the spatial organization of these communication systems, the interconnection hierarchy, and the functions of their main elements. Further reading may be started, for example, from the book of Keshav [32], which provides a comprehensive introduction to a wide range of networking concepts and technologies.

1.1.1 Static Telephone Network

The telephone network offering a two-way voice connection between a pair of users is nowadays by far the most popular communication service with the number of its subscribers passing a billion mark. Since the late 70s of the last century, when the first public telephone network was conceived by Bell Telephone Company, technological innovations were constantly increasing the performance of the system. However, the basic architecture principles have remained almost unchanged.

The telephone service is based on the concept of *circuit switching*, from where the name Public Switched Telephone Network (PSTN). A *circuit* is a temporary communication path that the network sets up between two endpoints by switching the existing links. Once established, the circuit lasts for the duration of the call and is then dismantled; the links become available for reuse.

The telephone network is organized hierarchically (Figure 1.1). The lowest level of the hierarchy is formed by the end-systems, most often ordinary

telephone sets, sometimes fax machines and modems. All the end-systems within a particular geographical zone are connected to a switch at the *central office* (CO). By switching the local links, the CO can complete calls from the end-systems within its local zone. This local part of connection is called the *local loop*, as it is usually done by a pair of wires.

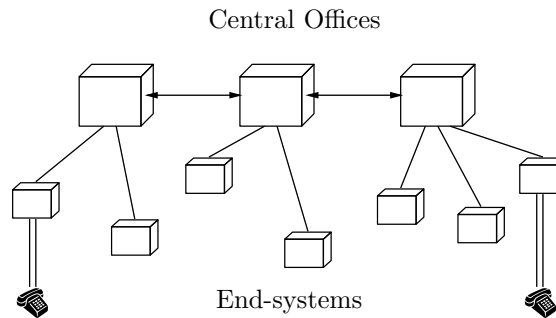


Figure 1.1: Public Switched Telephone Network

In order to be able to pass calls outside of local zones, the local COs are connected to less numerous COs of higher level, and so on. The hierarchy of the COs consists of two to five levels; the top level COs are handling the long-distance calls at the national and the international scale. Each of the COs of higher level can perform switching of the links to the lower-level COs, as the local COs can perform switching of wires to the end-systems. The top-level COs are interconnected by high-capacity backbone links so that any two COs can either communicate directly, or establish a path in a few hops using other COs as intermediate relays. These links form the *core network*. Depending on the capacity that is required for the transmission links at different levels, different types of media can be used: twisted pair, coaxial cable, fiber optics; the transmission can also be performed over wireless links.

A number of other communication systems make use of the global span of the telephone network. For example, Internet service providers use the local loop to reach customers at the households. The wireless systems that we consider below are closely integrated with PSTN and may use the core network as a relay medium for long-distance calls.

1.1.2 Wireless Networks with Mobile Users

Wireless networks are designed to provide voice and data connection to mobile users. The concept of the wireless systems is to deploy a number of low-power stations in the service area and let the mobile user communicate with the station providing the best quality of transmission. The whole service area is thus partitioned into subareas served by the stations, called *cells*. The size and shape of a cell is defined by the transmission and propagation factors. Low transmission power and low interference between stations makes it possible to reuse frequencies some distance away, which considerably increases the capacity of the system.

The acronym PLMN (Public Land Mobile Network) is often used as a general reference to the land-based cellular networks. Let us look more closely at the architecture of a cellular network on the example of GSM. A complete description of GSM system can be found in [47], [53]; see [56] and [57] for an overview. Other cellular networks are organized similarly, the principal difference between them lies in the technology of signal transmission.

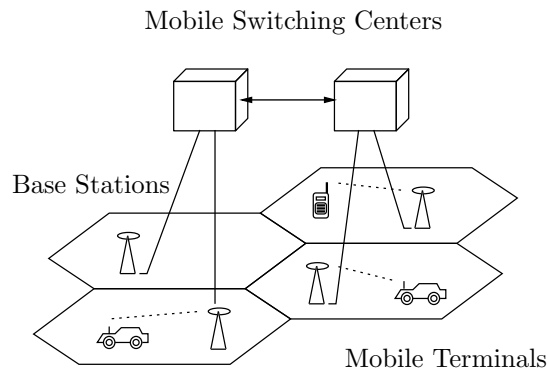


Figure 1.2: Wireless Telephone Network

A GSM network consists of three superposed layers (Figure 1.2):

- mobile terminals carried by the subscribers;
- base stations;
- network subsystem and switching centers.

Mobile terminals are portable handset transceivers used by subscribers. The mobile terminals communicate over the radio links with the *base stations*. The geographical area in which the base station can be best heard is called a *cell*. The cells are grouped in clusters, each station is assigned a unique set of frequencies so that the frequencies in the same cluster do not repeat, and the frequencies of different clusters do not interfere. The clusters are called *location areas*.

The base stations of each location area are controlled by a *mobile switching center* (MSC), which sometimes is also called mobile telephone switching office (MTSO). The switching centers are interconnected by *trunk lines* so that they can transfer data and exchange signaling information. The gateways are implemented in some of the switching centers, which provide an interface to the fixed telephone network and other services.

Such hierarchical organization allows for effective handling of calls from mobile terminals. The two main problems arising from the mobility of a subscriber are location tracking and communicating with mobile terminals.

When a mobile subscriber in active call mode moves from one cell to another, the call has to be switched between the two base stations. This action is called *handover*. Generally, it is initiated by a mobile terminal, which monitors the signal quality from neighboring stations and signals to its current switching center when the quality of the signal degrades beyond a certain limit. A mobile center can also perform handovers if it is unable to handle all the mobile terminals in its cell. There are two types of handovers: between cells controlled by the same switching center and belonging to the same local area, and between cells controlled by different switching centers.

The problem of effective handover policy is one of the major challenges in wireless networks. The signal power levels are subject to sudden fluctuations caused by natural obstacles. Because each handover involves a signaling cost, it seems unreasonable to perform switching each time the signal power falls, as it might result in the call being bounced back and forth between two stations. From the other side, if the reason of the signal degradation is the increasing distance between the mobile and the station, not performing handover may result in call dropping. An effective handover policy must then balance the cost and the reliability of service.

1.1.3 Mobile Wireless Networks

Another rapidly evolving sector of wireless communications are the networks in which not only the customers, but also part of the infrastructure is mobile. An example from this class are the systems of low-orbit satellite

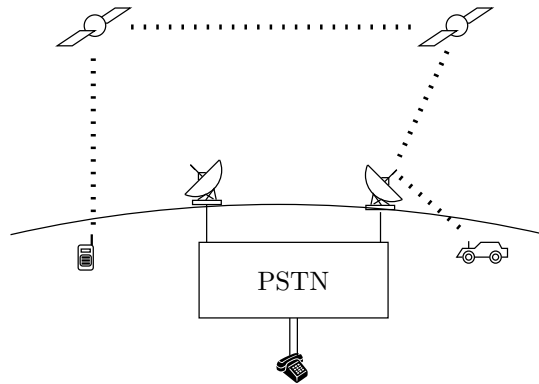


Figure 1.3: Satellite Communication Network

communications, designed as an extension to the existing wired and wireless land-based telephone networks (Figure 1.3). The most known commercial implementations, Iridium and Globalstar, offer point-to-point voice connection, messaging and other low-rate data services. The technology to provide multimedia data transfer with small delays is currently under development.

The worldwide coverage is achieved by deploying a constellation of satellites on low-earth orbits (LEO), at 750-1500 km over the land surface. The orbits are configured so that one or more satellites is always visible from any terrestrial location. The advantage of LEO satellites is that they can be reached directly from low-power mobile terminals. For voice communications, it is also important that the propagation delay from the LEO satellites is relatively small.

The ground-based segment of the satellite network consists of mobile satellite terminals (satellite telephones) and gateways to PSTN/PLMN. There is also a number of control centers that oversee satellite operations and manage the radio resources.

The mobile satellite terminal operates as a typical mobile terminal when the land-based cellular network is within reach. When the land-based network is unavailable, it establishes connection with a satellite. Next, the call is either relayed from satellite to satellite (Iridium), or is immediately bounced back to the land-based gateway (Globalstar), and is then completed via the PSTN/PLMN network. Thus the satellites act as “enhanced” base stations in conventional cellular networks.

An *ad hoc network* (Figure 1.4) is formed by a number of mobile hosts communicating over wireless links without any centralized infrastructure

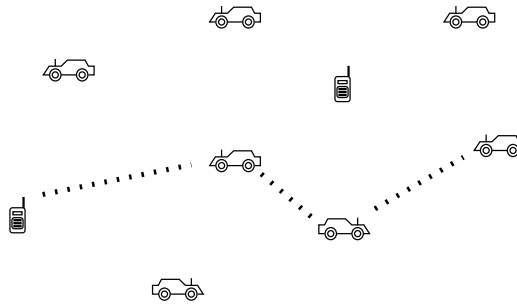


Figure 1.4: Ad Hoc Network (Mobile Radio Network)

(see e.g. [38], [39]). Such a situation occurs, for example, at emergency rescue operations, when communication services must be rapidly deployed in a region where the wired infrastructure is unavailable or inexistent. Frequently the networks of this type are called *mobile radio networks*, since the mobile hosts usually communicate over radio channels. If the source and the destination hosts are out of the radio range, other hosts participate in transmission by receiving and forwarding bits of information one to another.

1.1.4 Routing in Packet Switched Networks

The mechanism of *routing* ensures that the information transmitted from a source to a destination in the network finds its way along the link structure. There are two major ways of doing this: either to establish a communication path, a circuit, from source to destination for the whole period of connection (this is called *circuit switching*), or to split the information in small units, packets, and let the network independently choose the best way for each packet (called *packet switching*). Most of the telephone networks use circuit switching, which allows to guarantee the transmission quality. Internet, satellite communications, and mobile networks use packet switching, which better exploits the transmission capabilities of the networks and is more robust against link failures.

In packet switched networks, each station must be capable of forwarding information to the next hop on the way to the destination, i.e. must possess a so-called routing table matching each destination address to the address of the next hop in the routing path. The procedure of creating and maintaining such tables is called the *routing protocol*. The routing protocol defines which part of the global information on the network topology should be collected

and made available to each station so that it can create a coherent routing table. The protocol also implements the rules on how such informations should be exchanged between the stations.

For a routing protocol, at least three requirements can be formulated [32]:

- Size of routing tables and overhead signal messages should be minimized, to save useful bandwidth.
- Failures of communication links should not cause loss of information or loops.
- Paths used by the protocol should be optimal to minimize the network congestion and to maximize the overall network performance.

The last requirement depends on the choice of metric for the links. The optimal path may be the one with the minimal number of hops, with the least total length, or with the smallest delay. The metric may also depend on current link load and hence vary in time. We will look at mathematical models addressing the problems of path choice in Chapter 2.

Routing in the fixed telephone networks is largely predefined by the hierarchical network topology. Each CO maintains the list of phone numbers in its local zone and communicates it to the CO of superior level to which it is connected. When a call arrives, a CO checks whether the destination number is located within its local zone. If it is, the call is forwarded to the corresponding lower-level CO. If it is not, the call is forwarded to the superior level of the hierarchy.

Multiple routing decisions are possible when the call is forwarded to the top level of the telephone network (the core), and hence a path has to be established between two top-level COs. Because the network configuration at this level is essentially static, the links seldom fail, and the traffic is quite predictable, the common solution is to precalculate several variants of paths between each pair of top-level COs and to use the appropriate variant according to the traffic situation.

In wireless networks, in order to route incoming calls to subscribers, mobile phone numbers should be matched to the address of controlling base stations. In order to do this, the system must be able to rapidly determine the subscriber location. One way of doing this would be to page every cell of the network producing an excess of service messages. Another way would be to track every mobile and update this information at some global database each time a mobile changes cells. The solution is usually a trade-off: the system permanently keeps track only of the location area of a mobile and

pages every cell of this location area when the mobile has to be located. Mobile tracking is thus replaced by tracking of the corresponding MSC.

The routing scheme is thus the following. In the global database, the phone number of each subscriber is matched to the address of a *home* MSC to which the subscriber is permanently assigned. This home MSC stores and updates the address of the MSC that currently controls the mobile of the roaming subscriber. The calls *to* a roaming mobile are first routed to its home MSC and then to the MSC controlling its current location. The calls *from* a roaming mobile are routed to the destination via the current MSC and the home MSC. A scheme of this kind scales well and makes billing and accounting simple. The calls to and from the subscribers of fixed networks are forwarded through a number of PSTN/PLMN gateways. An update of the routing path is necessary each time when the mobile phone moves out of the cell of its current base station or out of the area of current MSC.

One of the most important engineering challenges is the design of routing protocols for distributed packet switched networks where no centralized information on the network topology is available [29], [28]. In such situations each host broadcasts to the others its local view of the network; the task of the routing protocol is that the information received by each host is consistent and as up-to-date as possible.

The two major types of distributed routing protocols use *distance vector* or *link state* algorithms. In the first, each host communicates to the neighbors its view of the distance to all hosts, and computes the optimal path to each host using the information received from its neighbors. In the second, each host broadcasts information containing the state and the cost of its adjacent links. Each host builds its own complete view of the network based on the information received from the others, and computes the optimal paths from this view. Both algorithms are also used in conventional wired networks.

1.2 Stochastic Geometry Network Models

The aim of this section is to show how models of different communication networks can be cast within the common mathematical framework of stochastic geometry. Common design principles make it possible to represent specific network architectures by combinations of abstract geometrical objects: point processes, graphs, and tessellations. A survey of results presents the examples of the analytical treatment of a number of evaluation and op-

timization problems. Applications of point processes to network modeling have also been reviewed by Schmidt & Frey in [20] and [21].

1.2.1 Model Design Principles

The locations of central offices of a large telephone network form an irregular point pattern. This irregularity is caused by spatial variations of population density, consumer demand, and a number of other geographical and technological factors. Though the picture looks essentially static, the development and upgrade of the system make it change in the long run. The dynamics is more evident for snapshots of wireless networks with mobile subscribers and mobile relay hosts.

With this irregularity and possible dynamics in mind, we argue that stochastic point processes provide good representations of locations of different network entities. The distributions of such processes can be chosen so that their realizations will look quite similar to observed point patterns. At the same time, a point process is in some way a much simpler object than the complete set of locations, because we care only about its distribution and not about the coordinates of many individual points.

For the sake of unity, in what follows, we will use the generic term *station* for network entities at each hierarchy level including the subscribers, and we will call *link* any form of physical connection between them, regardless of the media type.

In §1.1 we outlined the hierarchical organization of functional elements in several types of communication networks. From this viewpoint, the links between stations can be divided in two classes.

Inter-level links. Connections between stations of different levels of the hierarchy. This class comprises, for example, the local loops connecting subscribers to central offices, or the radio links between mobile terminals and base stations. Any two elements connected by a link of this class are in “parent–offspring” relation.

Intra-level links. Connections between the stations of the same level. Example from this class are the backbone links between the top-level COs and direct radio channels between mobile hosts in ad hoc networks.

A general design principle in communication networks is to exploit locality and to minimize lengths of physical and radio links, thus saving resources and facilitating transmission. Following this line, we will assume that the

inter-level links always connect an offspring station to the *closest* station of the parent level. In geometric terms this means that each level of parent stations generates a Voronoi tessellation of the space (see Definition A.2.1 in Appendix A), and the offspring stations that are located in the same Voronoi cell are connected to the parent station associated with its nucleus. We call two stations of the same level *neighboring* if they have adjacent service zones. In the basic models, we will assume that the intra-level links connect only neighboring stations. Thus the set of intra-level links constitutes a Delaunay graph (see Definition A.2.3) with stations as vertices.

The above assumptions on connections are, of course, idealistic. Natural obstacles and different engineering constraints influence the practical implementations of communication systems. The models discussed here capture only general tendencies and should be regarded as first-order approximations of reality. Hence, some attention should be paid, whether the assumptions apply in the context of each special case.

Here is the summary of the basic principles that define the structure of the forthcoming spatial stochastic models:

- Stations form an irregular point pattern represented by a spatial point process.
- Inter-level links connect a station to the closest station of the upper level. A Voronoi tessellation is thus generated by the upper-level stations, with cells corresponding to service zones. A station is connected to a station of the upper level, if it is located in its Voronoi cell.
- Intra-level links connect stations of adjacent cells. The set of links is thus represented by a Delaunay graph with the vertices at the locations of the stations.

1.2.2 Basic Cell Model

A simple representation of a generic network with a single level of stations can be built in the plane (or in \mathbb{R}^d) with only three components: a Poisson point process $\Pi = \{x_i\}$, the Voronoi tessellation $\Theta = \{C(x_i)\}$ generated by Π , and the Delaunay graph D having Π as the vertex set.

The Poisson process is perhaps the simplest non-trivial way of representing irregular point patterns formed by stations. Most often we will use a homogeneous Poisson process Π . It is clear that the homogeneity assumption ignores several important features of the networks. However, it reflects

the main quality of randomness of station locations in a region where the demographic density is approximately constant and it serves as a good starting point in the absence of additional information. With such an assumption, the model depends on the single parameter, the intensity λ of Π , and a number of network characteristics may be explicitly evaluated.

In cases when this assumption does not apply, an inhomogeneous process Π may be considered. Its intensity measure $\Lambda(\cdot)$ may be chosen proportional to the demographic density, the density of demand for the service, or to the hardware concentration. The estimation of $\Lambda(\cdot)$ may be performed from one realization e.g. by the maximal likelihood method (see [35], [36], and [52]).

So far, the model makes no distinction between the individual subscribers; they can be located anywhere in the space.

This construction serves as a primary block to build more complex systems. Used as a model in its own right, it admits several interpretations:

- Top level (core) of a fixed telephone network. The Voronoi tessellation corresponds to the division of space into service areas, and the Delaunay graph corresponds to the infrastructure of backbone links.
- Fixed part of a wireless communication system in the ideal signal propagation environment. Voronoi cells correspond to radio cells, and the stations are mobile switching centers, interconnected by land lines.
- Snapshot of configuration of mobile hosts in a mobile radio network. The Voronoi cells are local coverage areas, and the nodes of the Delaunay graph denote the radio channels established between the hosts.

1.2.3 Hierarchical Model

The hierarchical model is an extension of the basic cell model and it is based on the same assumptions. Consider a sequence of independent Poisson point processes

$$\Pi_0, \Pi_1, \dots, \Pi_n,$$

with $\Pi_k = \{x_i^k\}$ representing the stations of the k -th level (k -stations). If only homogeneous processes are considered, let λ_k be the intensity of Π_k . Denote by $\Theta^k = \{C^k(x_i^k)\}$ the Voronoi tessellation generated by the k -stations. Stations of Π_{k+1} that are closer to x_i^k thus are contained in $C^k(x_i^k)$. The inter-level links connect each $(k+1)$ -station x_i^{k+1} belonging to $C^k(x_i^k)$ to the nucleus x_i^k . These links constitute a family of spanning trees in the phase space, see Figure 1.5. The intra-level links connect each pair of

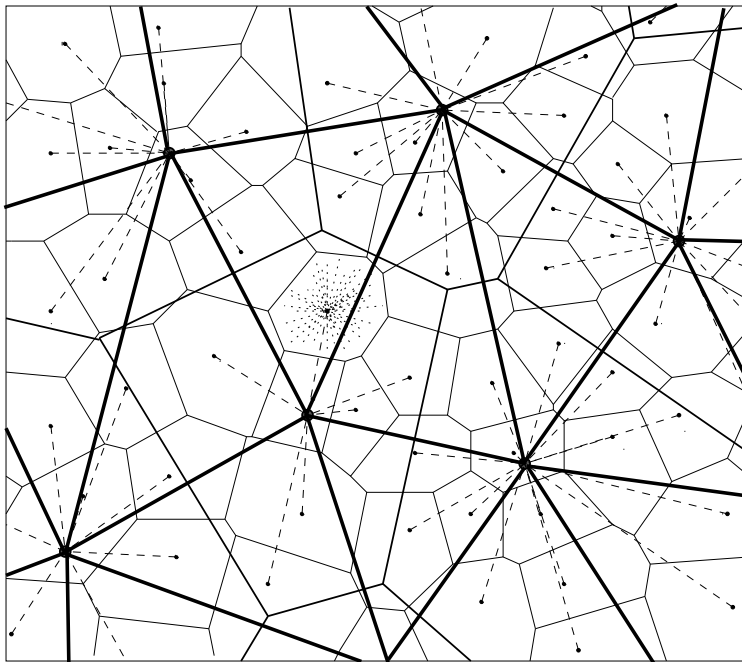


Figure 1.5: Hierarchical model of a communication network

top-level stations x_i^0 and x_j^0 whose Voronoi cells $C^0(x_i^0)$ and $C^0(x_j^0)$ share a $(d-1)$ -dimensional face. Thus, the intra-level links form a Poisson–Delaunay graph.

This model describes the fixed part of the infrastructure of wired and wireless networks, with the end subscribers represented by the lowest-level process Π_n . Alternatively, we may think of points of Π_n as of the base stations, and use a separate representation for the subscribers, like the one defined in the next section.

The connection rules that apply to the hierarchy of stations may be generalized in a number of ways by changing the type of tessellations associated with the point processes Π_k . For example, to each station x_i^k we may assign a random mark $w(x_i^k)$ reflecting its individual capacity or usage cost. Such a characteristic can be incorporated in the model by considering *weighed* Voronoi tessellations defined by (multiplicatively or additively)

weighed distances

$$\begin{aligned}d(y, x_i^k) &= w(x_i^k) \|y - x_i^k\|, \\d(y, x_i^k) &= w(x_i^k) + \|y - x_i^k\|.\end{aligned}$$

Systems in which for reliability reasons a station must be linked to *several* parent-level stations can be modeled with *higher-order* VTs, in which an area is assigned to the closest m -tuple of nuclei. See [42] and [51, Chapter 3] for definitions and a detailed account of properties of generalized Voronoi tessellations.

The strict hierarchical principle is seldom rigorously observed in real-world networks, which means that stations of non-adjacent levels may sometimes be connected directly. To reflect this fact, the topology of inter-level links can be modified by introducing direct connections between stations of non-adjacent levels, for example, k -stations connected to the closest stations of levels $0, 1, \dots, k - 1$.

It is also possible to use other types of graphs of intra-level links, for instance, the *Euclidean minimum spanning tree* on some bounded subset of \mathbb{R}^d . This is a connected graph that has $\Pi_0 \cap B$ as a vertex set and the minimal sum of edge lengths among all connected graphs with the vertex set $\Pi_0 \cap B$. A well-known result is that the minimum spanning tree is a subset of the Delaunay graph constructed on the same vertex set.

1.2.4 Wireless Communications Model

Mathematical representation for the fixed part of a cellular network is provided by a basic cell model or by a hierarchical model. Let us see how the aspects related to mobility of the subscribers can be integrated in this environment.

A simple way to model mobile subscribers would be to assume that their initial positions at time instant 0 are given by a Poisson process $\Pi = \{x_i\}$ and to let the subscribers move independently without interaction. Denote by d_i the displacement of the mobile x_i after time t . Bartlett's theorem (see e.g. [34]) states that the distribution of the set of new locations of subscribers $\{x_i + d_i\}$ is again Poisson provided that all d_i are mutually independent. Hence, such a model is essentially equivalent to the fixed case.

A more realistic model was proposed in [7]. Assume that the trajectories of subscribers are all straight lines (roads) in the plane. Each line is defined by a pair of parameters (p, α) , where p is the distance from the origin, and α is the inclination. Let the road system be represented by a Poisson line

process $\Pi_l = \{D_i\}$ in the space of parameters $\mathbb{R} \times [0, \pi)$, with the intensity measure

$$M(dD) = \lambda_{rd} dp \mathcal{O}(d\alpha). \quad (1.1)$$

Here λ_{rd} is the road density, and $\mathcal{O}(d\alpha)$ is the orientation distribution of a typical road. When the orientation distribution is homogeneous, the model is isotropic with all the road inclinations being equivalently probable. If the orientation has atomic distribution there is only a fixed number of possible inclinations of the roads corresponding to the atoms.

We now turn to definition of the traffic patterns on a given road $D = (p, \alpha)$. In the local coordinates, the subscribers on this road are characterized by three parameters: position, velocity, and calling state. Let the position and velocity at time instant 0 be represented by a two-dimensional Poisson process

$$\Pi_{pv}^D = \{(x_i(0), v_i(0))\}$$

with the intensity measure

$$\lambda_{tr}^D \mathcal{V}^D(dv).$$

Here λ_{tr}^D is the traffic intensity, and \mathcal{V}^D is the velocity distribution of a typical subscriber at the road D .

The velocities are marks of the subscribers, and we suppose that they remain constant in time so that a subscriber at $x_i(0)$ after the time period t moves to $x_i(t) = x_i(0) + v_i t$. Since the process $\{x_i(0)\}$ is homogeneous and the displacements of the points are independent, the distributions of the processes $\{(x_i(t), v_i)\}$ and $\{(x_i(0), v_i)\}$ coincide. This result is a consequence of Bartlett's theorem. It highly simplifies the analysis of the model.

The calling state $s_i(t)$ is another independent mark of $x_i(t)$. It equals 0 if the user is not active at the time instant t , and 1 if the user is in the call mode. We assume that the idle periods and the calling periods are independent exponentially distributed random variables with parameters κ_0^D and κ_1^D , respectively, and that

$$\mathbf{P}(s_i(0) = 0) = \frac{\kappa_0^D}{\kappa_0^D + \kappa_1^D},$$

which makes the distribution of the calling state stationary in time.

Thus, the mobility component of the model is represented by a marked Poisson line process $\Pi_l = \{D_i\}$ with each of its lines marked by a traffic configuration: locations of the subscribers, velocities, calling states. Marks related to different lines are assumed independent.

1.3 Analytic Results for Stochastic Geometry Models

Poisson–Voronoi cell characteristics

Point processes form the basis of a large number of probabilistic models, and an extensive theory has been developed for them. A thorough theoretical introduction and an advanced review of applicable mathematical tools are contained in Daley and Vere-Jones [15]. Of all the point processes, the Poisson process is the most important and the best studied special case. An extended account of its properties can be found in Kingman [34].

Interest in the geometry of random graphs and tessellations derived from stationary point processes has persisted due to a vast number of potential applications. The most common type of results imply moments, distributions and correlations of various cell characteristics, such as the volume, number of faces, surface area, etc. The results, initially scattered over the literature, have been united in Stoyan *et al.* [58], and in Okabe *et al.* [51], who also provide the research history and organized lists of references. We will review only some of the results that have direct applications in network analysis.

In the settings of stochastic geometry models, many network characteristics related to individual stations and their cells can be represented as marks of underlying point processes. A ready example is the area of a service zone assigned to a base station (used to estimate the volume of the expected traffic), or the number of mobile phone users communicating to a base station. Another example of a mark is the number of faces of a cell, i.e. the number of neighbors with whom a station has direct connections.

The Palm probability approach provides a framework to study the distributions of such marks. Consider the empirical mark distribution of a stationary marked point process $\{x_i, m(x_i)\}$, constructed from the observation of a stationary simple point process $\mathcal{N} = \{x_i\}$ through a bounded window $W = b(0, R)$

$$\bar{\mathbf{P}}(m < x) = \frac{1}{\mathcal{N}(W)} \sum_{x_i \in \mathcal{N}} \mathbb{I}(m(x_i) < x) \mathbb{I}(x_i \in W). \quad (1.2)$$

Here we suppose that the marks are observable for all points $x_i \in W$. When the marked point process $\{x_i, m_i\}$ is ergodic, the empirical distribution (1.2) converges to the Palm distribution \mathbf{P}^0 of the mark $m(0)$ as the size of the window R tends to infinity (for the definition of \mathbf{P}^0 , see Appendix). Thus, the Palm distribution can be interpreted as the distribution of the mark of

a point randomly chosen in \mathcal{N} . We will also refer to it as the distribution of a *typical* mark.

The notion of a mark can be naturally extended to geometric objects. For example, the cell $C(x_i)$ itself can be regarded as a mark of its nucleus x_i . Let \mathcal{H} contain all positive measurable functions on the set of the polytopes contained in \mathbb{R}^d . Denote by \mathbf{E}^0 the expectation corresponding to \mathbf{P}^0 . Let θ_t be a shift by $t \in \mathbb{R}^d$ (see Appendix). The Palm distribution of a typical cell $C(0)$ may be completely defined through $\mathbf{E}^0 h(C(0))$ for different $h(\cdot) \in \mathcal{H}$ such that

$$h(\theta_t C(x_i)) = h(C(x_i)).$$

As follows from the definition (see Appendix), the $(d - k)$ -facets of d -dimensional Voronoi tessellation can be indexed by $(k + 1)$ -tuples

$$[x]_{k+1} = (x_{i_0}, x_{i_1}, \dots, x_{i_k})$$

from the nuclei process \mathcal{N} . A *centroid* associated with the facet $F([x]_{k+1})$ is a point $z([x]_{k+1})$ covariant under translations

$$z(\theta_t [x]_{k+1}) = \theta_t z([x]_{k+1}).$$

Such centroids can be defined in several ways, for example, $z([x]_{k+1})$ may be the gravity center of $F([x]_{k+1})$. We can now consider the stationary marked process of centroids

$$\mathcal{N}_{d-k} = \{z([x]_{k+1})\}$$

with the marks being the characteristics of the corresponding facets. The density λ_{d-k} and the intensity I_{d-k} of $(d - k)$ -facets in \mathbb{R}^d are given by

$$\begin{aligned} \lambda_{d-k} &= \frac{1}{|B|} \mathbf{E} \sum_{[x]_{k+1}} |F([x]_{k+1}) \cap B|_{d-k} \\ I_{d-k} &= \frac{1}{|B|} \mathbf{E} \sum_{[x]_{k+1}} \mathbb{I}(z([x]_{k+1}) \in B). \end{aligned}$$

Due to the stationarity of the underlying nuclei process, these characteristics do neither depend on the choice of B , nor on the definition of centroid.

The values of λ_{d-k} for Poisson–Voronoi Tessellations (PVTs) were found for arbitrary $k = 1, 2, \dots, d$, a result due to Miles [44]. A wide range of results for stationary tessellations comes from the relations between λ_{d-k} , I_{d-k} , and other mean cell characteristics. General expressions in \mathbb{R}^d are given in [45], for $d = 2, 3$ see [58, §10.3]. Mean value relations of similar type

also exist for the tessellations induced by the intersection of a d -dimensional PVT with a k -dimensional hyperplane [45].

Consider the following cell characteristics

$$\begin{aligned} N &= \text{mean number of vertices,} \\ L &= \text{mean perimeter,} \\ S &= \text{mean surface area,} \\ V &= \text{mean volume,} \\ B &= \text{mean average breadth of a typical cell.} \end{aligned}$$

From the mean-value relations, in the planar case ($d = 2$) it follows that

$$\begin{aligned} I_0 &= 2\lambda, & I_1 &= 3\lambda, & I_2 &= \lambda, & N &= 6, \\ L &= 4/\sqrt{\lambda}, & S &= 1/\lambda. \end{aligned}$$

In the spatial case ($d = 3$)

$$\begin{aligned} I_0 &= 24\pi^2\lambda/35, & I_1 + I_2 &= 3I_0 + \lambda, & I_3 &= \lambda, & N &= 24\pi^2/35, \\ \lambda_1 &= (16/15)(3/4)^{1/3}\pi^{5/3}\Gamma(4/3)\lambda^{2/3}, & \lambda_2 &= 4(\pi/6)^{1/3}\Gamma(5/3)\lambda^{1/3}, \\ S &= (256\pi/3)^{1/3}\Gamma(5/3)\lambda^{-2/3}, & V &= 1/\lambda, \\ B &= (\pi/3)^{-5/3}4^{2/3}\Gamma(1/3)\lambda^{-1/3}/5. \end{aligned}$$

A number of other mean cell characteristics can be expressed as functions of the above values, see [58, §10.4, §10.6.2], [51, §5.4], [45, §7], [43].

The boundary Γ of a Voronoi tessellation is defined as the union of the boundaries of its cells. Let B be a compact star-shaped set in \mathbb{R}^d containing the origin. The *contact distribution function* $H_B(r)$ is the probability that the random set Γ hits the set B scaled by r on the condition that the origin does not belong to Γ

$$H_B(r) = \mathbf{P}(\Gamma \cap rB \neq \emptyset \mid 0 \notin \Gamma).$$

Integral formulas of $H_B(r)$ for Voronoi tessellations generated by a simple stationary process are presented in [25]. Typical choices of B are the unit ball $b(0, 1)$, or the segment $[0, 1]$. They yield, respectively, the *spherical* and the *linear* contact DFs. Integral representations for these functions for stationary Poisson–Voronoi tessellations are given in [22] and [49].

The contact DFs may be interpreted e.g. as a probability measure of the interference that a mobile terminal with the emission range r creates

in the neighboring cells of a wireless system. Specific shapes of the set B correspond to unidirectional or non-directional types of broadcast.

Consider the one-dimensional point process induced on a line l by the intersections with the boundary of a stationary PVT. Let $\{T_k, k \in \mathbb{Z}\}$ be the points of this process in local coordinates on l such that $T_{k-1} < T_k$ and $T_{-1} < 0 \leq T_0$. In wireless network context, T_k corresponds to the locations along the mobile's trajectory l at which handovers between the base stations are performed. The chords $[T_{i-1}, T_k]$ correspond to the parts of the trajectory when the mobile is controlled by different stations; these parts can be regarded as the marks of T_k . Clearly, $\mathbf{P}(\|T_0\| \leq r)$ coincides with the linear contact DF. The typical chord length distribution $L(r)$ is defined as the Palm distribution of $\|T_k - T_{k-1}\|$ with respect to the process $\{T_k\}$. The inversion formula of Palm distribution (see e.g. [3]) yields the relation

$$H_{[0,1]}(r) = \frac{1}{\bar{L}} \int_0^r (1 - L(r)) dr,$$

where $\bar{L} = \int_0^\infty (1 - L(r)) dr$ is the mean chord length. For stationary PVTs of the intensity λ , in [22] it was shown that

$$\bar{L} = \lambda^{-1/d} \frac{d \Gamma\left(d - \frac{1}{2}\right) \left[\Gamma\left(\frac{d+1}{2}\right)\right]^2}{2 \Gamma(d) \Gamma\left(2 - \frac{1}{d}\right) \left[\Gamma\left(\frac{d}{2} + 1\right)\right]^{(2d-1)/d}}. \quad (1.3)$$

General forms of contact DFs of stationary Voronoi tessellations were obtained in [25]. The contact DFs were expressed there in terms of the two-point Palm distribution and the pair correlation function. Expressions for the mean chord lengths follow as a corollary.

Apart from mean characteristics, there are quite a few explicit results on the distributional characteristics of Poisson–Voronoi cells. The situation is somewhat better for the Delaunay graph and for the triangulation of the plane that it defines: typical cell size and shape have been completely characterized in [44], [31], and all moments of the volume were found in [45]. For the Delaunay graph corresponding to a Poisson–Voronoi tessellation, the density function for the length of the typical Delaunay edge was obtained in planar and spatial cases in [48].

Cost of the infrastructure

Consider a model of a two-level hierarchical network generated by the Poisson processes Π_0 and Π_1 . Several cost-related characteristics associated with

a typical station of Π_0 can be expressed as functionals of the form

$$S[f] = \sum_{x_i^1 \in \Pi_1} f(x_i^1) \mathbb{I}(x_i^1 \in C_0(0)).$$

For instance, with $f(x) = 1$ this functional becomes the number of subscribers of a typical Π_0 -station, which we will denote by S_N ; with $f(x) = \|x\|$ it becomes the total length of the links from this station to the subscribers in its zone and will be denoted by S_L . The first two moments of these characteristics can be calculated using Campbell's theorem and numerical integration (see [19]).

$$\begin{aligned} \mathbf{E} S_N &= \lambda_1/\lambda_0, & \mathbf{E} S_L &= \lambda_1/(2\lambda_0^{3/2}), \\ \mathbf{Var} S_N &= \lambda_1/\lambda_0 + 0.28\lambda_1^2/\lambda_0^2, & \mathbf{Var} S_L &= \lambda_1/(\pi\lambda_0^2) + 0.147\lambda_1^2/\lambda_0^3, \\ \mathbf{Cov}(S_N, S_L) &= \lambda_1/(2\lambda_0^{3/2}) + 0.197\lambda_1^2/\lambda_0^{5/2}. \end{aligned}$$

Further problems of evaluating the cost of the infrastructure in multilevel hierarchical networks were considered in [8]. As follows from the description of the hierarchical model, each station x_i^k can be viewed as the root of the tree of inter-level links connecting x_i^k to the stations of lower levels $k+1, k+2, \dots, n$. The cost functions $G(x_i^k)$ introduced in [8] associate with such a tree the cost of all stations and links that belong to it. These functions are defined recursively as follows

$$\begin{aligned} G(x_i^n) &= I_n \\ G(x_i^k) &= I_k + \sum_{x_j^{k+1} \in \Pi_{k+1}} \left(G(x_j^{k+1}) + L(x_i^k, x_j^{k+1}) \right) \mathbb{I}(x_j^{k+1} \in C_k(x_i^k)). \end{aligned}$$

Here I_k corresponds to the cost of installation and maintenance of a k -station, and $L(x_i^k, x_j^{k+1})$ corresponds to the cost of the link connecting x_i^k to x_j^{k+1} . The definition of L takes into account two factors:

- capacity of the link, which in its turn is a function of $S(x_i^k)$, the number of subscribers (n -stations) managed by x_i^k ;
- cost of the medium, a function of the length of the link and of the level number.

In the simplest case,

$$L(x_i^k, x_j^{k+1}) = c_k S(x_i^k) \|x_i^k - x_j^{k+1}\|^{\alpha_k}, \quad (1.4)$$

with some constants $c_k > 0$ and $\alpha_k > 0$, $k = 0, 1, \dots, n - 1$.

From the formal viewpoint, the marks $G(x_i^k)$ are associated with the process of station locations Π_k . In this setting, the average total cost assigned to a typical k -station is expressed as $\mathbf{E}_{k,n}^0 G(0)$ (a shorthand for the expectation with respect to $\Pi_k \cup \{0\}, \Pi_{k+1}, \dots, \Pi_n$). An expectation of this kind can be evaluated using Campbell's theorem and Neveu's exchange formula (see [50]), the final form of the expressions depends on the definition of L . For example, for a three-level network with the link cost defined by (1.4),

$$\begin{aligned} \mathbf{E}_{0,2}^0 G(0) &= I_0 + I_1 \frac{\lambda_1}{\lambda_0} + I_2 \frac{\lambda_2}{\lambda_0} \\ &\quad + \frac{c_0 \lambda_2}{\pi^{\alpha_0/2} \lambda_0^{\alpha_0/2+1}} \Gamma\left(\frac{\alpha_0}{2} + 1\right) + \frac{c_1 \lambda_2}{\lambda_0 \lambda_1^{\alpha_1/2} \pi^{\alpha_1/2}} \Gamma\left(\frac{\alpha_1}{2} + 1\right). \end{aligned}$$

Here is an example of optimization problems that may be stated in these settings: given the intensity λ_0 of the process of top-level stations Π_0 and the intensity λ_2 of the process of subscribers, find λ_1 that minimizes the average cost of the infrastructure $\mathbf{E}_{0,2}^0 G(0)$. Generally, such parametric optimizations require numerical calculations. Some special cases can be treated analytically, for instance, for $I_2 = 0$, $\alpha_k = 1$, and $c_k = 1$, the value of $\mathbf{E}_{0,2}^0 G(0)$ attains its minimum

$$I_0 + \frac{3I_1^{1/3} c_1^{2/3} \lambda_2^{2/3}}{\lambda_0 8^{1/3}} + \frac{c_0 \lambda_2}{2\lambda_0^{2/3}} \quad \text{at} \quad \lambda_1^* = \left(\frac{c_1 \lambda_2}{4I_1}\right)^{2/3}.$$

The hierarchical model may be adapted to incorporate somewhat more general connection principles. For example, in [8] an hierarchical network was considered in which a k -station is directly connected to the closest station chosen of $\Pi_0, \Pi_1, \dots, \Pi_{k-1}$. Expression for the corresponding cost functions are obtained by similar methods of Palm calculus.

It is also possible to evaluate the costs associated with the individual "branches" of the spanning trees. Consider a hierarchical model generated by the processes $\Pi_0, \Pi_1, \dots, \Pi_n$, with the last level representing the subscribers. Suppose, a subscriber $x^n \in \Pi_n$ is placing a call that should be routed to the top level of the hierarchy. Under the model assumptions, the path used for this call is one of the "branches" rooted at a top-level station. Denote the vertices of such path by

$$(x^n, x^{n-1}, \dots, x^0),$$

where $x_k \in \Pi_k$ and $x^{k+1} \in C_k(x^k)$, for all $k = 0, 1, \dots, n - 1$. Suppose that the cost $L(x^{k+1}, x^k)$ assigned to each link is given by (1.4) with $S \equiv 1$.

Then, using the independence of the processes Π_n , it is easy to verify that the mean cost of the hierarchical path constructed from a typical subscriber is given by

$$\mathbf{E}_{0,n-1} \mathbf{E}_n^0 \sum_{k=0}^{n-1} L(x^{k+1}, x^k) = \sum_{k=0}^{n-1} \lambda_k^{-\alpha_k/d} \frac{c_k \alpha_k}{\pi^{-\alpha_k/2}} \Gamma\left(\frac{\alpha_k}{d}\right) \left[\Gamma\left(1 + \frac{d}{2}\right)\right]^{\alpha_k/d}.$$

Traffic in cellular networks

Consider a mobile networks model represented by superposition of the basic cell model of §1.2.2 and the mobility component described in §1.2.4. Several important characteristics of a mobile communication system than can be expressed as

$$X = \sum_{D_i \in \Pi_i} \tau(D_i),$$

where $\tau(D_i)$ is the value of some random field $\{\tau(D)\}$ at D_i . For example, if $\tau(D_i)$ is the number of cars in the call mode on the intersection of the road D_i with the zone $Z \subset \mathbb{R}^2$, then $X \equiv X_C(Z)$ is the total number of communicating mobiles in Z . If $\tau(D_i)$ is the number of active mobiles on D_i entering and leaving the zone Z during the time period Δt , then $X \equiv X_H(Z, \Delta t)$ becomes the total number of handovers for the zone Z over the period Δt .

Let ϕ_{D_i} be the characteristic function of $\tau(D_i)$. By [7, Th.1], if all $\tau(D_i)$ are mutually independent, the ch.f. of X has the form

$$\Phi(s) = \exp\left(\int (\phi_D(s) - 1) M(dD)\right),$$

where M is given by (1.1). From here, the moments of X can then be derived, in particular,

$$\begin{aligned} \mathbf{E} X &= \int \mathbf{E}^\tau \tau_D M(dD), \\ \mathbf{Var} X &= \int \mathbf{E}^\tau \tau_D^2 M(dD), \end{aligned}$$

where \mathbf{E}^τ denotes the expectation with respect to the distribution of $\tau(D)$.

In the case of the isotropic road system with constant λ_{tr} and with constant calling probability $\kappa = \kappa_1/(\kappa_0 + \kappa_1)$, the ch.f. of the number of the communicating vehicles in zone Z is given by

$$\Phi(s) = \exp\left(\frac{\lambda_{rd}}{\pi} \int_{\text{hit}(Z)} (\exp(\kappa \lambda_{tr} l(p, \alpha)(e^{is} - 1)) - 1) d\alpha dp\right),$$

where $\text{hit}(Z) = \{(p, \alpha) : \text{line } D = (p, \alpha) \text{ intersects } Z\}$, and $l(p, \alpha)$ equals the length of the intersection of the line $D = (p, \alpha)$ with Z . From here,

$$\begin{aligned} \mathbf{E} X_C(Z) &= \kappa \lambda_{tr} \lambda_{rd} |Z|, \\ \mathbf{Var} X_C(Z) &= \mathbf{E} X_C(Z) + \frac{\kappa^2 \lambda_{tr}^2 \lambda_{rd}}{\pi} \int_{\text{hit}(Z)} l^2(\alpha, p) d\alpha dp. \end{aligned} \quad (1.5)$$

The ch.f. and the first two moments are calculated in a similar way for the number of border crossings for the zone Z during a fixed period of time Δt . For Z being a convex, bounded domain, the probability of large deviations of $X_C(Z)$ is given in [7, Th.2]. Finally, (1.5) can be extended to the case of Z being a random cell of a typical base station C_0 , constructed with respect to a Poisson process Π_0 of intensity λ_0 . The first two moments of the above characteristics are then given by

$$\begin{aligned} \mathbf{E} X_C(C_0) &= \frac{\kappa \lambda_{tr} \lambda_{rd}}{\lambda_0} \\ \mathbf{E} X_H(C_0, \Delta t) &= \Delta t \frac{8\kappa \lambda_{tr} \lambda_{rd} \bar{V}}{\pi \lambda_0^{1/2}} + O((\Delta t)^2) \\ \mathbf{Var} X_C(C_0) &\approx \mathbf{E} X_C(C_0) + 0.672 \frac{\kappa^2 \lambda_{tr}^2 \lambda_{rd}}{\lambda_0^{3/2}} + 0.280 \frac{\kappa^2 \lambda_{tr} \lambda_{rd}}{\lambda_0^2} \\ \mathbf{Var} X_H(C_0, \Delta t) &\approx \mathbf{E} X_H(C_0, \Delta t) + 1.890 \Delta t \frac{\kappa \lambda_{tr} \lambda_{rd} \bar{V}}{\pi \lambda_0} + O((\Delta t)^2), \end{aligned}$$

where \bar{V} is the first moment of the velocity distribution \mathcal{V} .

The problem of optimal size of local areas can be addressed in the settings of a three-level hierarchical model representing the mobiles, switching centers, and local area stations. Clustering of radio cells in location areas reduces the number of update messages in the network, but increases the search costs. The definition of the cost of mobile tracking introduced in [8] takes into account these two factors.

Let the cost of location updating be proportional to the frequency at which the mobile crosses the borders of the local areas (Π_0 -cells). Suppose \bar{V} is the mean velocity of a mobile, and α is the cost of one operation of location updating. Using the fact that the intensity of cell border crossings by a straight line equals $4\lambda^{1/2}/\pi$ (see e.g. [58]), we can define the location update cost per time and per space unit as

$$G_1 = 4\alpha \bar{V} \lambda_2 \lambda_0^{1/2} / \pi.$$

Let $S(n)$ be the cost of locating a mobile in a Π_0 -cell containing n base stations, and let μ be the temporal intensity of calls directed to a mobile. Then the mobile search cost per time and per space unit writes as

$$G_2 = \mu\lambda_2 \mathbf{E}Y(\Pi_1(\tilde{C}_0)), \quad (1.6)$$

where \tilde{C}_0 is the Π_0 -cell containing the origin. Suppose, $Y(n) = \beta n$ for some constant $\beta > 0$, then

$$\mathbf{E}Y(\Pi_1(\tilde{C}_0)) = \beta\lambda_0\lambda_1 \mathbf{E}|\tilde{C}_0| = \frac{35\lambda_1\beta}{8\pi\lambda_0},$$

and the minimal value of the total cost function

$$G(\lambda_0) = G_1 + G_2$$

is attained at

$$\lambda_0^* = \left(\frac{35\lambda_1\mu\beta}{32\alpha\lambda_2\pi\bar{V}} \right)^{2/3}.$$

Thus, λ_0^* is the optimal intensity of the location area stations in these settings.

Stochastic gradients

The statistical approach to network optimization is applicable when no closed-form expressions can be obtained for the network characteristics. The optimization is based on the estimation of the gradients of functionals of point processes, see [54], [2], [46], [5], and [61].

Let $F(\mathcal{N})$ be some characteristic of a point process \mathcal{N} observed through a window $W \subset \mathbb{R}^d$. If the process is ergodic, an estimator of the expectation of $F(\mathcal{N})$ can be constructed using a *single* configuration of \mathcal{N} . For the stationary and Palm distributions, it is given, respectively, by

$$\begin{aligned} \widehat{\mathbf{E}}F(\mathcal{N}) &= \frac{1}{|W|} \int_W F(\theta_{-x}\mathcal{N}) dx, \\ \mathbf{E}^0 \widehat{F}(\mathcal{N}) &= \frac{1}{\mathcal{N}(W)} \sum_{x_i \in \mathcal{N} \cap W} F(\theta_{-x_i}\mathcal{N}). \end{aligned} \quad (1.7)$$

Suppose, $W = W_t$ is a sequence of bounded convex sets such that each W_t contains a ball of radius t , and $W_t \subset W_{t+1}$ for $t = 0, 1, \dots$. By the ergodic theorem [15, Prop. 10.2.II], the estimators (1.7) converge as $t \rightarrow \infty$

respectively to $\mathbf{E}F(\Pi)$ and $\mathbf{E}^0F(\Pi)$ a.s. and in $\mathcal{L}_p(\Pi)$, $p \geq 1$. The convexity of W_t is not required for the convergence if \mathcal{N} is a Poisson process.

In practice, the point process \mathcal{N} is usually observed through a finite-size window W . Thus, problems arise with the application of the estimator (1.7): for some statistics, $F(\theta_{-x}(\mathcal{N} \cap W))$ is not defined, for others, a bias is introduced by the edge effects.

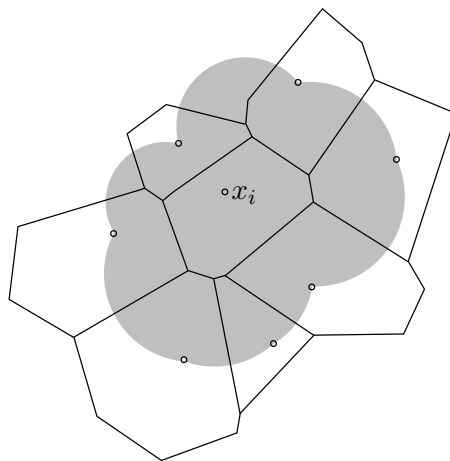


Figure 1.6: Fundamental region of the cell $C(x_i)$.

Call the statistic $F(\mathcal{N})$ *local* if there exists a compact set $B(\mathcal{N})$ such that $F(\mathcal{N})$ is completely determined by the restriction of the process configuration \mathcal{N} on $B(\mathcal{N})$.

For example, any translation-invariant characteristic of a Voronoi cell $C(x_i)$ generated by a Poisson process Π is a local statistic, because the Voronoi cell is completely determined by the restriction of Π on the so-called *fundamental region* (also known as the *Voronoi flower*) defined as a union of closed balls centered in the vertices of $C(x_i)$ and having x_i in its boundary (see Figure 1.6). The length of the paths on the Poisson–Delaunay graph that we will be considering in Chapter 2 is another example of local statistics.

For local statistics, the edge effects in (1.7) can be treated with a naive *border* method (see e.g. [55], [58]). It consists in reducing the observation to the window $W' = \{x \in W : \theta_x B(\theta_{-x}\mathcal{N}) \subset W\}$. Replacing W for W' in (1.7) reduces the bias. Of course, this method discards a large part of observed information, which may be unacceptable when the estimator bases on a single configuration of \mathcal{N} . For several basic characteristics of a sta-

tionary point process (intensity, pair-correlation function, nearest-neighbor distance, etc.) more sophisticated edge-corrected estimators were developed, see e.g. the surveys [9], [58, §4.6], [21].

Let $F(\Pi)$ be a local statistic on the realization of a homogeneous Poisson process of the intensity λ , representing, say, some infrastructure costs. We would like to find the value of the parameter λ at which the optimal value of $\mathbf{E} F(\Pi)$ is attained and would like to implement, for example, the steepest descent method. For this we need an estimator for the gradient $\frac{d}{d\lambda} \mathbf{E}_\lambda F$ for a given λ .

A random variable D is called a *stochastic gradient* of F if

$$\frac{d}{d\lambda} \mathbf{E}_\lambda F = \mathbf{E}_\lambda D.$$

If such a random variable exists for F , the estimation of the derivative $\frac{d}{d\lambda} \mathbf{E}_\lambda F$ can be reduced to the estimation of the expectation of D using (1.7).

For Poisson point processes, stochastic gradients exist under certain conditions (see [5]) and have the form

$$\begin{aligned} \frac{d}{d\lambda} \mathbf{E}_\lambda^0 F &= \mathbf{E}_\lambda^0 \int [F(\Pi \cup \{x\}) - F(\Pi)] dx \\ &= \int \mathbf{E}_\lambda^0 [F(\Pi \cup \{x\}) - F(\Pi)] dx. \end{aligned} \quad (1.8)$$

The expression remains valid if \mathbf{E}_λ^0 is replaced by \mathbf{E}_λ . Note that for the local statistics, $F(\Pi \cup \{x\}) - F(\Pi) = 0$ if x does not belong to the dependence region $B(\Pi)$. With this fact and (1.7), the estimator for the subintegral expectation in (1.8) is given by

$$\frac{1}{\Pi(W')} \sum_{x_i \in \Pi \cap W'} [F(\theta_{-x_i} \Pi \cup \{x\}) - F(\theta_{-x_i} \Pi)] \mathbb{1}(x \in B(\theta_{-x_i} \Pi)),$$

Taking the integral, we obtain

$$\frac{1}{\Pi(W')} \sum_{x_i \in \Pi \cap W'} \int_W [F_i(\Pi \cup \{x\}) - F_i(\Pi)] dx,$$

where $F_i = F \circ \theta_{-x_i}$. Using the Monte-Carlo method, we obtain the following estimator for stochastic gradients

$$\widehat{\frac{d}{d\lambda} \mathbf{E}_\lambda^0 F} = \frac{|W|}{\Pi(W')} \sum_{x_i \in \Pi \cap W'} \frac{1}{M} \sum_{m=1}^M [F_i(\Pi \cup \{u_m\}) - F_i(\Pi)], \quad (1.9)$$

where u_m , $m = 1, 2, \dots, M$ are independent uniformly distributed in W random variables. The asymptotic variance of the estimator (1.9) has the order $O(|W|^{-1} + M^{-1})$.

1.4 Contribution of This Thesis

1.4.1 Short Paths and Routing Algorithms.

Routing algorithms are designed to find communication paths connecting distant subscribers. On many occasions, call routing is performed in homogeneous environment, for instance, between two top-level stations of PSTN, or between two hosts in mobile radio network. In conventional wired or wireless networks, the routing protocols are usually based on modifications of one of the two schemes for the search of the shortest path on the graph of links. The *distance-vector routing* uses the algorithm of Bellman–Ford [11], [18], which prescribes the exchange of distance vectors between network neighbors. This allows one to distribute the routing process among the hosts and if all links stay up all the time, every host eventually ends up with a table containing the next hop in the shortest path to every destination. The classical algorithm is unstable against links failures, which may cause infinite exchanges between hosts (the famous “counting to infinity” problem). To avoid this, in different modifications of the algorithm the distance vector is completed with some path information (at the expense of the size of the routing tables), see e.g. [13]. In *link-state routing*, each host broadcasts the cost and the state of the links to its neighbors over the whole network and collects such information from the other hosts. This information is united by the host in global network picture. Then the host usually applies Dijkstra’s algorithm [16] to construct a spanning tree of shortest paths from itself to every destination.

Both types of algorithms require certain relaxation time: either for the distance vectors to converge, or for the link state information to reach every host. Routing in mobile networks requires this time to be short: when the actual network image and the image perceived by a host are significantly different, routing through this host is impossible. From the other hand, host mobility and frequent changes of the network topology significantly increase the quantity of overhead information and therefore slow down the convergence between the perceived and the real network states.

This difficulties cannot be entirely eliminated as soon as routing protocols aim at finding shortest paths, because shortest paths, by their nature, rely on comparison of many possible routing decisions, and hence, on interaction between many hosts. The aim of the first part of the thesis is to examine some path-finding algorithms that do not require extensive exchange of information between the stations and still yield reasonably short paths.

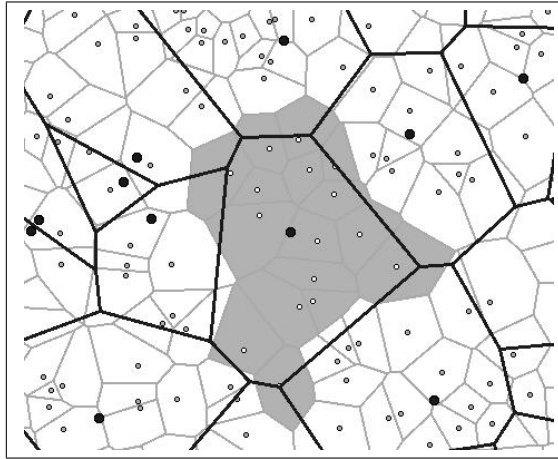


Figure 1.7: Aggregate cell of the first order (filled).

Stochastic geometry provides a framework for testing different routing algorithms by evaluating the corresponding paths' characteristics. In Chapter 2 we consider a simple ray-shoot algorithm in the context of basic network model and give a probabilistic analysis of a class of “short” paths that it generates on the Poisson–Delaunay graph. One of the main results of the chapter is the expression for the mean length of such paths, which is then compared to the length of the shortest path and the Euclidean distance between the two endpoints. The length results may also be used for computation of costs of the infrastructure that is needed in order to connect two network nodes.

1.4.2 Aggregate Tessellations in Network Models

Tessellations naturally arise in network models whenever a partition of space between some network elements is considered. An example of such a partition is the division of the coverage area of a wireless network between the base stations. As we have seen in §1.3, the connection rules between different types of network entities can also be described by means of tessellations.

The models presented in §1.3 mainly use the concept of Voronoi diagrams, with the cells being convex non-empty polyhedra. A number of reasons suggest that one should use more sophisticated shapes to obtain accurate models of service zones. The variability of the radio cells is an intrinsic feature of the wireless networks, where possibility of connection to

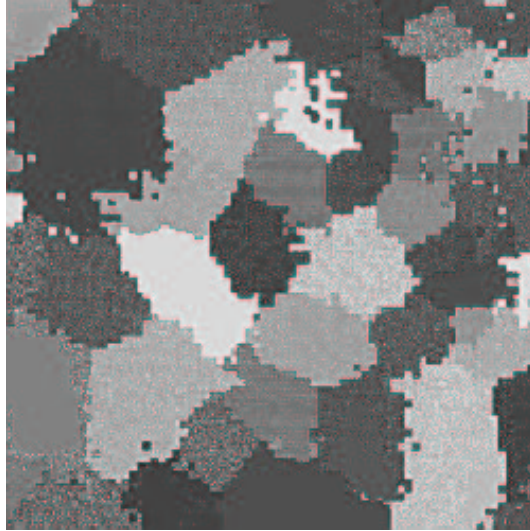


Figure 1.8: Radio cells in GSM network.
(Reproduced with permission of Prof. R. Mathar)

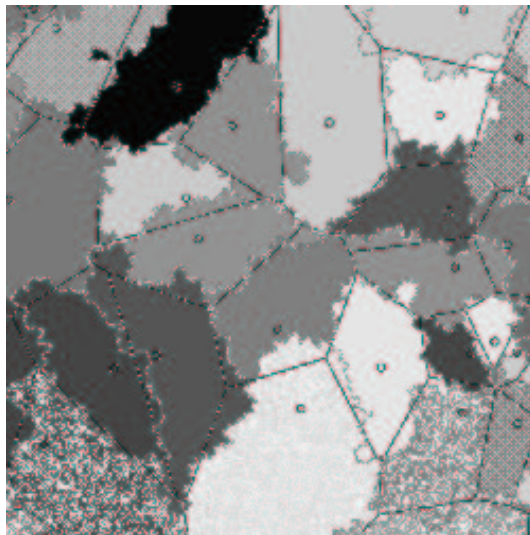


Figure 1.9: Realization of an aggregate tessellation.
(PVAT of order 3; $\lambda_n = 10^n$, $n = 0, \dots, 3$)

a base station is defined by the signal strength rather than by the Euclidean distance. Measurements of the signal quality in different locations of the service area show that the radio cells have irregular, distorted shapes and fuzzy boundaries (see Figure 1.8). The relative sizes of the cells are also affected by the different capacities of stations. Moreover, some of the stations may be made inactive and thus their zones will be empty.

Hence, in many cases the first-order approximation models oversimplify the complex geometry of service zones and radio cells. A refined representation for them is provided by the *aggregate tessellations* (ATs) that are introduced and studied in Chapter 3.

An AT of the first order is obtained from two arbitrary tessellations equipped with nuclei sets. The construction consists in merging (aggregating) those cells of tessellation 1 whose nuclei fall into the same cell of tessellation 0 (see Figure 1.7). By induction, an AT of order $n + 1$ is produced from a sequence of tessellations by merging those cells of tessellation $n + 1$ whose nuclei fall into the same cell of the aggregate tessellation of order n . The formal definition of ATs will be given in §3.1.

Special cases of aggregate tessellations arise in the models of hierarchically organized networks. Consider as an example a multilevel hierarchical model with stations and service zones represented, respectively, by the point processes Π_k , and by the tessellations $\Theta^k = \{C^k(x_i^k)\}$, $k = 0, 1$, as described in §1.2.3. The inter-level links connect a top-level station x_i^0 with every 1-station located in its cell $C^0(x_i^0)$. Every 1-station x_j^1 controls its local service zone $C^1(x_j^1)$. Thus, the area

$$C_0^1(x_i^0) := \bigcup_{j : x_j^1 \in C^0(x_i^0)} C^1(x_j^1)$$

is the territory controlled by the top-level station x_i^0 via the 1-stations. This territory corresponds to a cell of an AT of order 1 produced from Θ^0 and Θ^1 .

In the wireless context, ATs provide a model of cellular structure that fits well with observed cellular patterns (compare Figure 1.8 and Figure 1.9). The AT-based models can be used, for example, for the evaluation of coverage capacities of base stations and for testing the effectiveness of different handover policies. Some remarks on the interpretation of such models will be given in §3.7.

Chapter 3 is devoted to the study of the aggregate tessellations. We adopt a general viewpoint and introduce a sequence of ATs of increasing order generated by *arbitrary* stationary tessellations equipped with nuclei sets. The first group of obtained results concerns the evolution of this sequence:

we estimate different expansion and extinction probabilities of typical aggregate cells and find their coverage functions. The second group of results concerns the conditions of the existence and the characteristics of the limit tessellation. Special attention is given to the properties of ATs generated by Voronoi tessellations.

Chapter 2

Markov Paths on the Poisson–Delaunay Graph

The aim of the present chapter is to give a probabilistic analysis of a special class of paths on the Poisson–Delaunay graph constructed with a simple ray-shoot algorithm. The motivation for investigating such objects comes from two quite independent problems arising in communication networks.

- Development of an effective routing algorithm for mobile wireless networks. A ray-shoot packet relay may be useful as a tradeoff in situations when high host mobility makes computation of the shortest paths impossible and at the same time flooding of information packets to all hosts creates too large volumes of overhead messages. Thus, the properties of paths issued from the ray-shoot algorithm are worth exploring.
- Determination of a fair cost of a call between two locations of a large static network. Such a characteristic must account for the cost of the communication circuit between the end terminals. As we have seen in the previous chapter, when the network connectivity is achieved by linking the geographical neighbors, the link infrastructure can be modeled by a Delaunay graph. It is important to establish a relation between the costs of circuits that provide connection and the distance between the two end terminals.

In stochastic geometry terms, we will be interested in paths constructed on the Poisson–Delaunay graph that approximate well the Euclidean distance between the end points. The exposition is organized as follows. After

the preliminaries of §2.1, we introduce in §2.2 a class of paths on the Delaunay graph constructed along the segment connecting the end points. The use of the term *Markov paths* is justified in §2.3, where we prove that the segments of the paths of this kind form a Markov chain and derive its transition probabilities. Next, in §2.4 we use the embedding of the Markov path into an ergodic point process to formulate several ergodic results and find the stationary distribution of the corresponding Markov chain. As a corollary, we obtain in §2.5 an expression for the mean and asymptotic ratio of the path length to the Euclidean distance between the end-points. In the planar case, the ratio evaluates to $4/\pi$, for higher dimensions we give the results of numerical computations. Some implications of this result are discussed in §2.7. In §2.6 we show that conditions of the mean drift criterion are verified for the chain, which implies geometric rate of convergence of transition probabilities to the stationary regime. Several modifications of the Markov path that lead to shorter paths at the cost of additional complexity are introduced in §2.7. Finally, in §2.8 we discuss possible applications to routing in mobile communication networks; we introduce a family of distributed routing algorithms based on a local view of the network and use the analytical results to characterize their mean performance.

2.1 Paths Approximating the Euclidean Distance

For a graph constructed on the vertex set $\{x_i\}$, a *path* $p(x_i, x_j)$ between two nodes x_i and x_j is a sequence of segments

$$[x_i, x_{i_1}], [x_{i_1}, x_{i_2}], \dots, [x_{i_{n-1}}, x_j],$$

such that every segment is an edge of the graph. The *length* of the path $|p(x_i, x_j)|$ is the sum of the lengths of all of its segments.

We say that a class of paths *t-approximates the Euclidean distance* if for each path $p(x_i, x_j)$ in this class

$$|p(x_i, x_j)| \leq t \|x_i - x_j\|. \quad (2.1)$$

A class of paths *asymptotically t-approximates the Euclidean distance* if for each path $p(x_i, x_j)$ in this class

$$\limsup_{\|x_i - x_j\| \rightarrow \infty} \frac{|p(x_i, x_j)|}{\|x_i - x_j\|} \leq t. \quad (2.2)$$

In what follows, we will be considering paths on a random Delaunay graph having as its vertex set a homogeneous Poisson point process $\Pi = \{x_i\}$

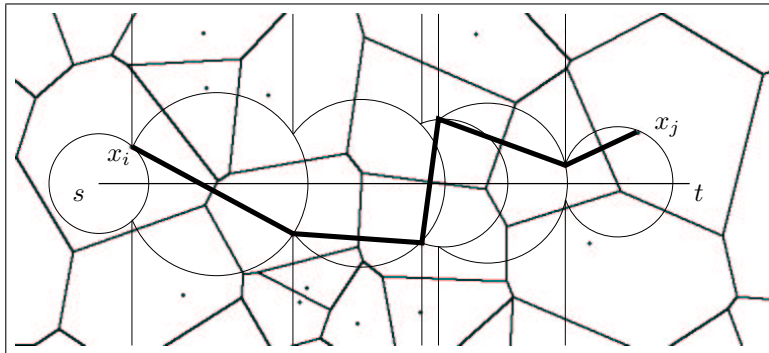


Figure 2.1: Markov path on the Poisson–Delaunay graph.

of intensity $\lambda = 1$ defined in \mathbb{R}^d . The paths constructed on such a graph are thus random closed sets and their lengths are random variables. For classes of random paths, we will speak of *t-approximation in mean* if (2.1) holds for the expectation of $|p|$, and of *asymptotic t-approximation* if (2.2) holds with probability one.

2.2 The Markov Path Algorithm

Let s and t be two points in \mathbb{R}^d . Suppose, x_i and x_j are the two points of Π which are the closest to s and t , respectively. A path on the Delaunay graph between x_i and x_j can be defined using the dual Voronoi tessellation $\Theta = \{C(x_i)\}$ as follows.

Consider the sequence $C(x_i), C(x_{i_0}), \dots, C(x_j)$ of cells successively crossed by the segment $[s, t]$. The sequence of nuclei of these cells defines a *Markov path* $\hat{p} = \hat{p}(s, t, \Pi)$ on the Delaunay graph from x_i to x_j (see Figure 2.1). This path is the main object of our study.

Another way to define the end-points of a random path is to add two fixed points s and t to the vertex set Π and consider the path $\hat{p}(s, t, \Pi')$ with $\Pi' = \Pi \cup \{s\} \cup \{t\}$. Relation (2.33) at the end of this section shows that both paths have the same asymptotic behavior.

We are interested in the distribution of \hat{p} . Because the underlying Poisson process Π is homogeneous and isotropic, without loss of generality we may assume s to lie at the origin and let t belong to the d -th coordinate axis, so that $t = (0, 0, \dots, \|t\|)$. The finite sequence of vertices of $\hat{p}(0, t, \Pi)$ is a subsequence of the infinite sequence $\{x_{i_0}, x_{i_1}, \dots\}$ of the nuclei of the

cells crossed by the ray $\{\alpha t, 0 \leq \alpha < \infty\}$. It is convenient to introduce for the infinite paths a special notation

$$\hat{p}(0, \infty, \Pi) = \{Z_0, Z_1, \dots\}.$$

Denote by $T(x, y)$ the point at which the bisector hyperplane of the segment $[x, y]$ intersects with the coordinate axis containing $[s, t]$. Observe that if for some x_i, x_j the ball $b(T(x_i, x_j), \|x_i - T(x_i, x_j)\|)$ contains no point of Π , then

- (a) the segment $[x_i, x_j]$ belongs to the Delaunay graph;
- (b) the axis containing $[s, t]$ crosses the border between $C(x_i)$ and $C(x_j)$ at the point $T(x_i, x_j)$.

The next proposition gives a criterion for an arbitrary sequence of points of Π to be the sequence of vertices of the path $\hat{p}(0, t, \Pi)$. Let

$$q_n = \{x_{j_0}, x_{j_1}, \dots, x_{j_n}\}$$

be an arbitrary sequence of points of Π . Denote $T_k = T(x_{j_{k-1}}, x_{j_k})$. Define the sets

$$B_0 := b(0, \|x_{j_0}\|)$$

$$B_k \equiv B_k(x_{j_{k-1}}, x_{j_k}) := b(T_k, \|x_{j_{k-1}} - T_k\|), \quad k = 1, 2, \dots, n$$

$$D_k \equiv D_k(x_{j_{k-2}}, x_{j_{k-1}}) := \{x \in \mathbb{R}^d : x^d > x_{j_{k-1}}^d\} \setminus B_{k-1}, \quad k = 1, 2, \dots, n.$$

Proposition 2.2.1 *A sequence $q_n = \{x_{j_0}, x_{j_1}, \dots, x_{j_n}\}$ coincides with the $n + 1$ first vertices $\{Z_0, Z_1, \dots, Z_n\}$ of the path $\hat{p}(0, \infty, \Pi)$ if and only if the following conditions are satisfied*

- (i) $\Pi(B_k) = 0, \quad k = 0, 1, \dots, n;$
- (ii) $x_{j_k} \in D_k, \quad k = 1, \dots, n.$

Proof. Condition (i) for some $k \geq 1$ is equivalent to saying that the cells $C(x_{j_{k-1}})$ and $C(x_{j_k})$ are adjacent and that their common border is crossed at point T_k by the coordinate axis containing $[0, t]$. For $k = 0$, this condition means that x_{j_0} is the nucleus of the cell containing 0. Condition (ii) is satisfied if and only if $0 < T_0^1 < T_1^1 < \dots < T_{n-1}^1$, which means that the cells are crossed in the same order as their nuclei appear in the sequence q_n .

Note that if q_n coincides with the vertices of $\hat{p}(0, t, \Pi)$ for some t , then the set $\{T_k\}$ is the restriction on the segment $[0, t]$ of the point process of cell border crossings by the coordinate axis containing $[0, t]$. Some properties of this process were discussed in §1.3.

2.3 Markov Property of the Path

A remarkable fact is that the sequence of segments $\{[Z_{n-1}, Z_n]\}_{n \geq 1}$ of the path $\hat{p}(0, \infty, \Pi)$ is a Markov chain. Here are some heuristic arguments (rigorous proof will be given below, after the introduction of appropriate parametrization). Fix the history of the process up to the n -th step, that is up to $[Z_{n-1}, Z_n]$. From Proposition 2.2.1, Z_{n+1} is a point of Π in D_{n+1} such that $\Pi(B_{n+1}) = 0$. There exists a.s. exactly one such point because the points of Π are a.s. in a general position. Due to the strong Markov property of the Poisson process, the numbers of points of Π in the disjoint sets $B_{n+1} \cap D_{n+1}$ and $B_{n+1} \cap D_{n+1}^c$ are independent. From the history, it follows that $\Pi(B_{n+1} \cap D_{n+1}^c) = 0$. Therefore, the event $\Pi(B_{n+1}) = 0$ has the same conditional probability as the event

$$\{\Pi(B_{n+1} \cap D_{n+1}) = 0\} = \{\Pi(B_{n+1} \setminus B_n) = 0\}. \quad (2.3)$$

Note that the shape of D_{n+1} and the form of Condition (2.3) depend only on the pair (Z_{n-1}, Z_n) , and not on the whole history of the process.

Spherical coordinates

Spherical coordinates provide a representation of points $x \in \mathbb{R}^d$ in the form $x = r \cdot s(\theta)$. Here $r \in [0, \infty)$ is the distance from the origin to x , and $s(\theta) \in \mathbb{R}^d$ is the direction to x defined by the *spherical angles*

$$\theta = (\theta^1, \theta^2, \dots, \theta^{d-1}) \in A := [-\pi, \pi) \times [0, \pi)^{d-2}$$

as follows

$$\begin{aligned} s^1(\theta) &= \sin \theta^1 \sin \theta^2 \cdots \sin \theta^{d-1} \\ s^2(\theta) &= \cos \theta^1 \sin \theta^2 \cdots \sin \theta^{d-1} \\ &\dots \\ s^{d-1}(\theta) &= \cos \theta^{d-2} \sin \theta^{d-1} \\ s^d(\theta) &= \cos \theta^{d-1}. \end{aligned}$$

The Jacobian of transition from Cartesian to spherical coordinates has the form $(r)^{d-1} J_d(\theta)$, where

$$J_d(\theta) = \prod_{i=2}^{d-1} \sin^{i-1} \theta^i. \quad (2.4)$$

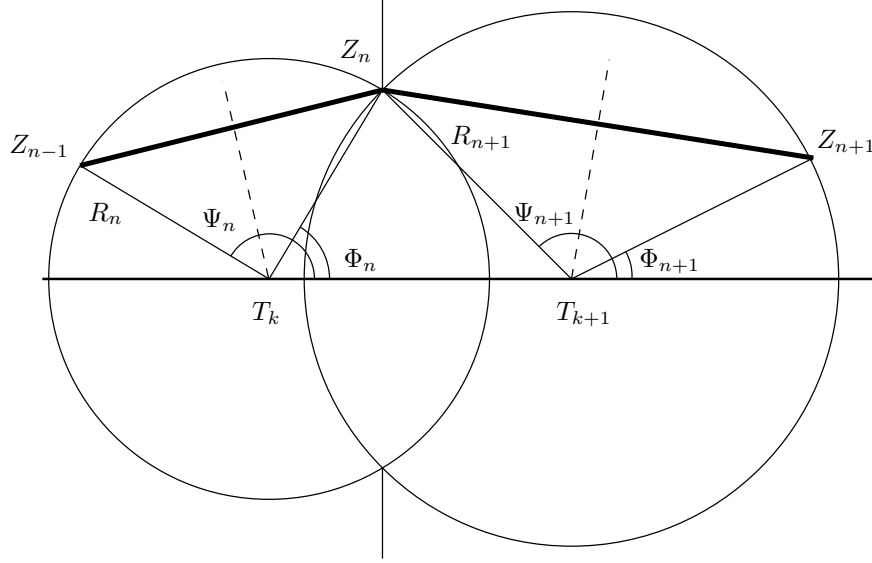


Figure 2.2: Two consecutive segments of the path $\hat{p}(0, t, \Pi)$.

Parameterization of the Markov path

Let us now introduce a more convenient coordinate system for $\hat{p}(0, \infty, \Pi) = \{Z_0, Z_1, \dots\}$. Define the following parameters (see Figure 2.2)

R_0 = distance from the origin to Z_0 ;

Φ_0 = spherical angles of Z_0 ;

R_k = distance from T_k to Z_k (equivalently, to Z_{k-1});

Φ_k = spherical angles of $Z_k - T_k$ (equivalently, of Z_k as seen from T_k);

Ψ_k = spherical angles of $Z_{k-1} - T_k$;

A segment $[Z_{k-1}, Z_k]$ is thus defined by $2d$ parameters

$$T_k, R_k, \Phi_k = (\Phi_k^1, \Phi_k^2, \dots, \Phi_k^{d-1}), \Psi_k = (\Psi_k^1, \Psi_k^2, \dots, \Psi_k^{d-1})$$

as follows

$$Z_{k-1} = T_k + R_k s(\Psi_k), \quad Z_k = T_k + R_k s(\Phi_k). \quad (2.5)$$

From the relations (see Figure 2.2),

$$Z_{k+1} = T_{k+1} + R_{k+1} s(\Phi_{k+1}) \quad (2.6)$$

$$R_{k+1} = \frac{R_k \sin |\Phi_k^{d-1}|}{\sin |\Psi_{k+1}^{d-1}|} = R_0 \prod_{j=0}^k \frac{\sin |\Phi_j^{d-1}|}{\sin |\Psi_{j+1}^{d-1}|} \quad (2.7)$$

$$T_{k+1} = \sum_{j=0}^k \left[R_k \cos \Phi_k^{d-1} - R_{k+1} \cos \Psi_{k+1}^{d-1} \right] \quad (2.8)$$

$$\Psi_{k+1}^l = \Phi_k^l, \quad l = 1, 2, \dots, d-2 \quad (2.9)$$

it follows that the first n segments of the path $\hat{p}(0, \infty, \Pi)$ are completely defined by the following $d(n+1)$ parameters

$$R_0, \Phi_0, \Phi_1, \Psi_1^{d-1}, \dots, \Phi_n, \Psi_n^{d-1}. \quad (2.10)$$

The following conditions on the parameters of the path are equivalent to the conditions of Proposition 2.2.1:

$$|\Phi_k^{d-1}| \leq |\Psi_k^{d-1}|, \quad |\Psi_k^{d-1}| \geq |\Phi_{k-1}^{d-1}|.$$

Transition probabilities

Theorem 2.3.1 *The sequence $\{(R_n, \Phi_n, \Psi_n)\}$ is a Markov chain in the state space $\mathbb{R}_+ \times \mathcal{A}$, where*

$$\mathcal{A} = \{(\phi, \psi) \in A \times A : 0 < |\phi^{d-1}| < |\psi^{d-1}|\}.$$

The transition probabilities are given by three components: by the conditional density of $\{\Phi_{n+1}, \Psi_{n+1}^{d-1}\}$ given $\{R_n = r_n, \Phi_n = \phi_n\}$

$$\begin{aligned} f(\phi, \psi^{d-1} | r_n, \phi_n) &= \exp\{-|B_{n+1} \setminus B_n|\} \times \\ &\times J_d(\phi) \left(\frac{r_n \sin |\phi_n^{d-1}|}{\sin |\psi^{d-1}|} \right)^d \frac{\cos \phi^{d-1} - \cos \psi^{d-1}}{\sin |\psi^{d-1}|} \end{aligned} \quad (2.11)$$

with the expression for $|B_{n+1} \setminus B_n|$ in (2.18), and by the equalities for R_{n+1} and Ψ_{n+1}^l , $1 \leq l \leq d-2$

$$R_{n+1} = \frac{r_n \sin |\phi_n^{d-1}|}{\sin |\Psi_{n+1}^{d-1}|} \quad (2.12)$$

$$\Psi_{n+1}^l = \phi_n^l, \quad l = 1, 2, \dots, d-2. \quad (2.13)$$

Proof. We start from deriving the distribution of parameters (2.10) of the first n segments of the path $\hat{p}(0, \infty, \Pi)$ from the distribution of the random vector $\{Z_0, Z_1, \dots, Z_n\}$ in $\mathbb{R}^{2(n+1)}$. From Proposition 2.2.1, it follows that this distribution admits a density with respect to the Lebesgue measure in $\mathbb{R}^{d(n+1)}$ given by

$$d(z_0, z_1, \dots, z_n) = \exp \left\{ - \left| \cup_{k=0}^n B_k \right| \right\} \prod_{k=1}^n \mathbb{1}_{D_k}(z_k). \quad (2.14)$$

Introduce the notation $p_n := (r_0, \phi_0, \phi_1, \psi_1, \dots, \phi_n, \psi_n)$, and consider the mapping $A : p_n \mapsto (z_0, z_1, \dots, z_n)$, defined by the following equations:

$$z_0 = r_0 s(\phi_0),$$

and for $k = 0, 1, \dots, n-1$,

$$\begin{aligned} z_{k+1}^1 &= r_{k+1} s^1(\phi_{k+1}) \\ z_{k+1}^2 &= r_{k+1} s^2(\phi_{k+1}) \\ &\dots \\ z_{k+1}^{d-1} &= r_{k+1} s^{d-1}(\phi_{k+1}) \\ z_{k+1}^d &= z_k^d + r_{k+1} (s^d(\phi_{k+1}) - s^d(\psi_{k+1})), \end{aligned}$$

with

$$r_{k+1} = r_0 \prod_{j=0}^k \frac{\sin |\phi_j^{d-1}|}{\sin |\psi_{j+1}^{d-1}|}.$$

According to (2.6–2.9),

$$(Z_0, Z_1, \dots, Z_n) = A(R_0, \Phi_0, \Phi_1, \Psi_1^{d-1}, \dots, \Phi_n, \Psi_n^{d-1}).$$

This mapping is a diffeomorphism between the two open subsets of $\mathbb{R}^{2(n+1)}$:

$$O = \{p_n : r_0 > 0, |\psi_k^{d-1}| > |\phi_k^{d-1}| > 0, |\psi_k^{d-1}| > |\phi_{k-1}^{d-1}| > 0, k = 1, 2, \dots, n\}$$

and

$$O' = \{z \in \mathbb{R}^{2(n+1)} : z_k \in D_k, z_k^d \neq 0, k = 1, 2, \dots, n\}.$$

Making in (2.14) the change of variables $(z_0, z_1, \dots, z_n) = A(p_n)$, we obtain the density $\bar{d}_n(p_n)$ of the path parameters (2.10). The Jacobian of the

mapping is equal to $\prod_{k=0}^n D_k(p_k)$, where

$$D_0(p_0) = J_d(\phi_0) (r_0)^{d-1}$$

$$D_k(p_k) = J_d(\phi_k) \left(r_0 \prod_{j=0}^k \frac{\sin |\phi_j^{d-1}|}{\sin |\psi_{j+1}^{d-1}|} \right)^d \frac{\cos \phi_k^{d-1} - \cos \psi_k^{d-1}}{\sin |\psi_k^{d-1}|},$$

and J_d is given by (2.4). It is easy to verify that $D_k \geq 0$ on the set O . Therefore,

$$\bar{d}_n(p_n) = \exp \left\{ -|\cup_{k=0}^n B_k| \right\} \prod_{k=0}^n D_k(p_k). \quad (2.15)$$

The conditional density $\bar{d}(\phi, \psi^{d-1} | p_n)$ of $(\Phi_{n+1}, \Psi_{n+1}^{d-1})$ given

$$\{R_0 = r_0, \Phi_0 = \phi_0, \Phi_k = \phi_k, \Psi_k^{d-1} = \psi_k^{d-1}, k = 1, 2, \dots, n\}$$

is equal to $\bar{d}_{n+1}(p_n, \phi, \psi^{d-1}) / \bar{d}_n(p_n)$. Since

$$(\cup_{k=0}^{n+1} B_k) \setminus (\cup_{k=0}^n B_k) = B_{n+1} \setminus B_n,$$

from (2.15) we obtain

$$\bar{d}(\phi, \psi^{d-1} | p_n) = \exp \left\{ -|B_{n+1} \setminus B_n| \right\} D_{n+1}(p_n, \phi, \psi^{d-1}). \quad (2.16)$$

Let us now calculate the volume of $B_{n+1} \setminus B_n$. The volume of the intersection of the unit ball $b(0, 1)$ with the half-space $\{x \in \mathbb{R}^d : x^d \leq \cos \alpha, \alpha \in (0, \pi]\}$ is given by

$$v(\alpha) := \frac{b_{d-1}}{d} \left((d-1) \int_{\alpha}^{\pi} \sin^{d-2} \theta d\theta + \cos \alpha \sin^{d-1} \alpha \right). \quad (2.17)$$

For $d = 2$ we have $v(\alpha) = \pi - \alpha + \sin \alpha \cos \alpha$; for $d = 3$ this results in $v(\alpha) = \frac{\pi}{3} \cos \alpha (2 + \sin^2 \alpha)$. In higher dimensions, the integral in (2.17) evaluates to (see e.g. [26])

$$\begin{aligned} \cos \alpha \sum_{i=0}^{(d-3)/2} \frac{(d-3)(d-5) \cdots (d-2i-1)}{(d-2)(d-4) \cdots (2-2i-2)} \sin^{d-2i-3} \alpha \\ + \frac{(d-3)!!}{(d-2)!!} [\mathbb{I}_{\{d \text{ odd}\}} + (\pi - \alpha) \mathbb{I}_{\{d \text{ even}\}}]. \end{aligned}$$

Using (2.17) and (2.7), we obtain

$$\begin{aligned} |B_{n+1} \setminus B_n| &= (r_n)^d (v(|\phi_n^{d-1}|) - b_d) + (r_{n+1})^d v(\pi - |\psi^{d-1}|) \\ &= (r_n)^d (v(|\phi_n^{d-1}|) - b_d) + \left(\frac{r_n \sin |\phi_n^{d-1}|}{\sin |\psi^{d-1}|} \right)^d v(\pi - |\psi^{d-1}|). \end{aligned} \quad (2.18)$$

Observe that the conditional density \bar{d} is a function of only ϕ , ψ^{d-1} , r_n , and ϕ_n . Indeed, as follows from (2.18), the volume of $B_{n+1} \setminus B_n$ depends only on r_n , ϕ_n^{d-1} , and ψ^{d-1} , whereas by (2.7),

$$D_{n+1}(p_n, \phi, \psi) = J_d(\phi) \left(\frac{r_n \sin |\phi_n^{d-1}|}{\sin |\psi^{d-1}|} \right)^d \frac{\cos \phi^{d-1} - \cos \psi^{d-1}}{\sin |\psi^{d-1}|}. \quad (2.19)$$

Hence, substitution of (2.18) and (2.19) into (2.16) gives the expression for transition density (2.11). Equality (2.12) follows from (2.7), and (2.13) from (2.9).

Remark 2.3.1 In the planar case ($d = 2$), the conditional density is defined in $\mathcal{A} = \{(\phi, \psi) \in [-\pi, \pi)^2 : 0 < |\phi| < |\psi|\}$ and is expressed as

$$\begin{aligned} f(\phi, \psi | r_n, \phi_n) &= (r_n \sin \phi_n)^2 \frac{\cos \phi - \cos \psi}{\sin^3 \psi} \times \\ &\times \exp \left\{ -(r_n \sin \phi_n)^2 (v(\psi) - v(\phi_n)) \right\} \mathbb{I}(|\psi| < |\phi_n|), \end{aligned} \quad (2.20)$$

where

$$v_2(y) := \frac{|y| - \sin |y| \cos |y|}{\sin^2 y}.$$

By Fubini's theorem, the conditional density (2.20) admits decomposition into a product of two conditional densities

$$f(\phi, \psi | r_n, \phi_n) = f_1(\phi | \psi) f_2(\psi | r_n, \phi_n), \quad (2.21)$$

where

$$f_1(\phi | \psi) = \frac{\cos \phi - \cos \psi}{2(\sin |\psi| - |\psi| \cos \psi)}, \quad \phi \in (-\psi, \psi); \quad (2.22)$$

$$f_2(\psi | r_n, \phi_n) = \frac{\partial}{\partial \psi} F(r_n, \phi_n, \psi), \quad |\psi| \in (\phi_n, \pi); \quad (2.23)$$

and

$$F(r_n, \phi_n, \psi) = -\frac{1}{2} \exp \left\{ -(r_n \sin \phi_n)^2 (v_2(\psi) - v_2(\phi_n)) \right\}. \quad (2.24)$$

This remark concludes the proof of Theorem 2.3.1.

2.4 Ergodic Properties and Stationary Distribution

It is clear even without detailed analysis of the transition probabilities that the Markov path $\hat{p}(0, \infty, \Pi)$ should inherit some ergodic properties of the embedding point process Π . In the present section we prove convergence to the equilibrium of the sequence of path segments and find its stationary distribution in the explicit form.

Consider the process $\mathcal{N} = \{T_n, n \in \mathbb{Z}\}$ of cell border crossings by the coordinate axis containing $[0, t]$. Since the generating Poisson process Π is stationary, the point process $\{T_n, n \in \mathbb{Z}\}$ is also stationary with respect to shifts along the line containing $[0, t]$. Its intensity λ_T can be obtained by inverting (1.3). The parametrization introduced in §2.3 extends naturally to the path $\hat{p}(0, -\infty, \Pi)$. Consider now a stationary marked point process $\mathcal{N}_M = \{(T_n, M_n), n \in \mathbb{Z}\}$ with the marks $\{M_n = (R_n, \Phi_n, \Psi_n), n \in \mathbb{Z}\}$ such that (R_n, Φ_n, Ψ_n) coincide with the parameters of $\hat{p}(0, \infty, \Pi)$ for $n \geq 0$, and with the parameters of $\hat{p}(0, -\infty, \Pi)$ for $n \leq 0$.

Proposition 2.4.1 *The process $\mathcal{N}_M = \{T_n, M_n\}$ is mixing (and hence, ergodic) with respect to the family of shifts $\{\theta_s, s \in \mathbb{R}\}$ along the line containing $[0, t]$.*

The following is an ergodic theorem for simple stationary point processes (see e.g. [15, Lemma 10.2.II and §12.4]).

Proposition 2.4.2 *Let $\{(T_n, M_n), n \in \mathbb{Z}\}$ be a stationary ergodic marked point process, and $n(t)$ the number of points of $\{T_k\}$ in the segment $[0, t]$. Then for all $\mathbf{P}_{\mathcal{N}}^0$ -measurable functions L of marks M_n ,*

$$\lim_{\|t\| \rightarrow \infty} \frac{1}{n(t)} \sum_{n=1}^{n(t)} L(M_n) = \mathbf{E}_{\mathcal{N}}^0 L(M_0) \quad a.s. \quad (2.25)$$

and

$$\lim_{\|t\| \rightarrow \infty} \frac{n(t)}{\|t\|} = \lambda_T \quad a.s.$$

Also, as $N \rightarrow \infty$,

$$\lim_{N \rightarrow \infty} \frac{1}{N} \sum_{n=1}^N L(M_n) = \mathbf{E}_{\mathcal{N}}^0 L(M_0) \quad a.s. \quad (2.26)$$

By Campbell’s theorem, the limits (2.25–2.26) exist as well in $\mathcal{L}_1(\Pi)$.

Remark 2.4.1 In addition, the mixing property of the process \mathcal{N}_M implies that for all bounded continuous functions L of marks M_n ,

$$\lim_{n \rightarrow \infty} \mathbf{E} L(M_n) = \mathbf{E}_{\mathcal{N}}^0 L(M_0),$$

(see [15, Theorem 12.4.IV]), i.e. that the distribution of M_n converges weakly to the Palm distribution of M_0 .

In particular, when $L(M_n) = R_n \|s(\Psi_n) - s(\Phi_n)\| \equiv \|Z_n - Z_{n-1}\|$, we have

$$\begin{aligned} \lim_{\|t\| \rightarrow \infty} \frac{1}{\|t\|} |\hat{p}(0, t, \Pi)| &= \lim_{\|t\| \rightarrow \infty} \frac{n(t)}{\|t\|} \frac{1}{n(t)} \sum_{n=1}^{n(t)} \|Z_n - Z_{n-1}\| = \lambda_T \mathbf{E}_{\mathcal{N}}^0 L_0 \quad \text{a.s.}, \\ \lim_{N \rightarrow \infty} \frac{1}{N} \sum_{n=1}^N \|Z_n - Z_{n-1}\| &= \mathbf{E}_{\mathcal{N}}^0 L_0, \quad \text{a.s.}, \end{aligned}$$

and

$$\lim_{n \rightarrow \infty} \mathbf{E} \|Z_n - Z_{n-1}\| = \mathbf{E}_{\mathcal{N}}^0 L_0.$$

The next result establishes the relation between the distribution of $\{M_n\}$ and that of the embedding process $\{(T_n, M_n)\}$.

Proposition 2.4.3 *Assume that the marks M_n , $n \geq 0$ of a stationary ergodic marked point process $\{(T_n, M_n), n \in \mathbb{Z}\}$ form a Markov chain. Then the Palm distribution $\mathbf{P}_{\mathcal{N}}^0$ of the marks is a stationary distribution $\pi(\cdot)$ of the Markov chain $\{M_n, n \geq 0\}$.*

Using this result, we derive a stationary distribution for our special case of $M_n = (R_n, \Phi_n, \Psi_n)$.

Theorem 2.4.1 *The stationary distribution $\pi(\cdot)$ of the Markov chain $\{(R_n, \Phi_n, \Psi_n), n \geq 0\}$ in the state space $\mathbb{R}_+ \times \mathcal{A}$ has the density*

$$\frac{1}{\lambda_T} J_d(\phi) J_d(\psi) (\cos \phi^{d-1} - \cos \psi^{d-1}) r^{2d-2} \exp\{-b_d r^d\}, \quad (2.27)$$

where λ_T is the intensity of the process $\mathcal{N} = \{T_n, n \in \mathbb{Z}\}$ of cell border crossings:

$$\lambda_T = \frac{2 \Gamma(d) \Gamma\left(2 - \frac{1}{d}\right) \left[\Gamma\left(\frac{d}{2} + 1\right)\right]^{(2d-1)/d}}{d \Gamma\left(d - \frac{1}{2}\right) \left[\Gamma\left(\frac{d+1}{2}\right)\right]^2}.$$

Remark 2.4.2 In particular, in the planar case ($d = 2$), the density of the stationary distribution of the Markov path becomes

$$\frac{\pi}{4}(\cos \phi - \cos \psi) r^2 e^{-\pi r^2}, \quad 0 \leq |\psi| \leq |\phi| \leq \pi. \quad (2.28)$$

The rest of the section contains the proofs of formulated statements.

Proof of Proposition 2.4.1. By definition, the process \mathcal{N}_M in $\mathbb{R} \times \mathbb{R}_+ \times \mathcal{A}$ is mixing if for any $A, B \in \mathcal{F}_{\mathcal{N}_M} = \mathcal{F}_{\mathcal{N}} \otimes \mathcal{B}(\mathbb{R}_+ \times \mathcal{A})$,

$$\mathbf{P}(\mathcal{N}_M \in A, \theta_t \mathcal{N}_M \in B) \rightarrow \mathbf{P}(\mathcal{N}_M \in A) \mathbf{P}(\mathcal{N}_M \in B) \quad \text{as } |t| \rightarrow \infty. \quad (2.29)$$

By construction, \mathcal{N}_M is a measurable transformation of the Poisson point process Π ; thus $\{\mathcal{N}_M \in A\}$ corresponds to $\{\Pi \in A'\}$ for some event $A' \in \mathcal{B}(\Pi)$. Moreover, $\theta_t \mathcal{N}_M \in A$ if and only if $\theta_t \Pi \in A'$. The proposition now follows from the mixing property of the Poisson process.

Proof of Proposition 2.4.3. Recall that $\theta_t \mathcal{N} = \{T_n - t\}_{n \in \mathbb{N}}$. The Palm probability is invariant with respect to the shift θ_{T_n} (see e.g. [3, Remark 3.2.1], and therefore

$$\mathbf{P}_{\mathcal{N}}^0(M_n \in \cdot) = \mathbf{P}_{\theta_{T_1} \mathcal{N}}^0(M_n \in \cdot) = \mathbf{P}_{\mathcal{N}}^0(M_{n+1} \in \cdot).$$

From the other hand, if $\mathbf{P}((r, \phi, \psi), \cdot)$ is the transition probability of the Markov chain $\{M_n = (R_n, \Phi_n, \Psi_n)\}$, then

$$\mathbf{P}_{\mathcal{N}}^0(M_{n+1} \in \cdot) = \mathbf{E}_{\mathcal{N}}^0 \mathbf{P}(M_{n+1} \in \cdot | M_n).$$

Therefore, $\mathbf{P}_{\mathcal{N}}^0$ is the stationary distribution of the chain $\{(R_n, \Phi_n, \Psi_n)\}$.

Proof of Theorem 2.4.1. As Proposition 2.4.3 shows, it is the Palm distribution of M_n that we are interested in. We start from finding the distribution density of $(T_1, R_1, \Phi_1, \Psi_1)$, and act as in the proof of Theorem 2.3.1: take the density (2.14) for (Z_0, Z_1) and make the change of variables

$$(z_0, z_1) \rightarrow (t_1, r_1, \phi_1, \psi_1),$$

with the mapping defined by (2.5). The Jacobian of the mapping has the form

$$r^{2d-2} \begin{vmatrix} 0 & \dots & 0 & 1 & 0 & \dots & 0 & 1 \\ s^1(\phi) & \dots & s^{d-1}(\phi) & s^d(\phi) & s^1(\psi) & \dots & s^{d-1}(\psi) & s^d(\psi) \\ \frac{\partial(s^1(\phi), \dots, s^d(\phi))}{\partial(\phi^1, \dots, \phi^{d-1})} & & & & & & 0 & \\ 0 & & & & & & \frac{\partial(s^1(\psi), \dots, s^d(\psi))}{\partial(\psi^1, \dots, \psi^{d-1})} & \end{vmatrix}.$$

Calculating it, we obtain the density of $(T_1, R_1, \Phi_1, \Psi_1)$:

$$c(t, r, \phi, \psi) = r^{2d-2} (\cos \phi^{d-1} - \cos \psi^{d-1}) \times \\ \times J_d(\phi) J_d(\psi) \exp\{-|B_0 \cup B_1|(t, r, \psi)\},$$

defined in the state space $\mathbb{R}_+^2 \times \mathcal{A}$.

To find the explicit form of the Palm probability, we use its local interpretation (see e.g. [3, §6.2]): for each Borel set $B \in \mathbb{R}_+ \times \mathcal{A}$,

$$\mathbf{P}_{\mathcal{N}}^0(M_1 \in B) = \lim_{h \downarrow 0} \mathbf{P}(M_1 \in B \mid T_1 \leq h).$$

Hence

$$\mathbf{P}_{\mathcal{N}}^0(M_1 \in B) = \lim_{h \downarrow 0} \frac{\int_{\mathbb{R}_+ \times \mathcal{A}} \int_0^h \mathbb{I}_B(r, \phi, \psi) c(t_1, r, \phi, \psi) dt_1 d(r, \phi, \psi)}{\int_{\mathbb{R}_+ \times \mathcal{A}} \int_0^h c(t_1, r, \phi, \psi) dt_1 d(r, \phi, \psi)}. \quad (2.30)$$

Since for each $t \geq 0$ and $(r, \phi, \psi) \in \mathbb{R}_+ \times \mathcal{A}$

$$c(t, r, \phi, \psi) \leq c(0, r, \phi, \psi) \\ = r^{2d-2} (\cos \phi^{d-1} - \cos \psi^{d-1}) J_d(\phi) J_d(\psi) \exp\{-b_d r^d\},$$

by the Dominated Convergence Theorem, the limit in (2.30) is equal to

$$\mathbf{P}_{\mathcal{N}}^0(M_1 \in B) = \frac{\int_{\mathbb{R}_+ \times \mathcal{A}} \mathbb{I}_B(r, \phi, \psi) c(0, r, \phi, \psi) d(r, \phi, \psi)}{\int_{\mathbb{R}_+ \times \mathcal{A}} c(0, r, \phi, \psi) d(r, \phi, \psi)}.$$

The denominator in the last expression equals

$$\lim_{h \downarrow 0} \mathbf{P}(T_1 \leq h)/h = \lambda_T.$$

This follows from Dobrushin's estimate (see e.g. [3, p. 39])

$$\mathbf{P}(T_1 \leq h) = \lambda_T h + o(h),$$

which can be obtained from the inversion formula of the Palm distribution. Therefore, evaluating the integral

$$\begin{aligned} & \int_{\mathbb{R}_+ \times \mathcal{A}} r^{2d-2} (\cos \phi^{d-1} - \cos \psi^{d-1}) J_d(\phi) J_d(\psi) \exp\{-b_d r^d\} d(r, \phi, \psi) \\ &= \frac{\Gamma\left(2 - \frac{1}{d}\right)}{b_d^{2-1/d} d} ((d-1)b_{d-1})^2 \times \\ & \times 2 \int_0^\pi \int_0^\psi \cos \phi^{d-1} (\sin \phi^{d-1})^{d-2} (\sin \psi^{d-1})^{d-2} d\phi^{d-1} d\psi^{d-1} \\ &= \frac{2\Gamma(d)\Gamma\left(2 - \frac{1}{d}\right) \left[\Gamma\left(\frac{d}{2} + 1\right)\right]^{(2d-1)/d}}{d\Gamma\left(d - \frac{1}{2}\right) \left[\Gamma\left(\frac{d+1}{2}\right)\right]^2} \end{aligned}$$

we obtain as a byside result the intensity of the process of cell border crossings $\lambda_T = \bar{L}^{-1}$ given by (1.3).

2.5 Path Length

For a non-negative measurable function $L : \mathbb{R}_+ \times \mathcal{A} \rightarrow \mathbb{R}$, by Campbell's formula,

$$\mathbf{E} \sum_k L(M_k) \mathbb{1}_{T_k \in [0, t]} = \lambda_T \|t\| \mathbf{E}_{\mathcal{N}}^0 L(M_0). \quad (2.31)$$

The path length is probably the most important of the characteristics which follows from (2.31). Obviously, we may consider other cost functions L of the marks M_k ; an example with power function is given below, in Corollary 2.5.2.

The following assertions follow from Theorem 2.4.1.

Corollary 2.5.1 *For each $s, t \in \mathbb{R}^d$*

$$\begin{aligned} \mathbf{E} |\hat{p}(s, t, \Pi)| &= \frac{\|s - t\|}{d \pi^d} \left[\Gamma\left(\frac{d}{2} + 1\right)\right]^2 \times \\ & \times \int_{\mathcal{A}} \|s(\phi) - s(\psi)\| J_d(\phi) J_d(\psi) (\cos \phi^{d-1} - \cos \psi^{d-1}) d\phi d\psi. \end{aligned}$$

In the planar case, the path length can be calculated explicitly.

Corollary 2.5.2 *For each $s, t \in \mathbb{R}^2$*

$$\mathbf{E} |\hat{p}(s, t, \Pi)| = \frac{4}{\pi} \|s - t\|.$$

If, more generally,

$$L(M_k) = \|Z_k - Z_{k-1}\|^\alpha, \quad \alpha > -1,$$

then

$$\mathbf{E} \sum_k L(M_k) \mathbb{1}_{T_k \in [0, t]} = \frac{4\|t\|}{\pi} \left(\frac{2}{\sqrt{\pi}} \right)^\alpha \Gamma \left(\frac{\alpha + 2}{2} \right). \quad (2.32)$$

Note that $J_d(\phi)$ is the density of the spherical angles of a point uniformly distributed on the surface of the unit ball $\partial b(0, 1)$. From here follows a simple interpretation of the expression in Corollary 2.5.1. Let S_1, S_2 be two independent random vectors, uniformly distributed on $\partial b(0, 1)$ in \mathbb{R}^d . Then

$$\mathbf{E} |\hat{p}(s, t, \Pi)| = c \|s - t\| \cdot \mathbf{E} [\|S_1 - S_2\| \|S_1^d - S_2^d\|],$$

where

$$c = \frac{2\pi^{d-2}}{d} \left[\Gamma \left(\frac{d}{2} + 1 \right) \right]^2.$$

This representation provides a basis for numerical simulations. A program written in C (the source is available from the author) calculated the expression in Corollary 2.5.1 by the Monte-Carlo method. The results of a numerical experiment producing 10^7 iterations of vectors S_1 and S_2 are grouped in Table 2.1.

Dim	3	4	5	6	7	8	9	10
Length	1.499	1.698	1.874	2.040	2.178	2.352	2.478	2.669

Table 2.1: Simulation results for the relative path length $\mathbf{E} |\hat{p}(s, t, \Pi)| / \|s - t\|$ in higher dimensions.

The mean path length $\mathbf{E} |\hat{p}(s, t, \Pi)|$ does not depend on the intensity of the generating Poisson process: for the process of the intensity λ , the typical segment length is scaled by $\lambda^{-1/d}$, while the intensity of the process \mathcal{N} is multiplied by $\lambda^{1/d}$.

The next results show that the Markov paths defined in §2.2 are asymptotically equivalent in approximating the Euclidean distance in the mean.

Theorem 2.5.1 *The mean lengths of the paths $\hat{p}(s, t, \Pi)$ and $\hat{p}(s, t, \Pi')$ differ by at most a constant, i.e.*

$$\left| \mathbf{E} |\hat{p}(s, t, \Pi)| - \mathbf{E} |\hat{p}(s, t, \Pi')| \right| < C, \quad (2.33)$$

where C depends only on the intensity of the underlying Poisson process.

Proof. Assume that the paths $\hat{p}(s, t, \Pi)$ and $\hat{p}(s, t, \Pi')$ are defined in the same probability space. Our proof bases on the following fact: if

$$\hat{p}(s, t, \Pi') = \{s, Z'_1, Z'_2, \dots, Z'_n, t\}, \quad (2.34)$$

then $\{Z'_1, Z'_2, \dots, Z'_n\}$ is a subpath of $\hat{p}(s, t, \Pi)$. In order to verify this, denote

$$B(x, y) = b(T(x, y), \|x - T(x, y)\|).$$

From (2.34) it follows that no point of Π lies in the interior of the balls

$$B(s, Z'_1), B(Z'_n, t), B(Z'_i, Z'_{i+1}), \quad i = 1, 2, \dots, n-1.$$

Hence the points $T(s, Z'_1)$, $T(Z'_n, t)$, and $T(Z'_i, Z'_{i+1})$, $i = 1, 2, \dots, n-1$ on the segment $[s, t]$ belong, respectively, to the closures of the Voronoi cells $C(Z'_1)$, $C(Z'_n)$, and $C(Z'_i)$, $i = 1, 2, \dots, n-1$. Consequently, the nuclei of these cells belong to $\hat{p}(s, t, \Pi)$.

Define a family of regions in \mathbb{R}^d as follows:

$$\begin{aligned} S_1(s, t, Z) &= b(s, \|s - Z\|) \cup b(t, \|t - Z\|) \cup B(s, t) \\ S_2(s, t, Z, Z') &= b(s, \|s - Z\|) \cup b(t, \|t - Z'\|) \cup B(s, t) \\ S_3(s, t, Z) &= B(s, Z) \cup B(t, Z) \\ S_4(s, t, Z, Z') &= B(s, Z) \cup B(t, Z'). \end{aligned}$$

Consider the following events, which form a partition of the probability space (see Figure 2.3):

$$\begin{aligned} E_1 &= \{\exists Z \in \Pi : \Pi(S_1(s, t, Z)) = 0\} \\ E_2 &= \{\exists Z, Z' \in \Pi : Z \neq Z' \text{ and } \Pi(S_2(s, t, Z, Z')) = 0\} \\ E_3 &= \{\exists Z \in \Pi \cap B(s, t) : \Pi(S_4(s, t, Z)) = 0\} \\ E_4 &= \{\exists Z, Z' \in \Pi \cap B(s, t) : Z \neq Z' \text{ and } \Pi(S_3(s, t, Z, Z')) = 0\}. \end{aligned}$$

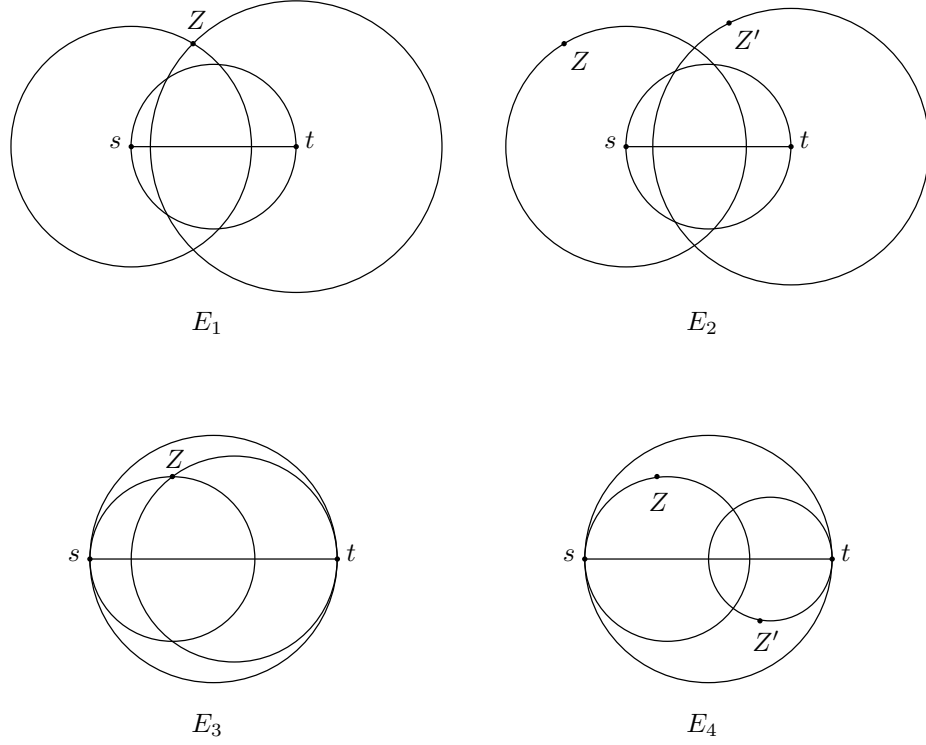


Figure 2.3: Events E_1 – E_4 form a partition of the probability space.

The events E_1 and E_2 imply that $|\hat{p}(s, t, \Pi)| = \|s - t\|$. On E_1 , the points s and t belong to the Voronoi cell with the nucleus Z , and $|\hat{p}(s, t, \Pi)| = 0$. On E_2 , if some point $Z'' \in \hat{p}(s, t, \Pi)$, then $\Pi(b(v, \|v - Z''\|)) = 0$ for some $v \in [s, t]$, and thus

$$\|v - Z''\| \leq \min\{\|v - Z\|, \|v - Z'\|\} \leq \min\{\|t - Z\|, \|s - Z'\|\}.$$

This implies that all vertices of the path $\hat{p}(s, t, \Pi)$ lie in the figure

$$b(T(s, t), r(s, t, Z, Z')) \setminus S_2(s, t, Z, Z'), \quad (2.35)$$

where

$$r(s, t, Z, Z') = \|s - Z\| + \frac{3}{2}\|s - t\| + \|t - Z'\|.$$

On E_3 , $\hat{p}(s, t, \Pi) = \{s, Z, t\}$ and the common part for both paths consists of a single point Z . Moreover, for E_3 , the remaining two parts of $\hat{p}(s, t, \Pi)$

lie in the closure of

$$(b(s, \|s - Z\|) \cup b(t, \|t - Z\|)) \setminus S_3(s, t, Z), \quad (2.36)$$

whereas the remaining parts of $\hat{p}(s, t, \Pi')$ are just two segments $[s, Z]$ and $[t, Z]$. Situation is similar for E_4 , when both paths coincide between the points Z and Z' , the remaining two parts of $\hat{p}(s, t, \Pi)$ lie in the closure of

$$(b(s, \|s - Z\|) \cup b(t, \|t - Z'\|)) \setminus S_4(s, t, Z, Z'), \quad (2.37)$$

and the remaining parts of $\hat{p}(s, t, \Pi')$ are $[s, Z]$ and $[t, Z']$.

Note that due to the independence property of the Poisson process, the conditional distribution of Π in the interior of the domains (2.35–2.37) on the events E_2 – E_4 , respectively, is the same as the unconditional one.

For any open Borel set $B \in \mathbb{R}^d$ of diameter δ , the expectation of the maximal length of a path constructed on the vertices of the Poisson–Delaunay graph containing in B is less than $\delta \cdot \mathbf{E}(\Pi(B) - 1) < \lambda b_d 2^d \delta^{d+1}$.

Now, to estimate the expectation of

$$D(s, t) = \left| \mathbf{E} |\hat{p}(s, t, \Pi)| - \mathbf{E} |\hat{p}(s, t, \Pi')| \right|,$$

we make use of this fact and the total probability formula

$$\mathbf{E} [D(s, t) | E_4, Z = z, Z' = z'] \leq K(s, t, z, z'),$$

where

$$K(s, t, z, z') = \lambda b_d 2^d (\|z - s\|^{d+1} + \|z - s\|^{d+1}) + \|z - s\| + \|z' - t\|.$$

Similarly, in the case of E_3 , when the common path consists of a single point,

$$\mathbf{E} [D(s, t) | E_4, Z = z] \leq K(s, t, z, z).$$

The point Z from E_1 has a density $f(z | E_1)$. In Cartesian coordinates

$$f(z | E_1) \mathbf{P}(E_1) = \lambda \exp \{-\lambda |S_1(s, t, z)|\} \mathbb{I}_{\mathbb{R}^2 \setminus B(s, t)}(z).$$

Similar densities exist in the cases of E_2 – E_4 . Summarizing the above results, we have

$$\begin{aligned} \mathbf{E} D(s, t) &\leq \int \lambda \|s - t\| \exp \{-\lambda |S_1(s, t, z)|\} dz \\ &+ \int \lambda^3 b_d 2^d r^{d+1}(s, t, z, z') \exp \{-\lambda |S_2(s, t, z, z')|\} dz dz' \\ &+ \int \lambda^2 K(s, t, z, z') \exp \{-\lambda |S_4(s, t, z, z')|\} dz dz' \\ &+ \int \lambda K(s, t, z, z) \exp \{-\lambda |S_3(s, t, z)|\} dz. \end{aligned}$$

The first two integrals vanish as $\|s - t\|$ becomes large. The second two are bounded by constants. Hence, $\mathbf{E} D(s, t)$ is bounded by a constant, which depends only on λ .

2.6 Convergence of Transition Probabilities

As noted in Remark 2.4.1, the mixing property of the embedding Poisson point process Π guarantees weak convergence of the Markov chain $M_n = (R_n, \Phi_n, \Psi_n)$, $n \geq 0$ to its stationary distribution π . In this section we will use the explicit form of the transition probabilities of the chain derived in Theorem 2.3.1, and examine more closely its limiting behavior. We will be interested in convergence rate and its uniformity with respect to the starting point as well as in the uniqueness of the stationary distribution. We will test the chain for various forms of convergence by verifying mean drift conditions and invoking different forms of the Foster–Lyapunov criterion.

Several modifications of the Foster–Lyapunov criterion and related formalism are described in [41]. Roughly speaking, for a Markov chain $\{X_n\}$ in the state space \mathbf{X} , the criterion relies on the existence of a “basin of attraction” $C \subset \mathbf{X}$, and a test function $\mathbf{V} : \mathbf{X} \rightarrow \mathbb{R}_+$ such that the mean drift function

$$\Delta \mathbf{V}(x) = \mathbf{E} [\mathbf{V}(X_{n+1}) | X_n = x] - \mathbf{V}(x)$$

is bounded on C , and negative on $\mathbf{X} \setminus C$.

Before formulating the main result of this section, we need to introduce the definition of \mathbf{V} -uniform ergodicity. For a function $\mathbf{V} : \mathbf{X} \rightarrow [1, \infty)$, consider the norm of a probability measure \mathbf{P}

$$\|\mathbf{P}\|_{\mathbf{V}} = \sup_{g : |g| \leq \mathbf{V}} \int g(x) \mathbf{P}(dx).$$

(For $\mathbf{V} \equiv 1$ this is just the total variation norm.) Now define the \mathbf{V} -norm distance between two transition probabilities $\mathbf{P}_1(x, \cdot)$ and $\mathbf{P}_2(x, \cdot)$ as follows:

$$\|\mathbf{P}_1 - \mathbf{P}_2\|_{\mathbf{V}} = \sup_{x \in \mathbf{X}} \frac{|\mathbf{P}_1(x, \cdot) - \mathbf{P}_2(x, \cdot)|_{\mathbf{V}}}{\mathbf{V}(x)}. \quad (2.38)$$

Definition 2.6.1 (Meyn & Tweedie) *An ergodic Markov chain X_n with the n -step transition probabilities $\mathbf{P}^n(x, \cdot)$ and the stationary distribution $\pi(\cdot)$ is called \mathbf{V} -uniformly ergodic if*

$$\lim_{n \rightarrow \infty} \|\mathbf{P}^n - \pi\|_{\mathbf{V}} = 0.$$

The aim of the section is to prove the following statement, which we formulate, for simplicity, for the Markov chain in two dimensions.

Theorem 2.6.1 *The Markov chain $M_n = (R_n, \Phi_n, \Psi_n)$, $n \geq 0$ in the plane is regular, positive Harris recurrent, and \mathbf{V} -uniformly ergodic for the function \mathbf{V} defined in (2.44).*

This implies that for some positive constants C and $\rho < 1$, for \mathbf{V} defined in (2.44), and for the stationary distribution π given by (2.28),

$$\|\mathbf{P}^n - \pi\|_{\mathbf{V}} \leq C\rho^n.$$

Various limit theorems hold for \mathbf{V} -uniformly ergodic chains; see e.g. [41, Theorem 17.0.1], which formulates the Central Limit Theorem, the Law of Large Numbers, and the Law of the Iterated Logarithm for functions having the form $S_n(L) = \sum_{k=1}^n L(M_k)$.

The proof of Theorem 2.6.1 is divided into several lemmas. The first one shows that the chain is irreducible with respect to the Lebesgue measure on $\mathbb{R}_+ \times \mathcal{A}$.

Lemma 2.6.1 *The chain $\{(R_n, \Phi_n, \Psi_n)\}$ is ψ -irreducible.*

Proof. The assertion of the Lemma follows from the definition of ψ -irreducibility (see [41, p. 89]) and the following fact: if B is Borel subset of $\mathbb{R}_+ \times \mathcal{A}$ of positive Lebesgue measure, the two-step transition probability $\mathbf{P}^2((r, \phi, \psi), B)$ considered as a function of (r, ϕ, ψ) is strictly positive in $\mathbb{R}_+ \times \mathcal{A}$.

To prove this fact, we use the following form of the two-step transition probability

$$\begin{aligned} \mathbf{P}^2((r, \phi, \psi), B) &= \int_{\mathcal{A} \times \mathcal{A}} \mathbb{I}_B(r_2, \phi_2, \psi_2) f(\phi_2, \psi_2 | r_1, \phi_1) \times \\ &\quad \times f(\phi_1, \psi_1 | r, \phi) d\phi_2 d\psi_2 d\phi_1 d\psi_1, \end{aligned} \quad (2.39)$$

where f is defined in (2.20), and where

$$r_1 = r \left| \frac{\sin \phi}{\sin \psi_1} \right|, \quad \text{and} \quad r_2 = r \left| \frac{\sin \phi \sin \phi_1}{\sin \psi_1 \sin \psi_2} \right|. \quad (2.40)$$

For each $(\bar{r}_2, \bar{\phi}_2, \bar{\psi}_2)$ in the interior of $B \in \mathcal{B}(\mathbb{R}_+ \times \mathcal{A})$ and for each (r, ϕ, ψ) there exists $(\bar{\phi}_1, \bar{\psi}_1) \in \mathcal{A}$ such that

$$\bar{r}_2 = r \left| \frac{\sin \phi \sin \bar{\phi}_1}{\sin \bar{\psi}_1 \sin \bar{\psi}_2} \right|,$$

and in addition,

$$|\bar{\psi}_1| > |\phi|, \quad |\bar{\psi}_1| > |\bar{\phi}_1|, \quad |\bar{\phi}_1| < |\bar{\psi}_2|.$$

The indicator function in (2.39) is non-zero in some neighborhood of $(\bar{\phi}_2, \bar{\psi}_2)$. Also the product of the densities under the integral is positive in some neighborhood of $(\bar{\phi}_1, \bar{\psi}_1, \bar{\phi}_2, \bar{\psi}_2)$. Thus the integral in (2.39) is positive for every $(r, \phi, \psi) \in \mathbb{R}_+ \times \mathcal{A}$.

Recall the following definition (see [41, p. 106]).

Definition 2.6.2 *A set $C \subset \mathsf{X}$ is called ν -small for the chain X_n , if there exists a non-trivial measure ν such that for each $B \in \mathcal{B}(\mathbb{R}_+ \times \mathcal{A})$,*

$$\inf_{x \in C} \mathbf{P}^n(x, B) \geq \nu(B).$$

Lemma 2.6.2 *Define the set C_M of $(r, \phi, \psi) \in \mathbb{R}_+ \times \mathcal{A}$ such that for some $M > 0$,*

$$r > M, \quad r \sin |\phi| \leq M, \quad |\phi| \leq \pi/2 \quad \text{or} \quad r \leq M. \quad (2.41)$$

There exist non-trivial measures ν_i such that C_M is ν_i -small for $i \geq 3$.

Proof. For every $B^0 \in \mathcal{B}(\mathbb{R}_+ \times \mathcal{A})$ and $i \geq 3$,

$$\inf_{C_M} \mathbf{P}^i((r, \phi, \psi), B) \geq \inf_{C_M} \mathbf{P}((r, \phi, \psi), B^0) \left[\inf_{B^0} \mathbf{P}((r, \phi, \psi), B) \right]^{i-1}. \quad (2.42)$$

Consider

$$B^0 = \{(r, \phi, \psi) \in [2M, 3M] \times [\pi/11, \pi/10] \times [\alpha_1, \alpha_2]\},$$

where

$$\alpha_1 = \pi - \arcsin \frac{r \sin |\phi|}{2M}, \quad \alpha_2 = \pi - \arcsin \frac{r \sin |\phi|}{3M}.$$

First, we will show that for this special set B_0 and for some $\delta > 0$,

$$\inf_{C_M} \mathbf{P}((r, \phi, \psi), B^0) \geq \delta. \quad (2.43)$$

Note that $\max\{\pi/2, |\phi|\} < \alpha_1 < \alpha_2$. Next, use the decomposition of transition probability (2.21). From (2.22) it follows that when $\psi > \pi/2$, for some $\delta_1 > 0$ we have

$$\mathbf{P}(\Phi_n \in [\pi/11, \pi/10] \mid \Psi_n = \psi) > \delta_1.$$

Using (2.23) and (2.24), we verify that for $(r, \phi, \psi) \in C_M$ and some $\delta_2 > 0$,

$$\begin{aligned} \mathbf{P} \{ \Psi_{n+1} \in [\alpha_1, \alpha_2] \mid R_n = r, \Phi_n = \phi \} &= F(r, \phi, \alpha_1) - F(r, \phi, \alpha_2) \\ &\geq \frac{1}{2} e^{-5\pi M^2} (1 - e^{-\pi M^2}) > \delta_2. \end{aligned}$$

From here follows (2.43) with $\delta = \delta_1 \delta_2$.

The distribution $\mathbf{P}^i((r, \phi, \psi), B)$ does not depend on ψ , as can be easily seen from (2.20). As we have shown in the proof of Lemma 2.6.1, for each $i \geq 2$, it is a positive function of (r, ϕ) if only $|B| > 0$. Actually, a stronger fact holds: this distribution admits a conditional density $\gamma^i(r_1, \phi_1, \psi_1 \mid r, \phi)$ with respect to the Lebesgue measure in $\mathbb{R}_+ \times \mathcal{A}$. This density can be constructed by a change of variables in (2.14) in the same way as in the proof of Theorem 2.3.1. Choose a closed neighborhood U of (r_1, ϕ_1, ψ_1) in $\mathbb{R}_+ \times \mathcal{A}$ such that γ^i is strictly positive and continuous in $B^0 \times U$. Then, for some $\delta' > 0$,

$$\inf_{B^0} \mathbf{P}^i((r, \phi, \psi), U) \geq |U| \inf_{B^0 \times U} \gamma^i(r_1, \phi_1, \psi_1 \mid r, \phi) \geq \delta' |U|.$$

As it now follows from (2.42) and (2.43), a non-trivial minorizing measure for \mathbf{P}^i can be taken proportional to the Lebesgue measure restricted to the set U :

$$\nu_i(B) = \delta \delta' \int_{\mathbb{R}_+ \times \mathcal{A}} \mathbb{I}_{B \cap U}(r, \phi, \psi) d(r, \phi, \psi).$$

Recall the definition of aperiodicity from [41, p. 118]. From Lemma 2.6.2 immediately follows the next assertion.

Lemma 2.6.3 *The Markov chain $\{(R_n, \Phi_n, \Psi_n)\}$ is aperiodic.*

Let $\mathbf{V} : \mathbb{R}_+ \times \mathcal{A} \rightarrow \mathbb{R}_+$ be a measurable function. Denote

$$\mathbf{P}\mathbf{V}(r, \phi, \psi) = \mathbf{E} [\mathbf{V}(R_{n+1}, \Phi_{n+1}, \Psi_{n+1}) \mid R_n = r, \Phi_n = \phi, \Psi_n = \psi].$$

The mean drift function Δ is thus given by

$$\Delta \mathbf{V}(r, \phi, \psi) = \mathbf{P}\mathbf{V}(r, \phi, \psi) - \mathbf{V}(r, \phi, \psi).$$

Lemma 2.6.4 (Geometrical drift towards C_M) *For the function*

$$\mathbf{V}(r, \phi, \psi) = \max\{ r \sin |\phi/2|, 1 \} \tag{2.44}$$

defining a mapping from $\mathbb{R}_+ \times \mathcal{A}$ to $[1, \infty)$ there exist the constants $\beta, M > 0$, and $b < \infty$ such that

$$\Delta \mathbf{V}(r, \phi, \psi) \leq -\beta \mathbf{V}(r, \phi, \psi) + b \mathbb{I}_{C_M}(r, \phi, \psi).$$

Proof. We have

$$\begin{aligned} \mathbf{PV}(r, \phi, \psi) &\leq \mathbf{E} \left[R_{n+1} \sin |\Phi_{n+1}/2| \mid R_n = r, \Phi_n = \phi \right] + 1 \\ &= \mathbf{E} \left[R_{n+1} \mathbf{E} \left[\sin |\Phi_{n+1}/2| \mid \Psi_{n+1} \right] \mid R_n = r, \Phi_n = \phi \right] + 1. \end{aligned}$$

Using the conditional density (2.22), we verify that

$$\mathbf{E} \left[\sin |\Phi_{n+1}/2| \mid \Psi_{n+1} = \psi_1 \right] < |\psi_1|/5.$$

Therefore,

$$\begin{aligned} \mathbf{PV}(r, \phi, \psi) &\leq \mathbf{E} \left[R_{n+1} \cdot |\Psi_{n+1}|/5 \mid R_n = r, \Phi_n = \phi \right] + 1 \\ &= 2 \int_{|\phi|}^{\pi} \frac{r \sin |\phi|}{\sin |\psi_1|} \cdot \frac{\psi_1}{5} \cdot \frac{\partial}{\partial \psi_1} F(r, \phi, \psi_1) d\psi_1 + 1. \end{aligned} \tag{2.45}$$

First, suppose that $(r, \phi, \psi) \in C_M$ and let us show that $\mathbf{PV}(r, \phi, \psi)$ is bounded by a constant. If $r \leq M$ and $|\phi| > \pi/2$, then from (2.45) we have

$$\begin{aligned} \mathbf{PV}(r, \phi, \psi) &\leq \frac{\pi}{5} \mathbf{E} \left[R_{n+1} \mid R_n = r, \Phi_n = \phi \right] + 1 \\ &\leq \frac{\pi}{5} (2r + \mathbf{E} \left[R_{n+1} \mathbb{I}\{R_{n+1} > 2R_n\} \mid R_n = r, \Phi_n = \phi \right]) + 1 \\ &\leq \frac{2\pi M}{5} + \frac{\pi}{5} \int_{2r}^{\infty} \mathbf{P}(R_{n+1} > x \mid R_n = r, \Phi_n = \phi) dx + 1. \end{aligned} \tag{2.46}$$

From the geometrical viewpoint, the inequalities $|\phi| > \pi/2$ and $R_{n+1} > x > 2R_n$ imply that a disc of radius $x/2$ can be inscribed in the domain $B_{n+1} \setminus B_n$ containing no points of Π . Hence, the probability in the last integral of (2.46) does not exceed $\exp(-x^2/4)$, and

$$\mathbf{PV}(r, \phi, \psi) \leq \frac{\pi}{5} (2M + 1) + 1 \quad \text{for } (r, \phi, \psi) \in C_M, \quad |\phi| > \pi/2. \tag{2.47}$$

Now let $|\phi| \leq \pi/2$. Since $\psi_1/\sin \psi_1 \leq \pi/2$ for $\psi_1 \in (0, \pi/2]$, from (2.45) we have

$$\begin{aligned} \mathbf{PV}(r, \phi, \psi) &\leq \frac{\pi r \sin |\phi|}{10} + 1 \\ &+ \pi \mathbf{E} \left[R_{n+1} \mathbb{I}\{\Psi_{n+1} > \pi/2, R_{n+1} \leq M\sqrt{2}\} \mid R_n = r, \Phi_n = \phi \right] \\ &+ \pi \mathbf{E} \left[R_{n+1} \mathbb{I}\{\Psi_{n+1} > \pi/2, R_{n+1} > M\sqrt{2}\} \mid R_n = r, \Phi_n = \phi \right] \\ &\leq \frac{\pi M}{10} + \pi M\sqrt{2} + \pi \int_{M\sqrt{2}}^{\infty} \mathbf{P}(R_{n+1} > x \mid R_n = r, \Phi_n = \phi) dx + 1. \end{aligned}$$

By the same geometrical considerations as in (2.46), the probability under the integral does not exceed $\exp(-x^2/4)$, and

$$\mathbf{PV}(r, \phi, \psi) \leq \pi(M/10 + M\sqrt{2} + 1) + 1 \quad \text{for } (r, \phi, \psi) \in C_M, \quad |\phi| \leq \pi/2. \quad (2.48)$$

Now suppose that $(r, \phi, \psi) \in C_M^c$. Integrating (2.45) by parts, we get

$$\mathbf{PV}(r, \phi, \psi) \leq \frac{r|\phi|}{5} + I(r, \phi),$$

where

$$I(r, \phi) = - \int_{|\phi|}^{\pi} \frac{r \sin |\phi|}{5} \left(\frac{\psi_1}{\sin \psi_1} \right)' F(r, \phi, \psi_1) d\psi_1 + 1.$$

Then

$$\Delta \mathbf{V}(r, \phi, \psi) \leq r \sin |\phi/2| \left(\frac{|\phi|}{5 \sin |\phi/2|} - 1 \right) + I(r, \phi). \quad (2.49)$$

Using (2.12), (2.23), and (2.24), we note that

$$I(r, \phi) = \mathbf{E} \left[\frac{1}{10R_{n+1}} \mid R_n = r, \Phi_n = \phi \right] + 1.$$

As follows from (2.7),

$$R_{n+1} \geq \begin{cases} R_n & \text{if } |\phi| \leq \pi/2, \\ R_n \sin \Phi_n & \text{else.} \end{cases}$$

Therefore, $I(r, \phi) \leq 1/(10M) + 1$. Also in (2.49) for all ϕ ,

$$\left(\frac{|\phi|}{5 \sin |\phi/2|} - 1 \right) \leq -\frac{3}{10},$$

and thus we have

$$\Delta \mathbf{V}(r, \phi, \psi) \leq -\frac{3}{10} r \sin |\phi/2| + \frac{1}{10M} + 1.$$

Put $M = 20$. Then, for all $(r, \phi, \psi) \in C_M^c$,

$$\mathbf{V}(r, \phi, \psi) = r \sin |\phi/2| \geq \frac{M}{2} = 10,$$

and therefore

$$\Delta \mathbf{V}(r, \phi, \psi) \leq -\frac{1}{10} \mathbf{V}(r, \phi, \psi), \quad (r, \phi, \psi) \in C_M^c. \quad (2.50)$$

From (2.47), (2.48), and (2.50) follows the statement of the lemma with

$$M = 20, \quad \beta = -\frac{1}{10}, \quad b = 100.$$

Proof of Theorem 2.6.1. The assertion of Theorem 2.6.1 results from different modifications of the Foster–Lyapunov criteria. Let us summarize the properties of the test function \mathbf{V} defined in (2.44) and the test set C_M defined in (2.41). By Lemma 2.6.2, the set C_M is small. The function \mathbf{V} is finite everywhere and bounded on C_M . By Lemma 2.6.4, the condition of geometrical (and hence, uniform) drift towards a small set is satisfied. Moreover, by Lemma 2.6.1, the chain $\{(R_n, \Phi_n, \Psi_n)\}$ is ψ -irreducible, and by Lemma 2.6.3, aperiodic.

Therefore, by [41, Th.11.3.4], the chain $\{(R_n, \Phi_n, \Psi_n)\}$ is Harris recurrent and admits an invariant probability measure. This theorem uses the broader concept of a *petite* set; it is easy to see from the definition [41, p. 121] that every small set is petite. By [41, Th.11.3.15], the chain is regular. From [41, Th.16.1.2] it follows that the chain is \mathbf{V} -uniformly ergodic and that the transition probabilities $\mathbf{P}^n((r, \phi, \psi), \cdot)$ converge with geometric rate to the invariant probability measure in the special metric (2.38) induced by \mathbf{V} .

2.7 Other Short Paths on the Delaunay Graph

The shortest path Since each realization of Π is locally finite, for each pair of points x_i, x_j there exists the *shortest path* $p^*(x_i, x_j)$. We call the quantity $|p^*(x_i, x_j)|$ the *Delaunay distance* between x_i and x_j . In [30] it was shown that in the Euclidean plane, for an arbitrary vertex set, the ratio *Delaunay distance/Euclidean distance* does not exceed $2\pi/(3\cos(\pi/6)) \approx 2.42$. On the other hand, the example constructed in [14] shows that this ratio can be arbitrarily close to $\pi/2 \approx 1.57$. Since then it is a standing conjecture that $\pi/2$ is indeed the *worst case*, i.e. that there always exists a path $\pi/2$ -approximating the distance between its endpoints. As can be seen from Corollary 2.5.2, for the Delaunay graphs generated by an homogeneous Poisson process, the asymptotic value of the above ratio is bounded by $4/\pi \approx 1.27$, which is far less than $\pi/2$.

Let s and t be two fixed points. Denote by $p^*(s, t, \Pi)$ the shortest path between the two vertices of Π which are the closest to s and t , respectively.

The family of paths $\{p^*(s, t, \Pi)\}_{s, t}$ is *subadditive*: for any three collinear points s, v, t such that $v \in [s, t]$,

$$|p^*(s, t, \Pi)| \leq |p^*(s, v, \Pi)| + |p^*(v, t, \Pi)|.$$

Therefore, by Kingman's subadditive theorem (see e.g. [33]), the finite limit

$$\kappa(p^*) = \lim_{\|t\| \rightarrow \infty} \frac{1}{\|t\|} |p^*(0, t, \Pi)| \quad (2.51)$$

exists a.s. and in the mean. In other words, the class of shortest paths on the Poisson–Delaunay graph asymptotically $\kappa(p^*)$ -approximates the Euclidean distance.

Obviously, if some particular family of paths provides a κ -approximation to the Euclidean distance, then κ is an upper bound for $\kappa(p^*)$. By Proposition 2.4.2,

$$\kappa(\hat{p}) = \lim_{\|t\| \rightarrow \infty} \frac{1}{\|t\|} |\hat{p}(0, t, \Pi)| \quad \text{a.s. and in } \mathcal{L}_1(\Pi).$$

As Corollary 2.5.2 shows, in the plane $\kappa(p^*) \leq 4/\pi$; in higher dimensions numerical bounds for $\kappa(p^*)$ are listed in Table 2.1 on page 56.

The value of $\kappa(\hat{p})$ also facilitates the computation of the shortest path itself. Indeed all the paths between x_i and x_j of length smaller than $|\hat{p}(x_i, x_j)|$ lie within the ellipsoid \mathcal{E} defined by the focuses x_i, x_j , and the larger semi-axis $|\hat{p}(x_i, x_j)|/2$. Since Π is stationary and has intensity 1, the number of vertices of this graph has the order of $|\mathcal{E}|$. For each realization, the number of points of Π in \mathcal{E} is finite, and hence, one of the algorithms for finding the shortest path on a finite graph (see e.g. [23]) can be applied to the restriction of the Delaunay graph to the domain \mathcal{E} .

First-passage percolation The constant $\kappa(p^*)$ corresponds to the so-called *time constant* arising in first-passage percolation models. In these models a non-negative variable, the *passage time*, is associated with each edge of an infinite connected graph. The passage time along a path on the graph is the sum of the passage times of all the edges belonging to this path.

In many models, under appropriate conditions, the limit (2.51) exists, and the shortest path length corresponds to the minimal passage time between the vertices of the graph which are the closest to s and t . If the vertex set is given by a Poisson process, and if the edge set includes the edges of the Delaunay triangulation, then the Markov path may be useful for obtaining an upper bound for the time constant.

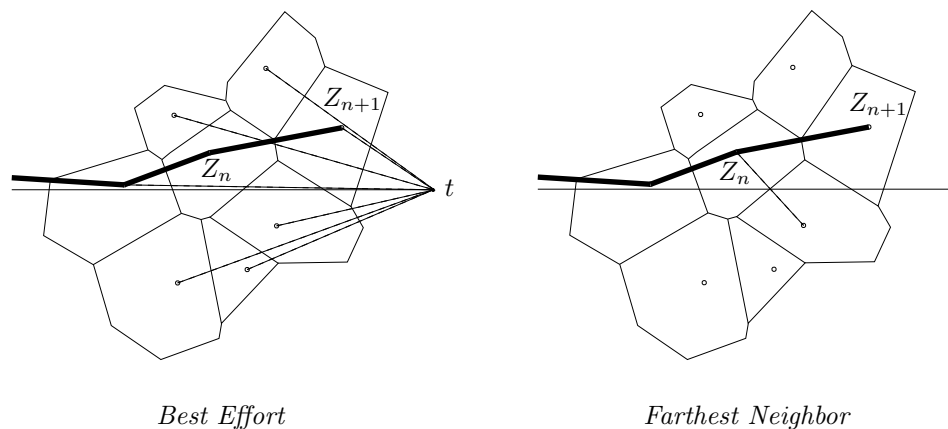


Figure 2.4: Modifications of the Markov path algorithm.

As an illustration, consider the planar first-passage percolation model on the Poisson–Delaunay graph, where the passage times along the edges are independent random variables $\{\tau_i\}$ with common distribution function F . As shown in [60], the time constant is finite in this model if and only if $\int_0^\infty [1 - F(t)]^3 dt < \infty$. Replacing in (2.31) the marks $L(M_k)$ by the passage times τ_k and using the fact that $\lambda_T = 4\sqrt{\lambda}/\pi$, we immediately obtain that $\kappa(p^*) \leq 4\sqrt{\lambda} \mathbf{E} \tau_0/\pi$, where λ is the intensity of the underlying Poisson process.

The next example concerns the model introduced in [27]. This model is based on complete graph whose vertex set is given by a Poisson process. The passage time between any two points x_i and x_j of the Poisson process is set to be equal to $\|x_i - x_j\|^\alpha$ for some $\alpha > 1$. Taking as $L(M_k)$ the length of an edge raised to the power α , we obtain from (2.32) that in the planar case

$$\kappa(p^*) \leq \frac{4\lambda^{\frac{1-\alpha}{2}}}{\pi} \left(\frac{2}{\sqrt{\pi}} \right)^\alpha \Gamma\left(\frac{\alpha+2}{2} \right).$$

Modifications of the Markov path For applications, it is important that the paths can be built in an incremental way. Here is an algorithm for constructing the Markov path: start from Z_0 , the point of Π which is the closest to s . Suppose that the path has been constructed to Z_n . If $t \notin C(Z_n)$, then choose among the neighbors of $C(Z_n)$ the next Voronoi cell that is crossed by the segment $[s, t]$. Take the nucleus of this cell for Z_{n+1} .

Several other algorithms for constructing short paths on the Delaunay graph can be derived from the Markov path algorithm. We consider here two simple modifications:

1. *Best Effort.* Take for Z_{n+1} the nucleus of the neighboring cell that is the closest to the destination t (see Figure 2.4).
2. *Farthest Neighbor.* Take for Z_{n+1} the nucleus of the neighboring cell that is last crossed by $[s, t]$ (see Figure 2.4). For each realization of Π , the length of this path cannot exceed $|\hat{p}(s, t, \Pi)|$, because its set of vertices is contained in the set of vertices of $\hat{p}(s, t, \Pi)$.

Note that the paths constructed with these modified algorithms do not satisfy the subadditivity conditions of Kingman's theorem, and thus the limit (2.51) for these paths may not exist.

Simulations were carried out in order to estimate the asymptotic ratio *Path length / Euclidean distance* for the shortest path (see Figure 2.5) and for both modifications of the Markov path. The Delaunay graph was constructed on 5000 points uniformly distributed in the rectangle $(-0.7 < x < 0.7; -0.25 < y < 0.25)$. The paths were searched between the two closest vertices to $(-0.5, 0)$ and $(0.5, 0)$, respectively. The results of the series of 30 experiments for each algorithm are presented in Table 2.2.

Algorithm	Relative length	Standard deviation
Markov Path	1.27	-
Best Effort	1.18	0.005
Farthest Neighbor	1.08	0.02
Shortest path	1.05	0.04

Table 2.2: Simulation results. The relative lengths $|p(s, t, \Pi)|/\|s - t\|$ of different short paths on the Poisson–Delaunay graph.

The Delaunay graph was constructed with the program QHULL¹, which uses a convex hull algorithm for computing Delaunay triangulations and Voronoi diagrams [10]. Modifications of the Markov path algorithm were programmed in MAPLE; for the shortest path, Dijkstra's algorithm was used from MAPLE package library. The program sources are available from the author.

¹The Qhull homepage is at <http://www.geom.umn.edu/software/qhull/>

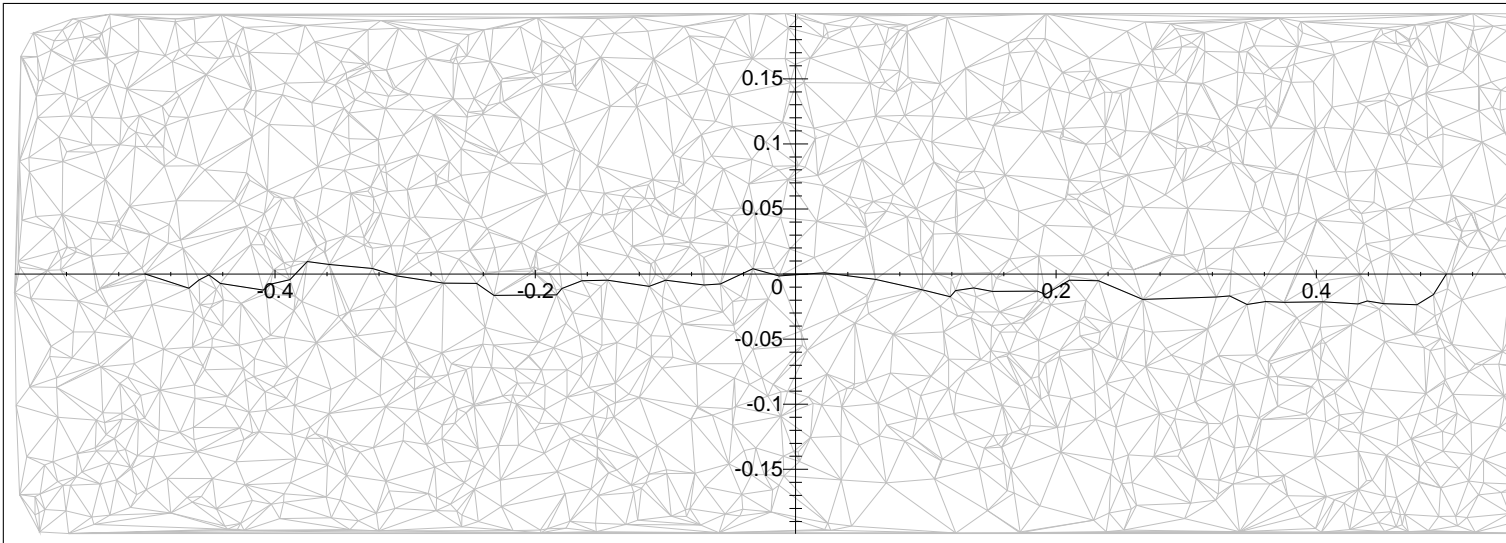


Figure 2.5: Shortest path on the Delaunay graph between the points $(-0.5, 0)$ and $(0.5, 0)$.

2.8 Routing Algorithms for Mobile Communication Networks

In §1.1.4 we outlined the basic principles of routing in packet switched networks. Some difficulties of implementation of routing protocols based on shortest path algorithms were discussed in §1.4.1. The conclusion is that the routing problems arise in mobile networks when the link topology changes much faster than the information about the changes propagates in the network.

Therefore, it is desirable to have a routing algorithm that would work well with a rapidly changing graph of links, yield reasonably short paths, and not require from a host the knowledge of entire network configuration in order to take a routing decision.

In view of this, the Markov path on the Delaunay graph and its modifications possess an attractive property. As it was mentioned in the previous section, such paths can be constructed incrementally, adding vertices one by one. It is important that the choice of the next vertex Z_{n+1} of the path is made between the *neighbors* of the current vertex Z_n (more precisely, between the neighbors belonging to the area D_{n+1} , see Proposition 2.2.1). Hence, if $F(Z_n)$ is the fundamental region of the cell Z_n (see Figure 1.6 on page 34), then Z_{n+1} is defined exclusively from the restriction of the Delaunay graph on $F(Z_n)$. Changes in the vertex set of the graph outside of $F(Z_n)$ do not affect the choice of Z_{n+1} . Consequently, the whole Markov path $\hat{p}(s, t, \Pi)$ is completely defined from the restriction of the vertex set to the union of the fundamental regions of the cells crossing $[s, t]$.

Let us now look, how this property can be translated in network terms. Consider a mobile wireless network that transfers packetized information between pairs of fixed end-stations (gateways) using mobile stations as intermediate relays. We assume that stations of the mobile layer move without any centralized control, as in an ad hoc network. In addition, we assume that

- Each mobile station can determine its own location in the space and the locations of its closest neighbors, so that at any time it can reconstruct its own Voronoi cell and Delaunay edges with respect to the point process of locations of the mobile stations.
- Each packet carries information on the locations of the source and the destination end-stations.

- The network configuration changes that might occur during the period of transfer of a single packet can be neglected.

In such settings, the Markov path algorithm (or one of its modifications) can be used. The routing procedure for each mobile station can be described as follows:

1. The source sends a packet to the closest mobile routing station.
2. The mobile station receives a packet and extracts the positions of the source and the destination end-stations.
 - If the cell of the current station contains the destination, the packet is relayed to it.
 - Else, the packet is relayed to the mobile station whose cell is crossed next by the source–destination line.

The advantage of this algorithm is that the decision on where to relay the packet is based only on the position of the closest neighbors, i.e. only on the *local* geometry of the network. Also note that if the mobile stations can be modelled by a Poisson point process, Corollary 2.5.2 gives explicitly the mean path length and the mean number of hops. The Markov property could also be used to determine variances or large deviations from this mean behavior.

The network configuration can be assumed static during the transfer of a single packet, but significant changes may occur over longer time periods. If the communication links are established along nodes of the Delaunay graph, as in the Markov path algorithm, then changes in the topology of the intra-level links correspond to changes in the topology of the Delaunay graph.

The last remark concerns the possible number of such changes. Suppose that the network consists of n mobile hosts that move in the Euclidean plane without collisions along straight lines maintaining constant velocities. It was shown in [24] that the number of topology changes of the corresponding Delaunay graph over time has a lower bound of $O(n^2)$ and an upper bound of $O(n^3)$. Bounds of this type were established also in higher dimensions and for arbitrary continuous point trajectories, see e.g. [1].

Chapter 3

Aggregate and Fractal Tessellations

In this chapter we look into the distribution properties of the so-called *aggregate tessellations*. ATs represent a spatial analog of branching processes generated by a sequence of stationary tessellations of the Euclidean space. As mentioned in §1.4.2, ATs can serve as a refinement to Voronoi-based models of service zone in wireless networks. Special cases of ATs arise in the hierarchical network models described in §1.2.3.

The organization of the chapter is the following. In §3.1 we introduce an operation of *aggregation*, which may be interpreted as an approximation of cells of the first tessellation by the union of the cells of the second. In §3.2 we find an expression for the *coverage probability* function of a typical aggregate n -cell via the corresponding characteristics of the generating tessellations $\Theta^0, \dots, \Theta^n$. This result is valid for *any* independent sequence of stationary tessellations although a closed-form expression can be obtained only in a few cases. In §3.3 we find a uniform upper bound on the diameter of a typical cell of a Poisson–Voronoi aggregate tessellation (PVAT). Here “typical” refers to the cell with the nucleus at the origin under the Palm distribution of the nuclei process. We also give estimates for the probability of the extinction of a cell and show that with positive probability there is a ball contained in all n -level aggregate cells $C_0^n(0)$. In §3.4 it is shown that for the self-similar tessellations this property guarantees the existence of a limit tessellation, with cells defined as lower set limits of $\{C_0^n(x_i^0)\}_{n \in \mathbb{N}}$. Further, we consider alternative definitions of limit cells and some generalizations of the existence condition.

Defined by a simple recursive procedure, the boundary of the limit PVAT

has an intricate self-similar structure at any scale allowing us to call it fractal. To characterize its degree of irregularity, we provide in §3.6 an upper bound for its Hausdorff dimension. It is based on the analysis of the boundary contact distribution function in the preceding §3.5. Note that the parts of fractal cell boundary are highly dependent making most of previously developed techniques for random fractals inapplicable in our case (a presentation of modern methods used in studying fractals can be found e.g. in the book of Falconer [17]). Finally, we discuss the construction of a cellular network model that would account for both large- and small-scale propagation factors, and show how ATs can be used for this purpose.

3.1 Operation of Aggregation on Tessellations

The main object of study in this chapter, the aggregate tessellations, are generated from a sequence of independent stationary tessellations. We assume that the cells of every considered tessellation $\Theta = \{C_i\}$ are equipped with nuclei $x_i = x(C_i)$ satisfying the obvious compatibility condition

$$\theta x(C_i) = x(\theta C_i)$$

for any shift transformation θ of \mathbb{R}^d for which the tessellation Θ is stationary. It is clear that if the cells of Θ have no nuclei, we may always assign them by some rule: for example, let x_i be the gravity center of C_i . Hence, in what follows we will index the cells of tessellations by the points of their nuclei sets.

The operation of *aggregation* combines two tessellations into one. Let $\Theta^0 = \{C^0(x_i^0)\}$ and $\Theta^1 = \{C^1(x_j^1)\}$ be two independent stationary tessellations equipped with nuclei sets. Define the aggregate cells of $\Theta_0^1 = \Theta^0 \circ \Theta^1$

$$C_0^1(x_i^0) = \bigcup_{j: x_j^1 \in C^0(x_i^0)} C^1(x_j^1).$$

In words, $C_0^1(x_i^0)$ is the union of all the cells of Θ^1 whose nuclei lie in $C^0(x_i^0)$ (see Figure 3.1). Due to the independence and stationarity assumptions, with probability 1 every x_j^1 lies in unique cell of Θ^0 , and hence Θ_0^1 is again a tessellation, though some of its cells may be empty.

It is easy to verify that the operation of aggregation is associative

$$\Theta^0 \circ (\Theta^1 \circ \Theta^2) = (\Theta^0 \circ \Theta^1) \circ \Theta^2,$$

and that the aggregate tessellation is stationary provided that the initial tessellations are stationary. Let $\{\Theta^n\}_{n \in \mathbb{N}}$ be a sequence of independent

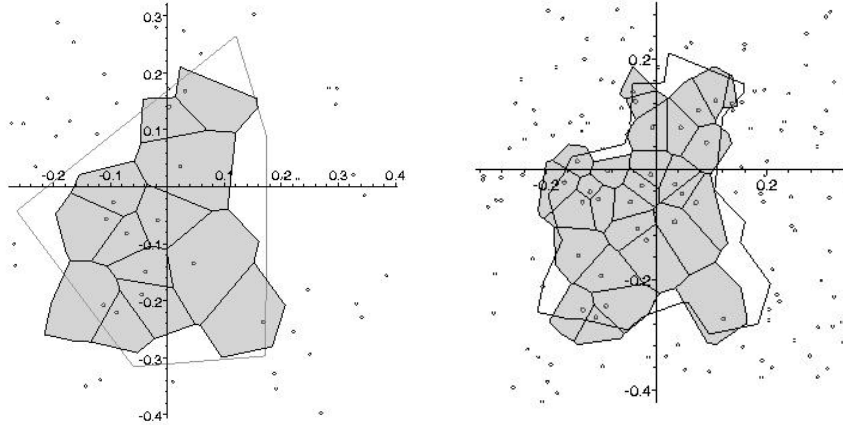


Figure 3.1: First and second iterations in the construction of aggregate cells. The boundary of the previous level cell is countered.

stationary tessellations with the nuclei sets $\Pi_n = \{x_i^n\}$, $n \in \mathbb{N}$. The aggregation of the first n terms of the sequence yields the *aggregate tessellation of order n*

$$\Theta_0^n = \Theta^0 \circ \Theta^1 \circ \dots \circ \Theta^n$$

with the nuclei set $\Pi_0 = \{x_i^0\}$. The cells of this tessellation will be called *aggregate n -cells* and denoted by $C_0^n(x_i^0)$. Of course, aggregate cells constructed in this way depend on positions of the nuclei and do not, in general, inherit the connectivity or convexity properties of the cells of generating tessellations. Figure 3.2 on page 76 shows simulated aggregate cells generated by independent Poisson–Voronoi plane tessellations with exponentially growing intensities.

It is clear that the more the intensities of the successive processes differ, the less the boundary of cell $C_0^{n+1}(x_i^0)$ deviates from the boundary of $C_0^n(x_i^0)$. On the other hand, for close intensity values the boundary becomes very irregular, cells are more likely to split and sometimes no points of Π_{n+1} fall into $C_0^n(x_i^0)$, so $C_0^{n+1}(x_i^0)$ is empty. Using an analogy with branching processes, we may think of the nuclei of the Θ^n -cells that make up the aggregate cell $C_0^n(x_i^0)$, as of n -generation *offspring* of a 0-level parent nucleus x_i^0 . If we connect by segments the nuclei Π_n of each level n with their offspring in the next level nuclei Π_{n+1} , we will obtain a family of spanning trees studied in the Poisson–Voronoi case by Baccelli and Zuyev [8]. We will

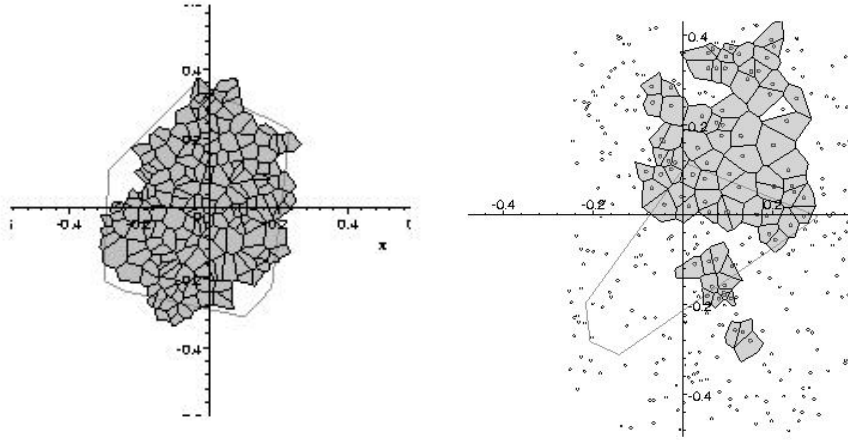


Figure 3.2: Aggregate cells $C_0^n(0)$ in PVAT model and the initial Voronoi cell $C^0(0)$. Left image: $n = 2$, $\lambda = 10$. Right image: $n = 20$, $\lambda = 1.1$.

be interested in the properties of the *aggregate cells* rather than those of the spanning trees.

New phenomena appear in the limit, when n tends to infinity. As we have seen above, there exist models in which with positive probability some of the aggregate cells are empty, i.e. the densities of 0-level nuclei that have not died out till the n -th generation form a decreasing sequence. *A priori* it is not clear if the limit is positive, i.e. that not all the 0-nuclei Π_0 end dying out with probability 1. Next, even if the limit is positive, will Θ_0^n converge in some sense to a limit, say, Θ_0^∞ that is a tessellation? It is easy to imagine that Θ_0^∞ may have a fractal boundary (it also may not: see Example 3.2.1 in §3.2) and thus it is unclear if the boundary has d -Lebesgue measure 0 and whether only a finite number of the limit aggregate cells hits a bounded set. Finally, if the boundary does have a positive measure and thus the cells overlap, does a typical cell contain with a positive probability a “core”—an open set with all the points belonging only to this cell?

As the examples in the text readily show, different models may manifest very different behavior. We illustrate this on two basic models: cubic lattices and *Poisson–Voronoi aggregate tessellations*, quoted as PVAT in the sequel, for which the elements of the sequence $\{\Theta^n\}_{n \in \mathbb{N}}$ are all Voronoi tessellations generated, respectively, by mutually independent homogeneous Poisson point processes Π_n , $n \in \mathbb{N}$.

The following notation is used throughout the rest of the chapter. By \mathbf{P}_n

we denote the distribution in a probability space carrying the sequence of independent stationary point processes $\{\Pi_k, k \geq n\}$. By \mathbf{P}_n^0 we denote the Palm distribution in this space constructed with respect to the process Π_n . Most frequently we will consider distributions with respect to $\{\Pi_0, \Pi_1, \dots\}$. In this case, instead of \mathbf{P}_0 and \mathbf{P}_0^0 we will use \mathbf{P} and \mathbf{P}^0 respectively as a shorthand. Similar notation will be used for the corresponding expectations. The intensity of Π_n is denoted by λ_n . We also assume that $\lambda_0 = 1$, which is just a matter of scale choice. Finally, in the next section we will use the convolution of two functions defined as follows

$$f * g(y) = \int_{\mathbb{R}^d} f(z) g(y - z) dz.$$

3.2 Coverage Probability

Consider a tessellation Θ^n of fixed level n . Under Palm probability \mathbf{P}_n^0 , there is almost surely a point of Π_n at the origin 0. Since the density of cells is λ_n , the volume of a typical cell is $\mathbf{E}_n^0 |C^n(0)| = \lambda_n^{-1}$ (see e.g. [45], Corollary 5.2, equation (5.6)). Therefore,

$$\begin{aligned} \lambda_n \int \mathbf{P}_n^0 \{y \in C^n(0)\} dy &= \lambda_n \mathbf{E}_n^0 \int \mathbb{I}(y \in C^n(0)) dy \\ &= \lambda_n \mathbf{E}_n^0 |C^n(0)| = 1, \end{aligned}$$

so that the function

$$f_n(y) = \lambda_n \mathbf{P}_n^0 \{y \in C^n(0)\}$$

is a distribution density in \mathbb{R}^d .

The next statement provides a formula for calculating the probability that an arbitrary point $y \in \mathbb{R}^d$ is covered by a typical aggregate cell of level n .

Theorem 3.2.1 *Let $f_{0,n}(y) = \mathbf{P}^0 \{y \in C_0^n(0)\}$. Then for every $n \in \mathbb{N}$,*

$$f_{0,n}(y) = f_0 * f_1 * \dots * f_n(y). \quad (3.1)$$

Proof. By definition, for $n = 0$, obviously,

$$f_0(y) = \mathbf{P}^0 \{y \in C^0(0)\}.$$

Suppose, the statement of the lemma holds for $n - 1$. By the Campbell theorem (see e.g. [58, p. 119]),

$$\begin{aligned} \mathbf{P}^0\{y \in C_0^n(0)\} &= \mathbf{E}^0 \sum_{x_i^n \in \Pi_n} \mathbb{I}(x_i^n \in C_0^{n-1}(0)) \mathbb{I}(y \in C^n(x_i^n)) \\ &= \lambda_n \int_{\mathbb{R}^d} \mathbf{P}^0\{z \in C_0^{n-1}(0)\} \mathbf{P}_n^0\{y - z \in C^n(0)\} dz. \end{aligned}$$

It is easy to see that this expression is equivalent to

$$f_{0,n}(y) = \int_{\mathbb{R}^d} f_{0,n-1}(z) f_n(y - z) dz.$$

Example 3.2.1 Consider a stationary tessellation Θ^n of \mathbb{R}^d obtained by shifting the regular mesh of d -hypercubes of side λ_n^{-1} with a vertex at the origin by a random vector uniformly distributed in $[0, \lambda_n^{-1}]^d$. Note that the d -dimensional stationary mesh is simply a Cartesian product of d one-dimensional independent components. Therefore, it is sufficient to study the one-dimensional case, when Θ^n is a stationary sequence of intervals of length λ_n^{-1} on a line.

Assume that $\{\lambda_n\}$ is a non-decreasing sequence and $\lambda_0 = 1$. Choose $\alpha \in [0, 1]$ and define the nuclei set as

$$\Pi_n = \{\lambda_n^{-1}(\alpha + k + u_n)\}, \quad k \in \mathbb{Z},$$

so that the nucleus of each cell divides that cell in proportion $\alpha : (1 - \alpha)$ from left to right. It is easy to see by induction that the size of any Θ_0^n -cell along each coordinate axis is at least λ_n^{-1} , so there is always at least one nucleus of Π_{n+1} in each cell. As a result, all aggregate cells are line intervals and the cells never die. Moreover, for each n , the sizes of the aggregate cells along the line do not change if λ_{n+1}/λ_n is a natural number and change periodically if λ_{n+1}/λ_n is a rational one. By construction, the boundaries of the Θ^n -cells have coordinates $\lambda_n^{-1}(k + u_n)$, $k \in \mathbb{Z}$, where u_n are independent uniformly distributed in $(0, 1)$ random variables describing the shift.

According to (3.1), the characteristic function of $f_0^n(y)$ is given by

$$\chi_0^n(z) = \prod_{k=0}^n \frac{\lambda_k}{iz} \left(e^{iz\lambda_k^{-1}(1-\alpha)} - e^{-iz\lambda_k^{-1}\alpha} \right).$$

In fact, a complete analysis of this model is possible. Let a_k^n be the right boundary point of the n -aggregate cell with the nucleus $\alpha + k + u_0$, $k \in \mathbb{Z}$. It is straightforward to verify that the evolution of the boundaries are given by the following recursion

$$\begin{aligned} a_k^n &= a_k^{n-1} + d_k^n, \quad \text{where} \\ d_k^n &= \lambda_n^{-1} (1 - \alpha - \langle \lambda_n a_k^{n-1} - \alpha - u_n \rangle), \end{aligned}$$

and $\langle z \rangle = z - \max\{k \in \mathbb{Z} : k \leq z\}$ is the fractional part of a real number z . Note that for any z and for any u uniformly distributed in $(0, 1)$, the r.v. $\langle z + u \rangle$ is again uniform in $(0, 1)$. Therefore,

$$\begin{aligned} \mathbf{E} d_k^n &= \lambda_n^{-1} (1/2 - \alpha) \\ \mathbf{var} d_k^n &= 1/(12\lambda_n^2), \end{aligned}$$

so that there is a systematic drift to the right or to the left if $\alpha < 1/2$ or $\alpha > 1/2$, respectively. We have $|d_k^n| \leq 1$. Using the well-known three-series convergence criterion (see e.g. [12, p. 239]), we conclude that the boundaries of the aggregate cells almost surely stabilize as $n \rightarrow \infty$ if and only if both series $(1/2 - \alpha) \sum_n \lambda_n^{-1}$ and $\sum_n \lambda_n^{-2}$ converge. We see a noticeable dependence on the nuclei choice when, for example, $\lambda_n = n$. In this case the cells stabilize only if $\alpha = 1/2$ and float to plus or minus infinity depending on whether α is less or greater than $1/2$.

Let us take a closer look at the coverage probability for Poisson–Voronoi aggregate tessellations. For PVAT we have:

$$f_n(y) = \lambda_n \exp \{ - \lambda_n b_d \|y\|^d \}. \quad (3.2)$$

The next two statements provide explicit formulas for the coverage probability in \mathbb{R}^1 and \mathbb{R}^2 .

Example 3.2.2 Consider PVAT in \mathbb{R}^1 and assume that all λ_i are pairwise different. Then

$$f_{0,n}(y) = \sum_{i=0}^n c_i \lambda_i \exp \{ - 2\lambda_i |y| \}, \quad (3.3)$$

where

$$c_i = 2 \prod_{\substack{l=0 \\ l \neq i}}^n \left(1 - \frac{\lambda_i}{\lambda_l} \right)^{-1} \sum_{j=0}^n \left(1 + \frac{\lambda_i}{\lambda_j} \right)^{-1} \prod_{\substack{m=0 \\ m \neq j}}^n \left(1 - \frac{\lambda_j}{\lambda_m} \right)^{-1}.$$

Indeed, from Theorem 3.2.1 it follows that $f_{0,n}(y)$ is the density of the sum $\sum_{i=0}^n \xi_i$ of independent r.v.'s ξ_i whose densities $f_i(y)$ are given by (3.2) with $d = 1$. Note that $\xi_i = \nu_i - \nu'_i$, where ν_i, ν'_i are independent exponentially distributed r.v.'s with parameter $2\lambda_i$. The density of $\sum_{i=0}^n \nu_i$ equals (see e.g. [12, p. 170])

$$\sum_{i=0}^n 2\lambda_i \exp\{-2\lambda_i y\} \prod_{\substack{l=0 \\ l \neq i}}^n \left(1 - \frac{\lambda_i}{\lambda_l}\right)^{-1} \mathbb{1}(y \geq 0).$$

Finding its symmetrization, we obtain (3.3).

Example 3.2.3 Consider PVAT in \mathbb{R}^2 . According to (3.2), in \mathbb{R}^2 the r.v. ξ_i has normal distribution with zero mean and the covariance matrix

$$\begin{pmatrix} (2\pi\lambda_i)^{-1} & 0 \\ 0 & (2\pi\lambda_i)^{-1} \end{pmatrix}. \quad (3.4)$$

Thus $\sum_{i=0}^n \xi_i$ is also normal with zero mean and the covariance matrix being the sum of (3.4):

$$\begin{pmatrix} (2\pi L_n)^{-1} & 0 \\ 0 & (2\pi L_n)^{-1} \end{pmatrix},$$

where

$$L_n = \left(\sum_{i=0}^n \frac{1}{\lambda_i} \right)^{-1}.$$

The corresponding density is therefore

$$f_{0,n}(y) = L_n \exp\{-L_n \pi \|y\|^2\}$$

that is the same as for a typical cell in the ordinary Voronoi tessellation with the nuclei intensity L_n . This “mean field” approximation is valid only in the planar case because of the stability of the distributions of ξ_i 's in $d = 2$.

Example 3.2.4 For PVAT in \mathbb{R}^d , as follows from (3.1), the characteristic function of $f_{0,n}(y)$ is given by

$$\prod_n \chi(t/\lambda_n^{-1/d}),$$

where $\chi(t)$ is the characteristic function of the density $f_0(y)$ in (3.2). It can be shown that

$$\chi(t) = \frac{\Gamma(\frac{d}{2})}{\pi^{1/2}} \sum_{m=0}^{\infty} \frac{(-1)^m \|t\|^{2m}}{(2m)! \pi^m} \left[\Gamma\left(1 + \frac{d}{2}\right) \right]^{2m/d} \times \frac{\Gamma(m + \frac{1}{2}) \Gamma(1 + \frac{2m}{d})}{\Gamma(m + \frac{d}{2})}.$$

An alternative representation may be given using Bessel functions of the first kind (see e.g. [37]):

$$\chi(t) = \frac{(2\pi)^{d/2}}{\|t\|^{d/2-1}} \int_0^{\infty} \rho^{d/2} e^{-b_d \rho^d} J_{d/2-1}(\rho \|t\|) d\rho.$$

3.3 Evolution of the Aggregate Cells

In this section we will investigate the behavior of the typical aggregate cell $C_0^n(0)$ as n tends to infinity on the Palm space of the process Π_0 . The maximal and the minimal distance from a point z to the cell's boundary can be defined, respectively, as

$$R_n(z) = \begin{cases} \min\{r : b(z, r) \supset C_0^n(0)\} & \text{if } C_0^n(0) \neq \emptyset, \\ 0 & \text{otherwise;} \end{cases}$$

$$r_n(z) = \begin{cases} \max\{r : b(z, r) \subset C_0^n(0)\} & \text{if } z \in C_0^n(0), \\ 0 & \text{otherwise.} \end{cases}$$

The definition takes into account the fact that an aggregate cell of order $n \geq 1$ might not contain z or might be empty. Our aim is to characterize the distribution of

$$R_{\infty}(z) = \sup_n R_n(z),$$

$$r_{\infty}(z) = \inf_n r_n(z).$$

Theorem 3.3.1 *Let $\phi(y)$ be the inverse of the function $y(x) = xe^x$. Assume that*

$$c = \sum_{n=1}^{\infty} \left(\frac{\phi(\lambda_n)}{\lambda_n} \right)^{1/d} = \sum_{n=1}^{\infty} e^{-\phi(\lambda_n)/d} < \infty. \quad (3.5)$$

Then for PVAT the following inequalities hold for all $\rho > c\sqrt{d}$ and any $z \in \mathbb{R}^d$:

$$\mathbf{P}^0\{R_\infty(z) > \rho + \|z\|\} \leq a_1 \sum_{n=1}^{\infty} e^{-\phi(\lambda_n)A(\rho)}, \quad (3.6)$$

$$\mathbf{P}^0\{r_\infty(z) = 0 \mid r_0(z) > \rho\} \leq a_1 \sum_{n=1}^{\infty} e^{-\phi(\lambda_n)A(\rho)}, \quad (3.7)$$

where

$$a_1 = 2((3/2)^d - 1)b_d d^{d/2} c^{d-1},$$

$$A(\rho) = \left(\frac{\rho}{c\sqrt{d}}\right)^d + 1/d - 1.$$

Proof. We begin with inequality (3.6). Since

$$\mathbf{P}^0\{R_\infty(z) > \rho + \|z\|\} \leq \mathbf{P}^0\{R_\infty(0) > \rho\},$$

it is sufficient to prove (3.6) for $z = 0$. Let $\{\rho_n\}$ be a monotonously increasing sequence of positive numbers converging to ρ . Then we have

$$\{R_\infty(0) > \rho\} \subset \cup_{n=0}^{\infty} \{R_n(0) > \rho_n\}.$$

Next, we use the following inequality: if $B \subset \cup_{n=0}^{\infty} B_n$, then

$$\mathbf{P}(B) \leq \mathbf{P}(B_0) + \sum_{n=1}^{\infty} \mathbf{P}(B_n \cap \bar{B}_{n-1}).$$

Hence,

$$\begin{aligned} \mathbf{P}^0\{R_\infty(0) > \rho\} &\leq \mathbf{P}^0\{R_0 > \rho_0\} \\ &\quad + \sum_{n=1}^{\infty} \mathbf{P}^0\{R_n(0) > \rho_n, R_{n-1}(0) \leq \rho_{n-1}\}. \end{aligned} \quad (3.8)$$

The event

$$\{R_n(0) > \rho_n, R_{n-1}(0) \leq \rho_{n-1}\}$$

implies the existence of a Voronoi cell $C^n(x_i^n)$ with the nucleus inside of the ball $b(0, \rho_{n-1})$ containing some point y on the sphere $\partial b(0, \rho_n)$. Therefore, the interior of the ball $b(y, \|y - x_i^n\|)$ contains no points of Π_n (see Figure 3.3).

the value of (3.9) does not exceed

$$2((3/2)^d - 1)b_d d^{d/2} (\rho/\Delta_n)^{d-1} \exp\{-\lambda_n(\Delta_n/\sqrt{d})^d\}. \quad (3.11)$$

Next, choose a special sequence $\{\rho_n\}$ with the increments $\Delta_n = \rho e^{-\phi(\lambda_n)/d}/c$ with c defined in (3.5). It is easy to see that ρ_n monotonously converges to ρ . For such a choice of $\{\rho_n\}$, from (3.11) it follows that the right-hand side of (3.8) is bounded by

$$a_1 c^{d-1} \sum_{n=0}^{\infty} \exp\{- (\rho/c\sqrt{d})^d \phi(\lambda_n) + (d-1)(\log c + \phi(\lambda_n)/d)\}, \quad (3.12)$$

which is equivalent to (3.6). We have used here the definition of ϕ , due to which $e^{-\phi(\lambda_n)} = \phi(\lambda_n)/\lambda_n$. The function $A(\rho) = O(\rho^d)$ increases to infinity and is greater than $1/d$ for all $\rho > c\sqrt{d}$. Therefore, for such ρ , the series in (3.6) converges and the whole bound tends to 0 as $\rho \rightarrow \infty$ providing the a.s. finiteness of $R_\infty(z)$.

Inequality (3.7) is proved much in the same manner. Fix a small $0 < \varepsilon < 1$ and consider a sequence $\{\rho'_n\}$ with $\rho'_0 = \rho$ that monotonously decreases to $\varepsilon\rho$. First, from

$$\{r_\infty(z) = 0, r_0(z) > \rho\} \subset \cup_{n=1}^{\infty} \{r_n(z) < \rho'_n, r_0(z) > \rho\}$$

it follows that

$$\begin{aligned} \mathbf{P}^0\{r_\infty(z) = 0 \mid r_0(z) > \rho\} \\ \leq \sum_{n=1}^{\infty} \mathbf{P}^0\{r_n(z) < \rho'_n, r_{n-1}(z) \geq \rho'_{n-1} \mid r_0(z) > \rho\}. \end{aligned} \quad (3.13)$$

The event

$$\{r_n(z) < \rho'_n, r_{n-1}(z) \geq \rho'_{n-1}\}$$

implies the existence of a Voronoi cell $C^n(x_i^n)$ with the nucleus outside of the ball $b(z, \rho'_{n-1})$ having some point $y \in C^n(x_i^n)$ inside $b(z, \rho'_n)$. Hence, there exists a ball of radius at least $\Delta'_n = \rho'_{n-1} - \rho'_n$ centered on the sphere $\partial b(z, \rho'_{n-1})$. Note that this event is independent of the event $\{r_0(z) > \rho\}$. Thus the summands in (3.13) can be bounded as in (3.9) with $\Delta'_n = (1 - \varepsilon)\Delta_n$. With that choice of Δ'_n the right hand side of (3.13) is bounded by an expression similar to (3.12) with c replaced by $(1 - \varepsilon)c$. Due to the arbitrariness of ε , expression (3.12) also provides an upper bound. The rest of the proof remains unchanged.

Remark 3.3.1 It follows by definition that $\log \phi(x) + \phi(x) = \log x$. Therefore, for $x \geq e$ one has $\phi(x) \leq \log x$. Since $e^{-\phi(\lambda_n)} = \phi(\lambda_n)/\lambda_n$ and $\lambda_n > e$ for all sufficiently large n , the condition

$$\sum_{n=1}^{\infty} \left(\frac{\log \lambda_n}{\lambda_n} \right)^{1/d} < \infty \quad \text{or} \quad \sum_{n=1}^{\infty} \lambda_n^{-1/d+\varepsilon} < \infty \quad (3.14)$$

for some $0 < \varepsilon < 1/d$ is sufficient for (3.5) to hold. We may also use another inequality: $\phi(x) \geq (1 + \log x)/2$ for all x . Then

$$a_1 \sum_{n=1}^{\infty} e^{-\phi(\lambda_n)A(\rho)} \leq a_1 e^{-A(\rho)/2} \sum_{n=1}^{\infty} \lambda_n^{-A(\rho)/2}$$

and the last function can also be used in (3.6-3.7).

Corollary 3.3.1 For PVAT with exponentially growing intensities $\lambda_n = \lambda^n$ for some $\lambda > 1$, one has for all $\rho > c_*$ and any $z \in \mathbb{R}^d$,

$$\mathbf{P}^0 \{ R_{\infty}(z) > \rho + \|z\| \} \leq c_1 \exp \{ -c_2 \rho^d \}, \quad (3.15)$$

$$\mathbf{P}^0 \{ r_{\infty}(z) = 0 \mid r_0(z) > \rho \} \leq c_1 \exp \{ -c_2 \rho^d \}. \quad (3.16)$$

One may take

$$\begin{aligned} c_1 &= a_1 \left(1 + d \frac{1 + \phi(\lambda)}{\phi(\lambda) \log \lambda} \right) e^{\phi(\lambda)}, \\ c_2 &= \phi(\lambda) (c\sqrt{d})^{-d}, \\ c_* &= ((\log c_1)/c_2)^{1/d}. \end{aligned}$$

Proof. Recall the following integral estimate:

$$\sum_{n=1}^{\infty} h(n) \leq h(1) + \int_1^{\infty} h(x) dx$$

for any non-increasing positive function $h(x)$. We have

$$\begin{aligned} \sum_{n=1}^{\infty} e^{-\phi(\lambda^n)A(\rho)} &\leq e^{-\phi(\lambda)A(\rho)} + \int_1^{\infty} e^{-\phi(\lambda^x)A(\rho)} dx \\ &= e^{-\phi(\lambda)A(\rho)} + \frac{1}{\log \lambda} \int_{\phi(\lambda)}^{\infty} (1 + y^{-1}) e^{-yA(\rho)} dy \end{aligned}$$

after the variable change $y = \phi(\lambda^x)$. Next, since $1 + y^{-1} \leq 1 + \phi(\lambda)^{-1}$ on the integration domain, the whole expression can be bounded by

$$e^{-\phi(\lambda)A(\rho)} + \frac{1 + \phi(\lambda)^{-1}}{A(\rho) \log \lambda} e^{-\phi(\lambda)A(\rho)} < \left(1 + \frac{1 + \phi(\lambda)^{-1}}{d^{-1} \log \lambda}\right) e^{-\phi(\lambda)A(\rho)},$$

so that (3.6-3.7) become (3.15-3.16), respectively. It can be immediately verified that these estimates are nontrivial if $\rho > c_*$ and that $c_* > c\sqrt{d}$.

Corollary 3.3.2 *For PVAT with polynomially growing intensities $\lambda_n = (1 + \alpha n)^\beta$ for some $\alpha > 0$, $\beta > d$, one has*

$$\sum_{n=1}^{\infty} e^{-\phi(\lambda_n)A(\rho)} \leq \frac{A(\rho)}{A(\rho) - \beta'} \left(e^{-\phi(\lambda_1)A(\rho)} + \frac{\Gamma(\beta', \phi(\lambda_1)(A(\rho) - \beta'))}{\alpha\beta(A(\rho) - \beta')^{\beta'}} \right),$$

where $\beta' = \beta^{-1}$ and $\Gamma(n, x) = \int_x^\infty z^{n-1} e^{-z} dz$ is the incomplete Gamma-function.

Proof. The reasoning is the same as in Corollary 3.3.1 with the variable change

$$z = (A(\rho) - \beta^{-1})\phi((1 + \alpha x)^\beta)$$

in the corresponding integral.

Corollary 3.3.3 *Under conditions of Theorem 3.3.1, with probability one, each family of cells $\{C_0^n(x_i^0)\}_{n \in \mathbb{N}}$ is uniformly bounded in \mathbb{R}^d .*

Proof. Let τ_x be the stationary shift defined on the probability space Ω such that $\Pi_n(\tau_x \omega)(B) = \Pi_n(\omega)(B - x)$ for any Borel set $B \subset \mathbb{R}^d$ and any n . In this notation, $\tau_{x_i^0} R_n(0)$ for $x_i^0 \in \Pi_0$ is the maximal distance from x_i^0 to the boundary of $C_0^n(x_i^0)$ that corresponds to the above definition of $R_n(0)$ with $C_0^n(0)$ replaced with $C_0^n(x_i^0) = \tau_{x_i^0} C_0^n(0)$. The probability that there exists an unbounded family of cells with the nucleus in a ball $b(0, N)$ equals

$$\begin{aligned} \mathbf{P} \bigcup_{x_i \in \Pi_0 \cap b(0, N)} \{ \tau_{x_i^0} R_\infty(0) = \infty \} \\ \leq \mathbf{E} \sum_{x_i \in \Pi_0 \cap b(0, N)} \mathbb{I}\{ \tau_{x_i^0} R_\infty(0) = \infty \} \\ = b_d N^d \mathbf{E}^0 \mathbb{I}\{ R_\infty(0) = \infty \} = 0, \end{aligned}$$

where we have used the Campbell theorem and (3.6). Letting N grow to infinity proves the assertion.

The following fact will be used later to show that the boundaries of the limit tessellation have zero Lebesgue measure.

Corollary 3.3.4 *Under conditions of Theorem 3.3.1, for any $y \in \mathbb{R}^d$ with positive probability, there exists $x_i^0 \in \Pi_0$ such that*

$$y \in \text{int} \left(\cap_n C_0^n(x_i^0) \right).$$

The lower bound for this probability is given in (3.19) below.

Proof. It is enough to show that the distance from y to the boundary of the Π_0 -cell containing y is sufficiently large so that the boundary of the progressing n -cells never reach y . The probability of the latter event is positive by (3.7).

Due to stationarity, we may put $y = 0$. Consider the following representation:

$$\mathbf{P} \left\{ \exists x_i^0 : 0 \in \text{int} \left(\cap_n C_0^n(x_i^0) \right) \right\} = \mathbf{E} \sum_{x_i^0 \in \Pi_0} \mathbb{I} \left(0 \in \text{int} \left(\cap_n C_0^n(x_i^0) \right) \right).$$

By the Campbell theorem, the right-hand side equals

$$\begin{aligned} \int_{\mathbb{R}^d} \mathbf{P}^0 \left\{ -z \in \text{int} \left(\cap_n C_0^n(0) \right) \right\} dz &\geq \\ \int_{\mathbb{R}^d} \mathbf{P}^0 \left\{ z \in \text{int} \left(\cap_n C_0^n(0) \right) \mid b(z, \rho) \subset C^0(0) \right\} \times \\ &\times \mathbf{P}^0 \left\{ b(z, \rho) \subset C^0(0) \right\} dz \end{aligned} \quad (3.17)$$

for arbitrary $\rho > 0$. By Theorem 3.3.1, the first factor under the integral in (3.17) is greater than $1 - a_1 \sum_{n=1}^{\infty} (\phi(\lambda_n)/\lambda_n)^{A(\rho)}$ provided that $\rho \geq c\sqrt{d}$. The second factor equals the probability that no points of Π_0 lie in the figure

$$\bigcup_{\|z-z'\|=\rho} b(z', \|z'\|).$$

This figure is obtained by rotation of a cardioid around its symmetry axis; by construction, it is contained in the ball $b(z, \|z\| + 2\rho)$. Therefore,

$$\mathbf{P}^0 \left\{ b(z, \rho) \subset C^0(0) \right\} > \exp \left\{ -b_d (\|z\| + 2\rho)^d \right\}.$$

Using this estimate we get

$$\begin{aligned} \int_{\mathbb{R}^d} \mathbf{P}^0 \{b(z, \rho) \subset C^0(0)\} dz &> \int_{\mathbb{R}^d} \exp \{ -b_d(\|z\| + 2\rho)^d \} dz \\ &> \int_0^\rho r^{d-1} db_d \exp \{ -b_d(3\rho)^d \} dr = b_d \rho^d \exp \{ -b_d(3\rho)^d \}. \end{aligned} \quad (3.18)$$

Hence

$$\begin{aligned} \mathbf{P} \{ \exists x_i^0 : y \in \text{int}(\cap_n C_0^n(x_i^0)) \} \\ > \sup_{\rho \geq c\sqrt{d}} \left[b_d \rho^d \exp \{ -b_d(3\rho)^d \} \left(1 - a_1 \sum_{n=1}^{\infty} \left(\frac{\phi(\lambda_n)}{\lambda_n} \right)^{A(\rho)} \right) \right] > 0. \end{aligned} \quad (3.19)$$

The following corollary gives bounds for the probability of the extinction of a cell

Corollary 3.3.5 *Under conditions of Theorem 3.3.1, for any N such that $1 \leq N \leq \infty$, one has $0 < \mathbf{P}^0 \{ C_0^N(0) = \emptyset \} < 1$. The corresponding bounds for the exponential case $\lambda_n = \lambda^n$ are given by (3.21) and (3.22) below.*

Proof. Obviously, the cell centered in the origin dies on level n if no points of Π_n fall into $b(0, R_{n-1}(0))$. Therefore,

$$\begin{aligned} \mathbf{P}^0 \{ C_0^N(0) = \emptyset \} &= \sup_{1 \leq n \leq N} \mathbf{P}^0 \{ C_0^n(0) = \emptyset \} \\ &\geq \sup_{1 \leq n \leq N} \mathbf{P}^0 \{ \Pi_n(b(0, R_{n-1}(0))) = 0 \} \\ &= \sup_{1 \leq n \leq N} \mathbf{E}^0 \exp \{ -b_d \lambda_n R_{n-1}^d(0) \} \\ &= \sup_{1 \leq n \leq N} \left[1 - \int_0^\infty db_d \lambda_n r^{d-1} \exp \{ -b_d \lambda_n r^d \} \mathbf{P}^0 \{ R_{n-1}(0) > r \} dr \right]. \end{aligned}$$

By Theorem 3.3.1, for $r \geq c\sqrt{d}$,

$$\mathbf{P}^0 \{ R_{n-1}(0) > r \} \leq \mathbf{P}^0 \{ R_\infty(0) > r \} \leq a_1 \sum_{n=1}^{\infty} \left(\frac{\phi(\lambda_n)}{\lambda_n} \right)^{A(r)}.$$

Choose $r_* > c\sqrt{d}$ such that the last expression is less than 1 for all $r > r_*$. Then we obtain the following estimate

$$\begin{aligned} \mathbf{P}^0\{C_0^n(0) = \emptyset\} &\geq 1 - \int_0^{r_*} db_d r^{d-1} \lambda^n \exp\{-b_d \lambda^n r^d\} dr \\ &\quad - \int_{r_*}^{\infty} db_d r^{d-1} \lambda^n a_1 \sum_{n=1}^{\infty} \left(\frac{\phi(\lambda_n)}{\lambda_n}\right)^{A(r)} dr, \end{aligned}$$

which can be worked out in each particular case. For instance, in the exponential case considered in Corollary 3.3.1, with $r_* = c_*$ and (3.15) we have

$$\begin{aligned} \mathbf{P}^0\{C_0^n(0) = \emptyset\} &\geq 1 - \int_0^{c_*} db_d r^{d-1} \lambda^n \exp\{-b_d \lambda^n r^d\} dr \\ &\quad - \int_{c_*}^{\infty} db_d r^{d-1} \lambda^n c_1 \exp\{-(b_d \lambda^n + c_2)r^d\} dr. \quad (3.20) \end{aligned}$$

Calculating the integrals in (3.20) and summing up the results, we obtain the estimate

$$\mathbf{P}^0\{C_0^N(0) = \emptyset\} \geq \sup_{1 \leq n \leq N} (2\lambda)^{-b_d \lambda^n / c_2} \left[1 - \frac{2db_d^2 \lambda^{n-1}}{c_2(b_d \lambda^n + c_2)} \right]. \quad (3.21)$$

In order to prove an upper bound, write

$$\begin{aligned} \mathbf{P}^0\{\exists n : C_0^n(0) = \emptyset\} &\leq \mathbf{P}^0\{r_\infty(0) = 0\} \\ &\leq \mathbf{P}^0\{r_\infty(0) = 0 \mid r_0(0) > r\} + \mathbf{P}^0\{r_0(0) \leq r\}, \end{aligned}$$

for arbitrary $r > 0$. The event $\{r_0(0) > r\}$ means that the ball $b(0, 2r)$ contains no points of Π_0 . Therefore its probability equals $\exp\{-b_d 2^d r^d\}$. Using the estimate (3.7) of Theorem 3.3.1, for $r > c\sqrt{d}$ we finally get

$$\mathbf{P}^0\{C_0^N(0) = \emptyset\} \leq 1 - \sup_{r \geq c\sqrt{d}} \left[\exp\{-b_d 2^d r^d\} \left(1 - a_1 \sum_{n=1}^{\infty} \left(\frac{\phi(\lambda_n)}{\lambda_n}\right)^{A(\rho)} \right) \right],$$

and in the exponential case, with $r_* = c_*$,

$$\begin{aligned} \mathbf{P}^0\{C_0^N(0) = \emptyset\} &\leq 1 - \sup_{r \geq c_*} \left[\exp\{-b_d 2^d r^d\} (1 - c_1 \exp\{-c_2 r^d\}) \right]. \quad (3.22) \end{aligned}$$

The next theorem reinforces, in some sense, Theorem 3.3.1 showing that not only the radius but also the range of the cells' boundaries evolution is related to the sum in (3.5). Recall the definitions of Minkowski operations \oplus and \ominus on two sets A, B in a vector space:

$$A \oplus B = \{a + b : a \in A, b \in B\}, \quad A \ominus B = (A^c \oplus B)^c.$$

For $0 \leq m < n \leq \infty$ introduce the variable γ_m^n , which shows how far the boundary of $C_0^n(0)$ stretches from the boundary of its predecessor $C_0^m(0)$. Put

$$\gamma_m^n = \inf\{r : C_0^m(0) \ominus b(0, r) \subseteq C_0^n(0) \subseteq C_0^m(0) \oplus b(0, r)\}$$

if both $C_0^m(0)$ and $C_0^n(0)$ are non-empty, otherwise put $\gamma_m^n = 0$.

Theorem 3.3.2 *Let $\phi(y)$ be the inverse of the function $y(x) = xe^x$ and let*

$$c(m, n) = \sum_{k=m+1}^n e^{-\phi(\lambda_k)/d}. \quad (3.23)$$

Then for $1 \leq m < n \leq \infty$, one has for all $\rho > c(m, n)\sqrt{d}$,

$$\begin{aligned} & \mathbf{P}^0\{\gamma_m^n > \rho \mid \text{diam } C_0^m(0) \leq r\} \\ & \leq b_d d^{d/2} c^d(m, n) \left(\frac{3}{2} + \frac{r}{\rho}\right)^d \sum_{k=m+1}^n e^{-\phi(\lambda_k) A(\rho, m, n)}, \end{aligned}$$

where $A(\rho, m, n) = (\rho/\sqrt{d}c(m, n))^d - 1$.

Proof. The proof mimics the one of Theorem 3.3.1 so we do not give details. The initial level m being fixed, denote $S_m^n = \sum_{k=m+1}^n \gamma_{k-1}^k$ and let $\{\rho_k\}_{k=m}^n$ be a monotonously increasing sequence of numbers such that $\rho_m = 0$ and $\rho_n = \rho$ (converging to ρ if $n = \infty$). Then, as in (3.13) we have

$$\begin{aligned} & \mathbf{P}^0\{S_m^n > \rho \mid \text{diam } C_0^m(0) \leq r\} \leq \mathbf{P}^0\{\gamma_m^{m+1} > \rho_{m+1} \mid \text{diam } C_0^m(0) \leq r\} \\ & + \sum_{k=m+2}^n \mathbf{P}^0\{S_m^k > \rho_k \mid S_m^{k-1} \leq \rho_{k-1}; \text{diam } C_0^m(0) \leq r\} \\ & \leq \mathbf{P}^0\{\gamma_m^{m+1} > \rho_{m+1} \mid \text{diam } C_0^m(0) \leq r\} \\ & + \sum_{k=m+2}^n \mathbf{P}^0\{\gamma_{k-1}^k > \Delta_k \mid S_m^{k-1} \leq \rho_{k-1}; \text{diam } C_0^m(0) \leq r\}, \end{aligned}$$

where $\Delta_k = \rho_k - \rho_{k-1}$. If $\gamma_{k-1}^k > \Delta_k$, there exist a Voronoi cell $C^k(x_i^k)$ and a point $y \in C^k(x_i^k)$ such that either $x_i^k \in C_0^{k-1}(0)$ and $y \in \partial(C_0^{k-1}(0) \oplus b(0, \Delta_k))$, or $x_i^k \notin C_0^{k-1}(0)$ and $y \in \partial(C_0^{k-1}(0) \ominus b(0, \Delta_k))$. In both cases the interior of the ball $b(y, \|y - x_i^k\|)$ contains no points of Π_k .

The event $E_m^{k-1} = \{S_m^{k-1} \leq \rho_{k-1}; \text{diam } C_0^m(0) \leq r\}$ implies the inclusions $C_0^{k-1}(0) \subseteq b(\zeta, r + \rho_{k-1})$ and $y \in b(\zeta, r + \rho_k)$ for some (random) center $\zeta \in \mathbb{R}^d$. Therefore,

$$\begin{aligned} \mathbf{P}^0 \{ \gamma_{k-1}^k > \Delta_k \mid E_m^{k-1} \} \\ \leq \mathbf{P}^0 \{ \exists y \in b(\zeta, r + \rho_k) : \Pi_k(b(y, \Delta_k)) = 0 \mid E_m^{k-1} \}. \end{aligned} \quad (3.24)$$

Now consider a collection of mesh cubes of side Δ_k/\sqrt{d} . Let N be the number of such cubes that lie inside the ball $b(\zeta, r + \rho_k + \Delta_k/2)$. The mesh cube containing y lies entirely in $b(y, \|y - x_i^k\|)$ and thus contains no points of Π_k . Hence (3.24) is bounded by the probability that at least one of those N cubes is empty (given by (3.9) with $n = k$) Note that this bound is independent of the distribution of the center ζ .

Acting as in the proof of Theorem 3.3.1 it can be shown that

$$N \leq b_d(\sqrt{d}/\Delta_k)^d (r + \rho_k + \Delta_k/2)^d < b_d \left(\frac{\sqrt{d}}{\Delta_k} \right)^d \left(r + \frac{3}{2}\rho \right)^d.$$

Using (3.10) we see that the value of (3.9) here does not exceed

$$b_d d^{d/2} \left(\frac{r + 3\rho/2}{\Delta_k} \right)^d \exp \{ -\lambda_k (\Delta_k/\sqrt{d})^d \}.$$

Choosing $\Delta_k = \rho e^{-\phi(\lambda_k)/d}/c(m, n)$ with $c(m, n)$ defined in (3.23) we obtain the theorem statement.

Corollary 3.3.6 *Assume that (3.5) is satisfied. Then $\lim_n \gamma_n^{n+k} = 0$ in probability, uniformly in $k \geq 1$.*

3.4 Existence of the Limit Tessellation

Heuristic arguments suggest that the difference between two successive aggregate cells becomes smaller and smaller if the intensities of the point processes grow sufficiently fast. In the case of PVAT, Corollary 3.3.6 shows that it is indeed the case. Moreover, by Corollary 3.3.4 with positive probability the family of cells $\{C_0^n(x_i^0)\}$ with the same nucleus x_i^0 possesses a non-empty

“core” $\text{int}(\cap_n C_0^n(x_i^0))$. Therefore, it is important to know, whether there exists a *limit* object for the process of tessellations, and if the answer is positive, whether this limit object is itself a tessellation (see Definition A.2.2). In the present section we will address these questions.

Let $\{A_n\}$ be a sequence of closed subsets of \mathbb{R}^d . Recall the definitions of the lower and upper set limits:

$$\begin{aligned}\liminf A_n &= \{x : \exists\{x_n\} \text{ such that } x_n \in A_n \text{ and } x = \lim_n x_n\}, \\ \limsup A_n &= \{x : \exists\{x_{n_k}\} \text{ such that } x_{n_k} \in A_{n_k} \text{ and } x = \lim_k x_{n_k}\}.\end{aligned}$$

In words, a point belongs to $\liminf A_n$ if and only if any its neighborhoods intersects with all sets A_n starting from some m ; a point belongs to $\limsup A_n$ if and only if any its neighborhood intersects infinitely many sets A_n . Both limits are closed sets (see e.g. [40, Prop. 1.2.3]). Now define the sets

$$\begin{aligned}C_0^\infty(x_i^0) &= \text{cl}(\cup_m \cap_{n \geq m} C_0^n(x_i^0)) \\ D_0^\infty(x_i^0) &= \text{cl}(\cap_m \cup_{n \geq m} C_0^n(x_i^0)) \\ E_0^\infty(x_i^0) &= \liminf_n C_0^n(x_i^0) \\ F_0^\infty(x_i^0) &= \limsup_n C_0^n(x_i^0).\end{aligned}\tag{3.25}$$

Our main purpose is to show that all four families under suitable conditions constitute the same tessellation in \mathbb{R}^d .

Let $C_m^n(x_i^m)$ be the cells of the aggregate tessellation Θ_m^n defined as

$$\Theta_m^n = \Theta^m \circ \Theta^{m+1} \circ \dots \circ \Theta^n.$$

Theorem 3.4.1 *Assume that the following condition is satisfied*

$$\mathbf{P}\{\exists m, \exists x_j^m \in \Pi_m : 0 \in \text{int}(\cap_{n \geq m} C_m^n(x_j^m))\} = 1.\tag{3.26}$$

Then the set families $C_0^\infty(x_i^0)$, $D_0^\infty(x_i^0)$, $E_0^\infty(x_i^0)$, and $F_0^\infty(x_i^0)$ defined by (3.25) have almost surely the same interior, may differ only on the set of a null measure, and constitute the same tessellation.

The following complementary result establishes the relation between the boundaries of Θ_0^n and Θ_0^∞ defined, respectively, as

$$\Gamma_0^n = \mathbb{R}^d \setminus \cup_i \text{int}(C_0^n(x_i^0)) \quad \text{and} \quad \Gamma_0^\infty = \mathbb{R}^d \setminus \cup_i \text{int}(C_0^\infty(x_i^0)).\tag{3.27}$$

Corollary 3.4.1 *Assume that a sequence of stationary aggregate tessellations satisfies condition (3.26). Then*

$$\Gamma_0^\infty \subset \liminf_n \Gamma_0^n = \limsup_n \Gamma_0^n \quad a.s.$$

The limit of Γ_0^n is the set defined in (3.28) below.

Proof of Theorem 3.4.1. The proof consists of two parts: in the first one we prove that the sets $C_0^\infty(x_i^0)$ constitute a tessellation, in the second we show that the interiors of the alternatively defined limit cells coincide.

Part I. Recall Definition A.2.2. We start by verifying condition (b). Consider disjoint open sets $A_i = \cup_m \text{int}(\cap_{n \geq m} C_0^n(x_i^n))$. Every $x_j^m \in \Pi_m$ is contained in an almost surely unique aggregate cell $C_0^{m-1}(x_i^0)$. If (3.26) holds, the set

$$\Gamma_A \equiv \mathbb{R}^d \setminus \cup_i A_i \quad (3.28)$$

misses the origin a.s., which implies that $|\Gamma_A| = 0$. Since $A_i \subset C_0^\infty(x_i^0)$, we have $C_0^\infty(x_i^0) \cap C_0^\infty(x_j^0) \subset \Gamma_0^\infty \subset \Gamma_A$ for $i \neq j$.

Let us verify (c). For a bounded Borel set $B \subset \mathbb{R}^d$ introduce a random variable

$$N(B) = \limsup_{n \rightarrow \infty} \sum_{x_i^n \in \Pi_n} \mathbb{I}\{C_n^\infty(x_i^n) \cap B \neq \emptyset\}$$

Obviously, if $N(B) < \infty$, only a finite number of cells $C_0^\infty(x_i^0)$ intersects B . Denote by σ_n the σ -algebra generated by the sequence of processes $\{\Pi_k, k \geq n\}$, and note that the event $\{N(B) = \infty\}$ belongs to the tail sigma-algebra $\sigma_\infty = \cap_n \sigma_n$. Since all the processes Π_k are independent, the zero-one law applies so that $\mathbf{P}\{N(B) = \infty\} = 0$ or 1. From (3.26) it follows that for some $\varepsilon > 0$,

$$\mathbf{P}\{\exists x_j^m \in \Pi_m : b(0, \varepsilon) \in \text{int}(\cap_{n=m}^\infty C_m^n(x_j^m))\} > 0,$$

and hence, $\mathbf{P}\{N(b(0, \varepsilon)) = \infty\} = 0$. Every bounded set $B \subset \mathbb{R}^d$ can be covered by a finite family $\{b(t_k, \varepsilon)\}_{k \leq K}$ of copies of $b(0, \varepsilon)$ shifted by t_k . Because of stationarity, $N(b(0, \varepsilon))$ and $N(b(t_k, \varepsilon))$ have the same distribution for each $t_k \in \mathbb{R}^d$, therefore

$$\mathbf{P}\{N(B) = \infty\} \leq \sum_{k=1}^K \mathbf{P}\{N(b(t_k, \varepsilon)) = \infty\} = 0.$$

In order to prove (a), we need to show that the set $\Phi = \mathbb{R}^d \setminus \cup_i C_0^\infty(x_i^0)$ is a.s. empty. Observe that $\Phi \subset \Gamma_0^\infty$, and therefore Φ contains only boundary

points if non-empty. For such a point $y \in \Phi$, there exists a sequence $\{y_k\} \subset \cup_i C_0^\infty(x_i^0)$ converging to y . Being itself a bounded set, this sequence visits only a finite number of limit cells $C_0^\infty(x_i^0)$. At least one of these cells contains an infinite subsequence $\{y_{k_n}\}$, and hence it contains y because cells are closed sets. We come to a contradiction with the non-emptiness of Φ .

Part II. We will show that the interiors of the cells defined in (3.25) coincide with $\text{int}(\text{cl}(A_i))$ a.s. Because $\text{cl}(A_i) \subset C_0^\infty(x_i^0) \subset D_0^\infty(x_i^0) \subset F_0^\infty(x_i^0)$ and $\text{cl}(A_i) \subset E_0^\infty(x_i^0) \subset F_0^\infty(x_i^0)$, it is sufficient to show that $\text{int}(\text{cl}(A_i)) = \text{int}(F_0^\infty(x_i^0))$.

Suppose $x \notin \text{int}(\text{cl}(A_i))$. Every open neighborhood $v(x)$ of x contains a point $y \notin \text{cl}(A_i)$. Therefore, $v(x)$ contains an open subset $v(y)$ disjoint of $\text{cl}(A_i)$. Since $|\Gamma_A| = 0$, there exists a point $z \in v(y) \cap A_j$ for some $j \neq i$. But $A_j \cap F_0^\infty(x_i^0) = \emptyset$ and thus $x \notin \text{int}(F_0^\infty(x_i^0))$.

Hence, the boundary Γ_0^∞ is common for the tessellations defined by (3.25).

Proof of Corollary 3.4.1. Let us show that the set Γ_A defined in (3.28) is the limit of the boundaries Γ_0^n . As it was shown in the proof of Theorem 3.4.1, $\Gamma_0^\infty \subset \Gamma_A$ and (3.26) implies that $|\Gamma_A| = 0$.

Let us verify that $\Gamma_A \subset \liminf_n \Gamma_0^n$. If $x \in \Gamma_A$, then any neighborhood $v(x)$ of x hits at least two disjoint sets A_i and A_j . Therefore, $v(x)$ hits $\cap_{n \geq m} C_0^n(x_i^0)$ and $\cap_{n \geq m} C_0^n(x_j^0)$ starting from some m . Then it must also hit Γ_0^n for all $n \geq m$.

Now we prove that $\limsup_n \Gamma_0^n \subset \Gamma_A$. Let n_k be a sequence of natural numbers such that $\lim_k n_k = \infty$. Suppose $x_{n_k} \in \Gamma_0^{n_k}$ and $x = \lim_k x_{n_k}$. If $x \notin \Gamma_A$, then $x \in A_i$ for some i . Then $x \in \text{int} \cap_{n \geq m} C_0^n(x_i^0)$ for some m , and the sequence of $x_{n_k} \in \Gamma_0^{n_k}$ cannot converge to x . From this contradiction it follows that $x \in \Gamma_A$.

Corollary 3.4.2 *Under condition (3.26), for each $y \in \mathbb{R}^d$,*

$$\begin{aligned} \lim_n \mathbf{P}^0 \{y \in C_0^n(0)\} &= \mathbf{P}^0 \{y \in C_0^\infty(0)\}, \\ \lim_n |C_0^n(0)| &= |C_0^\infty(0)| \quad a.s. \end{aligned}$$

and thus $\mathbf{E}^0 |C_0^\infty(0)| = \lambda_0$.

Proof. By Theorem 3.4.1, $\mathbf{P}^0 \{y \in C_0^\infty(0)\} = \mathbf{P}^0 \{y \in D_0^\infty(0)\}$. Using the

continuity property of the probability measures, we obtain

$$\begin{aligned}\mathbf{P}^0\{y \in C_0^\infty(0)\} &= \lim_m \mathbf{P}^0\{y \in \cup_{n \geq m} C_0^n(0)\} \geq \lim_n \mathbf{P}^0\{y \in C_0^n(0)\}, \\ \mathbf{P}^0\{y \in C_0^\infty(0)\} &= \lim_m \mathbf{P}^0\{y \in \cap_{n \geq m} C_0^n(0)\} \leq \lim_n \mathbf{P}^0\{y \in C_0^n(0)\}.\end{aligned}$$

The second equality is obtained by simply replacing $\mathbf{P}^0\{y \in \cdot\}$ by $|\cdot|$ above.

Call a sequence of tessellations Θ^n *self-similar* if there exists $\kappa > 0$ such that for all $n \in \mathbb{N}$ the scaled tessellation $\kappa\Theta^n$ with the boundary $\kappa\Gamma(\Theta^n) = \{\kappa y : y \in \Gamma(\Theta^n)\}$ has the same distribution as Θ^{n-1} .

Theorem 3.4.2 *For a self-similar sequence of tessellations, the condition*

$$\mathbf{P}\{\exists x_i^0 \in \Pi_0 : 0 \in \text{int}(\cap_{n=0}^\infty C_0^n(x_i^0))\} > 0 \quad (3.29)$$

implies (3.26). In particular, (3.29) implies the statements of Theorem 3.4.1 and its corollaries.

Proof. Suppose, the tessellations Θ^n are self-similar with the coefficient $\kappa > 0$. Let $v(0)$ be an open neighborhood of the origin, and let $x^n(0)$ be the point of Π_n such that $0 \in C^n(x^n(0))$. Consider the following r.v.'s:

$$\begin{aligned}T_1 &= \min\{n > 0 : v(0) \not\subset C_0^k(x^0(0))\}, \\ T_2 &= \min\{n > T_1 : v(0) \not\subset \kappa^{T_1+1} C_{T_1+1}^k(x^{T_1+1}(0))\}, \\ &\dots \\ T_{n+1} &= \min\{n > T_n : v(0) \not\subset \kappa^{T_n+1} C_{T_n+1}^k(x^{T_n+1}(0))\}, \text{ etc.}\end{aligned}$$

Thus defined r.v.'s are stopping times and the distribution of T_{n+1} given $\{T_n = k\}$ depends only on $\{\Pi_n\}_{n > k}$. By self-similarity we have $\mathbf{P}\{T_{n+1} < \infty \mid T_n < \infty\} = \mathbf{P}\{T_1 < \infty\} = p$, which is strictly smaller than 1 by assumption (3.29). Therefore,

$$\mathbf{P}\{T_1 < \infty, \dots, T_n < \infty\} = p^n. \quad (3.30)$$

Thus $\mathbf{P}\{\forall k, T_k < \infty\} = 0$ so that a.s. there exists n such that $T_n < \infty$, but $T_{n+1} = \infty$ and condition (3.26) is satisfied with $m = T_n + 1$.

Example 3.4.1 The existence of set limits of $\{C_0^n(x_i^0)\}_{n \in \mathbb{N}}$ alone does not guarantee that they form a tessellation. Consider a stationary tessellation Θ^n of the real line obtained by randomly shifting a regular mesh of intervals of size $1/3^n$. Define its cells as $C^n(i) = [i/3^n, (i+1)/3^n] + u_n$, where u_n is a r.v. uniformly distributed in $[-1/3^{n-1}, 1/3^{n-1}]$. For every $i \in \mathbb{Z}$, there exists unique $l \in \mathbb{Z}$ such that $i = 3l, 3l-2$, or $3l+2$. Define the nucleus x_i^n of the cell $C^n(i) \equiv C^n(x_i^n)$ as $(3^l + 1/2)/3^n + u_n$. By this definition, for every $l \in \mathbb{Z}$ the nuclei $x_{3l}^n, x_{3l-2}^n, x_{3l+2}^n$ are all located in the midpoint of $C^n(3l)$. Such midpoints are evenly spaced on the line at the distance $1/3^{n-1}$, and their distribution is stationary due to the choice of u_n .

Assume now that all u_n are independent and let us look into the evolution of the aggregate tessellation Θ_0^n . Each cell $C^{n-1}(i)$ contains exactly one midpoint of $C^n(3k)$ for some k . Therefore, $C_{n-1}^n(i) = C^n(3k-2) \cup C^n(3k) \cup C^n(3k+2)$. Denote by d_i^n the leftmost boundary point of $C_0^n(i)$. The evolution of this point is given by the following recursion

$$\begin{aligned} d_i^0 &= i + u'_0 \\ d_i^n &= d_i^{n-1} - 1/3^n + u'_n, \end{aligned}$$

where u'_n are all independent and uniformly distributed r.v.'s in $[-1/(2 \cdot 3^{n-1}), 1/(2 \cdot 3^{n-1})]$. Consequently,

$$C_0^n(i) = d_i^n + \bigcup_{i=0}^{3^n-1} \left[\frac{2i}{3^n}, \frac{2i+1}{3^n} \right].$$

The rightmost boundary point of $C_0^n(i)$ is thus $d_i^n + 2 - 1/3^n$. It is easy to see that all $d_i^n, i \in \mathbb{Z}$ converge almost surely as n grows, so that

$$\lim_n d_i^n = i + \xi, \text{ where } \xi = -1/2 + \sum_{k=0}^{\infty} u'_k.$$

Therefore, for all i ,

$$\liminf C_0^n(i) = \limsup C_0^n(i) = i + \xi + [0, 2].$$

Every point of \mathbb{R} turns out to be covered by at least two limit cells, therefore Θ_0^∞ is not a tessellation.

Remark 3.4.1 Theorem 3.4.2 together with Example 3.4.1 show that in the self-similar case $\{C_0^\infty(x_i^0)\}$ constitute a tessellation if and only if (3.29) holds.

Remark 3.4.2 The sequence of the Poisson-Voronoi tessellations with exponentially growing intensities $\lambda_n = \lambda^n$ for $\lambda > 1$ is self-similar (with $\kappa = \lambda^{1/d}$). In view of Corollary 3.3.4, the condition (3.29) is satisfied, and thus the family $\{C_0^\infty(x_i^0)\}$ constitutes a tessellation of \mathbb{R}^d . Closely examining the proof of Theorem 3.4.2 it is seen that the key step is to find a vanishing upper bound for the left-hand side of (3.30). For instance, for PVAT with super-exponential growth of intensities: $\liminf_n \lambda_{n+1}/\lambda_n > 1$, it will again be bounded by p^n , because $\mathbf{P}\{T_n < \infty \mid T_{n-1} = k\}$ is not increasing in k for all sufficiently large k . Thus (3.26) also holds for the super-exponential case.

3.5 Asymptotics of the Spherical Contact Distribution Function

From now on we confine ourselves to PVAT with exponentially growing intensities. As shown in Remark 3.4.2, the limit Poisson-Voronoi tessellations exist and the boundary of the limit cells Γ_0^∞ is a random closed set defined by (3.27). One of its important characteristics is the *spherical contact distribution function* $H(r)$, defined as

$$H(r) = \mathbf{P}\{\Gamma_0^\infty \cap b(0, r) \neq \emptyset \mid 0 \notin \Gamma_0^\infty\}, \quad r \geq 0.$$

Here the probability of the condition is one, thus $H(0) = 0$. Some information on the degree of variability of the cell boundary can be derived from the rate at which $H(r)$ decreases as r tends to zero. The aim of this section is to prove the following result.

Theorem 3.5.1 *For PVAT with exponentially growing intensities $\lambda_n = \lambda^n$ for some $\lambda > 1$, there exist constants $K > 0$ and $q \in (0, 1)$ given in (3.37) such that for all $r \geq 0$,*

$$H(r) = \mathbf{P}\{b(0, r) \cap \Gamma_0^\infty \neq \emptyset\} \leq Kr^{dq}.$$

Proof. Consider the cells of the limit tessellation $\{C_n^\infty(x_i^n)\}$ defined in the same way as in (3.25). Let $X(n, r)$ be the nuclei of those cells whose boundary crosses the ball $b(0, r)$, i.e.

$$X(n, r) = \{x_i^n \in \Pi_n : \partial C_n^\infty(x_i^n) \cap b(0, r) \neq \emptyset\}.$$

We will first prove the estimate: for each $n \geq 1$ and for each $s > 0$,

$$\mathbf{P}\{b(0, r) \cap \Gamma_0^\infty \neq \emptyset\} < f(r, n, s)^n, \quad (3.31)$$

where

$$f(r, n, s) = 1 - \mathbf{P}\{X(n, r) \subset b(0, s)\} \mathbf{P}\{b(0, s) \subset C^{n-1}(x^{n-1}(0))\},$$

and $x^{n-1}(0)$ denotes the closest point of Π_{n-1} to 0. Consider the events

$$E(m, r) = \{b(0, r) \cap \Gamma_m^\infty \neq \emptyset\},$$

where Γ_m^∞ is the boundary of the tessellation $\{C_m^\infty(x_i^m)\}$. Note that $E(0, r)$ is the event in the left-hand side of (3.31). Since $\Gamma_m^\infty \subset \Gamma_{m+1}^\infty$, we have $E(m, r) \subset E(m+1, r)$ and therefore

$$\begin{aligned} \mathbf{P}\{E(0, r)\} &= \mathbf{P}\{E(1, r)\} \mathbf{P}\{E(0, r) \mid E(1, r)\} \\ &= \mathbf{P}\{E(n, r)\} \prod_{m=1}^n \mathbf{P}\{E(m-1, r) \mid E(m, r)\} \\ &< \prod_{m=1}^n \mathbf{P}\{E(m-1, r) \mid E(m, r)\}. \end{aligned} \quad (3.32)$$

We assert that for every m and $s_m > 0$,

$$\mathbf{P}\{E(m-1, r) \mid E(m, r)\} \leq f(r, m, s_m). \quad (3.33)$$

Indeed, if $b(0, r) \cap \Gamma_m^\infty \neq \emptyset$ and

$$X(m, r) \subset b(0, s_m) \subset C^{m-1}(x^{m-1}(0))$$

then the cells $C_m^\infty(x_i^m)$ for which $x_i^m \in X(m, r)$ join in $C_{m-1}^\infty(x^{m-1}(0))$ so that $b(0, r) \cap \Gamma_{m-1}^\infty = \emptyset$.

Since the intensity of each Π_n equals λ^n , the distributions of

$$(\Pi_n, \Pi_{n+1}, \dots) \quad \text{and} \quad (\lambda^{1/d}\Pi_{n+1}, \lambda^{1/d}\Pi_{n+2}, \dots)$$

coincide. Consequently, the sets $X(m+1, r)$ and $\lambda^{-1/d}X(m, \lambda^{1/d}r)$ have the same distribution, and

$$\begin{aligned} \mathbf{P}\{X(m+1, r) \subset b(0, s_m)\} &= \mathbf{P}\{\lambda^{-1/d}X(m, \lambda^{1/d}r) \subset b(0, s_m)\} \\ &= \mathbf{P}\{X(m, \lambda^{1/d}r) \subset b(0, \lambda^{1/d}s_m)\} \\ &< \mathbf{P}\{X(m, r) \subset b(0, \lambda^{1/d}s_m)\}, \end{aligned}$$

as $X(m, r) \subseteq X(m, \lambda^{1/d}r)$. Also

$$\mathbf{P}\{b(0, s_m) \subset C^m(x^m(0))\} = \mathbf{P}\{b(0, \lambda^{1/d}s_m) \subset C^{m-1}(x^{m-1}(0))\}$$

so that $f(r, m-1, \lambda^{1/d}s_m) < f(r, m, s_m)$. Alternatively, $f(r, m, s_m) < f(r, m+1, \lambda^{-1/d}s_m) < f(r, n, \lambda^{-(n-m)/d}s_m)$ by induction. Thus, taking $s_m = \lambda^{(n-m)/d}s$ in (3.33), by (3.32) we obtain (3.31).

Next, we find a bound for $f(r, n, s)$. We have

$$\begin{aligned} 1 - \mathbf{P}\{X(n, r) \subset b(0, s)\} &= 1 - \mathbf{P}\{X(0, \lambda^{n/d}r) \subset b(0, \lambda^{n/d}s)\} \\ &< \mathbf{P}\{\exists x_i^0 : x_i^0 \notin b(0, \lambda^{n/d}s) \text{ and } C_0^\infty(x_i^0) \cap b(0, \lambda^{n/d}r) \neq \emptyset\} \\ &< \mathbf{E} \sum_{x_i^0 \in \Pi_0} \mathbb{I}(\|x_i^0\| > \lambda^{n/d}s \text{ and } C_0^\infty(x_i^0) \cap b(0, \lambda^{n/d}r) \neq \emptyset). \end{aligned}$$

By the Campbell theorem, the last expectation equals

$$\begin{aligned} &\int_{\|z\| > \lambda^{n/d}s} \mathbf{P}^0\{C_0^\infty(0) \cap b(-z, \lambda^{n/d}r) \neq \emptyset\} dz \\ &= \int_{\|z\| > \lambda^{n/d}s} \mathbf{P}^0\{R_\infty(0) > \|z\| - \lambda^{n/d}r\} dz \\ &= \lambda^n \int_{\|z\| > s} \mathbf{P}^0\{R_\infty(0) > \lambda^{n/d}(\|z\| - r)\} dz. \quad (3.34) \end{aligned}$$

Choose $s = 2r$. Then by (3.15), the right-hand side of (3.34) does not exceed

$$\begin{aligned} c_1 \lambda^n \int_{\|z\| > 2r} e^{-c_2 \lambda^n (\|z\| - r)^d} dz \\ &= c_1 \lambda^n \int_{2r}^\infty db_d \rho^{d-1} e^{-c_2 \lambda^n (\rho - r)^d} d\rho \\ &= c_1 \lambda^n \int_r^\infty db_d (\rho + r)^{d-1} e^{-c_2 \lambda^n \rho^d} d\rho \\ &\leq (2^{d-1} c_1 / c_2) e^{-c_2 \lambda^n r^d}. \end{aligned}$$

Denote $a = (1/c_2) \log(2^d c_1 / c_2)$ and choose $n = \lfloor d \log_\lambda(a/r) \rfloor + 1$, where $\lfloor x \rfloor = \max\{k \in \mathbb{Z} : k \leq x\}$. With such n , the inequality $a \leq \lambda^n r^d \leq \lambda a$ holds and $(2^{d-1} c_1 / c_2) e^{-c_2 \lambda^n r^d} \leq 1/2$. Therefore,

$$\mathbf{P}\{X(n, r) \subset b(0, s)\} \geq 1/2. \quad (3.35)$$

Since there is only one Voronoi cell that may contain a ball, we may

write

$$\begin{aligned}
& \mathbf{P}\{b(0, s) \subset C^{n-1}(x^{n-1}(0))\} \\
&= \mathbf{P}\{b(0, \lambda^{(n-1)/d}s) \subset C^0(x^0(0))\} \\
&= \mathbf{E} \sum_{x_i^0 \in \Pi_0} \mathbb{I}\{b(0, \lambda^{(n-1)/d}s) \subset C^0(x_i^0)\} \\
&= \int \mathbf{P}^0\{b(z, \lambda^{(n-1)/d}s) \subset C^0(0)\} dz.
\end{aligned}$$

Using the lower bound from (3.18), for s and n chosen as above we obtain

$$\begin{aligned}
\mathbf{P}\{b(0, s) \subset C^{n-1}(x^{n-1}(0))\} &> b_d \lambda^{n-1} s^d \exp\{-b_d \lambda^{n-1} (3s)^d\} \\
&\geq (2^d ab_d / \lambda) \exp\{-6^d ab_d\}.
\end{aligned} \tag{3.36}$$

Putting together (3.35) and (3.36) we get from (3.31)

$$\begin{aligned}
& \mathbf{P}\{b(0, r) \cap \Gamma_0^\infty \neq \emptyset\} \\
&\leq \left[1 - (2^{d-1} ab_d / \lambda) \exp\{-6^d ab_d\}\right]^{(d \log_\lambda(a/r)) + 1} \leq K r^{dq},
\end{aligned}$$

where

$$\begin{aligned}
q &= -\log_\lambda \left[1 - (2^{d-1} ab_d / \lambda) \exp\{-6^d ab_d\}\right] \\
K &= a^{-dq}.
\end{aligned} \tag{3.37}$$

Since $\lambda > 1$, we have $0 < q < 1$. The theorem is proved.

3.6 Properties of the Fractal Cell Boundary

In the case of exponentially growing intensities, the distributions of Γ_0^∞ and Γ_n^∞ scaled by $\lambda^{n/d}$ coincide, i.e. the boundary of the limit tessellation is statistically self-similar. This property is rather different from geometrical self-similarity in the sense of Γ_0^∞ being a union of scaled copies of self. However, by construction, Γ_{n-1}^∞ consists of parts of Γ_n^∞ , and therefore Γ_0^∞ has a similar structure at any scale of observation, which allows us to call it a fractal.

The primary characteristic of a fractal is its dimension, which can be defined in several ways. We will be interested in the *Hausdorff dimension* of Γ_0^∞ (see e.g. [17, p. 20–23] for the definitions of different dimensions that we use here).

Theorem 3.6.1 *Let q be the constant defined in (3.37). Then for PVAT with exponentially growing intensities: $\lambda_n = \lambda^n$ for some $\lambda > 1$, one has*

$$\begin{aligned} \dim_H \Gamma_0^\infty &= \mathbf{E} \dim_H \Gamma_0^\infty && \text{a.s.}, \\ \dim_H \Gamma_0^\infty &< d(1 - q) && \text{a.s.} \end{aligned}$$

Proof. Consider the collection of mesh cubes of size M in \mathbb{R}^d and let $\{\theta_\alpha\}$ be the family of shifts translating the cube at the origin $[0, M]^d$ by the vector $M\alpha$, where $\alpha = (\alpha_1, \dots, \alpha_d) \in \mathbb{Z}^d$. Introduce also

$$\Gamma_0^\infty(M) = \Gamma_0^\infty \cap [0, M]^d, \quad \theta_\alpha \Gamma_0^\infty(M) = \Gamma_0^\infty \cap \theta_\alpha [0, M]^d.$$

Since $\theta_\alpha \Gamma_0^\infty(M) \subset \Gamma_0^\infty$, with probability 1 for all $\alpha \in \mathbb{Z}^d$, we have

$$\dim_H \Gamma_0^\infty \geq \dim_H \theta_\alpha \Gamma_0^\infty(M).$$

Denote $\Lambda_N = \{\alpha : |\alpha_i| \leq N, i = 1, \dots, d\}$. Obviously,

$$\dim_H \Gamma_0^\infty \geq \sup_{\alpha \in \Lambda_N} \dim_H \theta_\alpha \Gamma_0^\infty(M).$$

Now by the ergodic theorem,

$$\begin{aligned} \dim_H \Gamma_0^\infty &\geq \lim_{N \rightarrow \infty} \sup_{\alpha \in \Lambda_N} \dim_H \theta_\alpha \Gamma_0^\infty(M) \\ &\geq \lim_{N \rightarrow \infty} \frac{1}{(2N)^d} \sum_{\alpha \in \Lambda_N} \dim_H \theta_\alpha \Gamma_0^\infty(M) \\ &= \mathbf{E} \dim_H \Gamma_0^\infty(M). \end{aligned}$$

Letting $M \rightarrow \infty$ in this inequality and using the property of monotonicity of the Hausdorff dimension, we get

$$\dim_H \Gamma_0^\infty \geq \mathbf{E} \dim_H \Gamma_0^\infty,$$

which implies the first equality of the theorem.

To prove the second inequality, we make use of the estimate of the Hausdorff dimension of a set by its upper box dimension (see e.g. [17, p. 24]). Let $N_\varepsilon(B)$ be the smallest number of closed balls of radius ε that cover B . Then

$$\dim_H \Gamma_0^\infty(M) \leq \limsup_{\varepsilon \rightarrow 0} \frac{\log N_\varepsilon(\Gamma_0^\infty(M))}{-\log \varepsilon}.$$

Take expectations at both sides of this inequality. It can be easily verified that $[0, M]^d$, and hence $\Gamma_0^\infty(M)$, can be covered by a family $\{b_i\}$ of less than $(M\sqrt{d}/2\varepsilon)^d$ balls of radius ε . Thus the function in the right-hand side under the limit is bounded by a constant not depending on ε , and therefore we can exchange the limit and the expectation. Moreover, the function $\log(\cdot)$ is concave, hence

$$\mathbf{E} \log(\cdot) \leq \log \mathbf{E}(\cdot).$$

Therefore,

$$\mathbf{E} \dim_H \Gamma_0^\infty(M) \leq \limsup_{\varepsilon \rightarrow 0} \frac{\log \mathbf{E} N_\varepsilon(\Gamma_0^\infty(M))}{-\log \varepsilon}.$$

Recalling the definition of the contact distribution $H(r)$ from the previous section, we get

$$\mathbf{E} N_\varepsilon(\Gamma_0^\infty(M)) \leq \mathbf{E} \sum_i \mathbb{I}(b_i \cap \Gamma_0^\infty(M)) \neq \emptyset \leq \left(\frac{M\sqrt{d}}{2\varepsilon} \right)^d H(\varepsilon).$$

From Theorem 3.5.1 it follows that

$$\begin{aligned} \mathbf{E} \dim_H \Gamma_0^\infty(M) & \\ & \leq \limsup_{\varepsilon \rightarrow 0} \frac{d \log(M\sqrt{d}/2) - d \log \varepsilon + \log K + dq \log \varepsilon}{-\log \varepsilon} = d(1 - q), \end{aligned}$$

and it remains to let $M \rightarrow \infty$ to obtain the second statement of the theorem.

3.7 Modeling Radio Cells of a Wireless Network

Optimization of a wireless network requires an adequate representation for the cellular structure. Its choice is important, for example, for testing different handover policies and for estimation of traffic load on base stations or mobile switching centers. In this section we present some motivation for the use of AT-based cell models.

In wireless communications, a radio cell of a base station can be defined as a set of locations where communication between the mobile terminal and the base station is possible with the signal quality above certain level. We start from the proposition that the quality of received signal is mainly due to the two factors:

- attenuation, which is a monotonous decrease of signal strength with the growth of the distance from the base station;
- fluctuations in propagation caused by land obstacles, channel interference, multipath reception, etc.

Voronoi models of radio cells take into account only the attenuation factor. An AT-based model may incorporate attenuation as a large-scale effect but also keep note of fluctuations at smaller scales.

For example, suppose that some additional information is available that makes it possible to partition the service area into a number of small zones with uniform propagation conditions and hence, uniform signal quality. Examples of such zones are a water area or a room in a building. A zone thus corresponds to an equivalence class on the set of possible mobile locations, with an obvious assumption that all mobile terminals within a zone are served by the same base station. A radio cell is then constructed as a cluster of zones. In order to decide whether a zone has to be assigned to a base station, it is sufficient to compare the signal strengths from different stations at some reference point chosen within that zone.

Denote by $\Theta^1 = \{C^1(x_i^1)\}$ the tessellation of \mathbb{R}^d corresponding to the partition of the service area into the zones of uniform signal quality, as described above. The nuclei $\{x_i^1\}$ represent the reference points placed, for example, at the gravity centers of the zones (the particular choice of x_i^1 within $C^1(x_i^1)$ is not important). Let $\{x_i^0\}$ be the coordinates of the base stations in the service area. For selected reference points $\{x_i^1\}$, it is natural to follow the general connection principle (see 1.2) and to assume that a mobile in x_i^1 is connected to the closest base station from $\{x_i^0\}$. Hence, if $\Theta^0 = \{C^0(x_i^0)\}$ is the Voronoi tessellation of \mathbb{R}^d generated by $\{x_i^0\}$, the radio cell of the station at x_i^0 is exactly the aggregate cell $C_0^1(x_i^0)$.

As follows from Theorem 3.2.1, an AT with its coverage function obtained by convolution may be interpreted as a spatial analog of the sum of independent random variables. A general stochastic model of a cellular structure is given by an aggregate tessellation of order n

$$\Theta_0^n = \Theta^0 \circ \Theta^1 \circ \dots \circ \Theta^n,$$

where Θ^0 is a Voronoi tessellation (ideal cellular system influenced only by the attenuation effect) and where $\Theta^1, \dots, \Theta^n$ are independent components introducing the effect of fluctuation of the signal strength. The fluctuations are modulated by the intensities λ_k of the nuclei processes $\{x_i^k\}$, $k = 1, 2, \dots, n$. As Figures 1.8 and 1.9 on page 38 show, ATs provide a promising model

of cellular structures with good resemblance to the patterns observed in practice.

Appendix A

Point Processes and Related Objects

A.1 Point Processes: Definitions and Basic Properties

The aim of this section is to give a definition of a random point process. This is done much in the same way as definition of a random variable: a point process is a measurable mapping from an abstract probability space $[\Omega, \mathcal{F}, \mathbf{P}]$ into the phase space of point patterns. However, it needs to be specified, what exactly is the state space, and what are the subsets of the state space that we consider events in these settings. We are concerned with the Euclidean d -dimensional space \mathbb{R}^d , a thorough introduction to the theory of point processes in complete separable metric spaces can be found in [15].

A.1.1 Random Point Patterns

A subset of \mathbb{R}^d is called *boundedly finite* if it has finite number of points in every bounded $A \in \mathcal{B}(\mathbb{R}^d)$. The state space of point processes is the set \mathcal{P} of all countable boundedly finite sets. Because \mathbb{R}^d has finite dimension, it coincides with the set of all closed boundedly finite sets.

For any $\mathcal{N} \in \mathcal{P}$ and $A \subset \mathbb{R}^d$, let $\mathcal{N}(A)$ be the number of points of \mathcal{N} containing in A . Define the σ -field of events on \mathcal{P} as the smallest σ -field with respect to which the mapping

$$\mathcal{N} \rightarrow \mathcal{N}(A)$$

is measurable for all bounded $A \in \mathcal{B}(\mathbb{R}^d)$. Equivalently, it can be defined as the σ -field generated by the sets

$$\{\mathcal{N} \in \mathcal{P} : \mathcal{N}(A) = k\}, \quad A \in \mathcal{B}(\mathbb{R}^d), k \in \mathbb{N}.$$

Denote this σ -field by $\mathcal{B}(\mathcal{P})$. Such notation is justified by the existence of a relevant metric on \mathcal{P} , see [15, Th.A2.6.III], with respect to which $\mathcal{B}(\mathcal{P})$ is a Borel σ -field.

Definition A.1.1 *A point process in \mathbb{R}^d is a measurable mapping from probability space $[\Omega, \mathcal{F}, \mathbf{P}]$ into $[\mathcal{P}, \mathcal{B}(\mathcal{P})]$.*

Thus, with every elementary outcome $\omega \in \Omega$ a particular realization $\mathcal{N}(\omega)$ is associated. By the above remark, $\mathcal{N}(A)$ is a well-defined random variable for every bounded $A \in \mathcal{B}(\mathbb{R}^d)$.

Finite-dimensional Distributions

Definition A.1.2 *The finite-dimensional distributions of a point process \mathcal{N} is the collection of joint distributions of the random variables*

$$\mathcal{N}(A_1), \mathcal{N}(A_2), \dots, \mathcal{N}(A_n)$$

for all finite families of bounded Borel sets A_1, A_2, \dots, A_n .

The distribution of a point process \mathcal{N} is completely defined by its finite-dimensional distributions. There exists an analogue of the Kolmogorov theorem establishing conditions for a family of distribution functions to define a point-process, see [15, Prop.6.2.III and Th.6.2.VII].

Stationarity For $t, x \in \mathbb{R}^d$ and $A \subset \mathbb{R}^d$, consider the group of transformations (shifts) $\{\theta_t\}$ such that

$$\theta_t x = x + t, \quad \theta_t A = A + t = \{x + t : x \in A\},$$

The shifts induce measurable transformations of \mathcal{P} , such that for all bounded $A \in \mathcal{B}(\mathbb{R}^d)$

$$\theta_t \mathcal{N}(A) = \mathcal{N}(\theta_t A).$$

Definition A.1.3 *A point process \mathcal{N} is stationary if for each $t \in \mathbb{R}^d$ the distributions of the processes \mathcal{N} and $\theta_t \mathcal{N}$ coincide.*

Representation of Point Processes as Measures Let \mathcal{M} be the space of all boundedly finite, integer-valued measures, called *counting measures*. There exists a one-to-one mapping between \mathcal{P} and \mathcal{M} : each boundedly finite countable set \mathcal{N} corresponds to a counting measure $\mu_{\mathcal{N}}$ on $\mathcal{B}(\mathbb{R}^d)$ such that for every bounded $A \in \mathcal{B}(\mathbb{R}^d)$

$$\mathcal{N}(A) = \mu_{\mathcal{N}}(A).$$

Indeed, let $\mathcal{N} = \{x_i\}$ (for some measurable numbering of points) and denote by \mathcal{N}' a maximal subset of \mathcal{N} with all disjoint points. Then

$$\mu_{\mathcal{N}} = \sum_{x_i \in \mathcal{N}'} n_i \delta_{x_i},$$

where $n_i = \mathcal{N}(\{x_i\})$ and δ_x is the Dirac measure. Conversely, if μ is a counting measure belonging to \mathcal{M} , then using the continuity of measures it is easy to show that the support of μ is a countable boundedly finite set satisfying the condition. Hence, point processes, though important in their own right, can be regarded as a particular case of random measures. Also, such view introduces certain uniformity in the general theory. For example, for corresponding \mathcal{N} and $\mu_{\mathcal{N}}$ in this context

$$\mathbf{E}\mathcal{N}(A) = \iint_{\Omega \times A} \mu_{\mathcal{N}}(\omega, dx) \mathbf{P}(d\omega).$$

Thus we may treat the elements of \mathcal{P} as measures where it is convenient.

Simple Point Processes Consider a subspace \mathcal{P}' of countable boundedly finite sets $\mathcal{N}' = \{x_i\}$ such that $x_i \neq x_j$, if $i \neq j$. Let $\mathcal{B}(\mathcal{P}')$ be the smallest σ -field with respect to which the mapping

$$\mathcal{N} \rightarrow \mathcal{N}(A)$$

is measurable for $\mathcal{N} \in \mathcal{P}'$ and for all bounded $A \in \mathcal{B}(\mathbb{R}^d)$. It can be easily seen that $\mathcal{B}(\mathcal{P}') \subset \mathcal{B}(\mathcal{P})$.

Definition A.1.4 A simple point process in \mathbb{R}^d is a measurable mapping from probability space $[\Omega, \mathcal{F}, \mathbf{P}]$ into $[\mathcal{P}', \mathcal{B}(\mathcal{P}')]$.

Throughout the thesis we consider only *simple* point processes.

Definition A.1.5 For a simple point process \mathcal{N} , the function of $A \in \mathcal{B}(\mathbb{R}^d)$

$$\Lambda(A) = \mathbf{E}\mathcal{N}(A)$$

is called the *intensity measure*.

The fact that Λ is a measure is proved e.g. in [15]. If a simple point process is stationary, then $\Lambda(B) = \lambda|B|$ for any $B \in \mathcal{B}(\mathbb{R}^d)$, where $|\cdot|$ is the Lebesgue measure on \mathbb{R}^d , and λ is the constant called the *intensity* of the process.

Definition A.1.6 Consider a simple point process $\mathcal{N} = \{x_i\}$ in $[\Omega, \mathcal{F}, \mathbf{P}]$ and a family $\{m_i\}$ of measurable mappings of $[\Omega, \mathcal{F}, \mathbf{P}]$ into a measurable space $[M, \mathcal{F}_M]$. The set $\mathcal{N}_m = \{[x_i, m_i]\} \subset \mathcal{P} \times M$ is called a *marked point process*. The random variables m_i are called *marks* of the points of \mathcal{N} .

Shifts act on marked point processes in the following manner

$$\theta_t \mathcal{N}_m = \{[x_i + t, m_i]\}.$$

Definition A.1.7 A marked point process \mathcal{N}_m is stationary if for each $t \in \mathbb{R}^d$ the distributions of the processes \mathcal{N}_m and $\theta_t \mathcal{N}_m$ coincide.

A.1.2 Palm Probability

The concept of Palm probability arised from the necessity to consider events “on condition that the point process has a point at a given location”.

Definition A.1.8 The *Palm probability* is a probability measure on $[\Omega, \mathcal{F}]$ defined by

$$\mathbf{P}^0(U) = \frac{1}{\lambda|A|} \mathbf{E} \sum_{x_i \in \mathcal{N}} \mathbb{I}_U(\theta_{x_i} \mathcal{N}) \mathbb{I}_A(x_i).$$

Formally, the Palm probability is defined on the subset \mathcal{P}^0 of \mathcal{P} of all point process configurations having a point at the origin. By stationarity, the definition does not depend on the choice of A . Its heuristic interpretation is the following. Let $\mathcal{N}(\omega) = \{x_i\}$ be a realization of a simple stationary point process, and let A be a bounded Borel subset of \mathbb{R}^d . Consider the family of shifted realizations $\{\theta_{x_i} \mathcal{N}(\omega)\}$ generated by $x_i \in \mathcal{N}(\omega) \cap A$. The Palm probability is the ratio of the two values: the average number of the occurrences when the shifted realizations verify the event U and the average number of the realizations in the family. The corresponding expectation is denoted by \mathbf{E}^0 .

The Palm probability can be inverted, i.e. the stationary distribution of \mathcal{N} can be determined from \mathbf{P}^0 and λ . For a configuration $\mathcal{N} \in \mathcal{P}^0$, consider the area

$$C(0, \mathcal{N}) = \{y \in \mathbb{R}^d : \|y\| \leq \|y - x_j\|\},$$

which is a cell of the Voronoi tessellation defined in the next section. Then, for any measurable non-negative function f ,

$$\mathbf{E} f(\mathcal{N}) = \lambda \mathbf{E}^0 \int_{C(0, \mathcal{N})} f(\theta_x \mathcal{N}) dx.$$

Campbell's theorem For any non-negative, measurable function f on $\mathbb{R}^d \times \mathcal{P}$,

$$\mathbf{E} \sum_{x_i \in \mathcal{N}} f(x_i, \mathcal{N}) = \lambda \int_{\mathbb{R}^d} \mathbf{E}^0 f(z, \theta_{-z} \mathcal{N}) dz.$$

The above expression is called the refined Campbell formula. It is a partial case of the so-called Mecke formula (see e.g. [3]), which is the Swiss Army knife of the Palm calculus. It may be understood as a form of Fubini's theorem in the context of point processes providing the relation between the stationary and the Palm probability.

A.1.3 Poisson Process

The Poisson process is, perhaps, the most widely used object in models involving random point patterns. Its characteristic property is complete randomness: for a family of disjoint test sets, the number and position of points in one set does not influence the number and position of points in the others. Hence, constructions based on Poisson process are sufficiently rich to represent a large number of real-world objects and sufficiently simple to allow for an analytical treatment. An elementary introduction to the structure and properties of the Poisson process may be found in [34], see also [15] for more technical discussion.

Definition A.1.9 Let $\Lambda(A)$ be a boundedly finite measure on $\mathcal{B}(\mathbb{R}^d)$. A Poisson process (usually denoted by Π) is a point process whose finite-dimensional distributions are defined as follows

- 1 For every bounded $A \in \mathcal{B}(\mathbb{R}^d)$, the random variable $\Pi(A)$ has Poisson distribution with the parameter $\Lambda(A)$:

$$\mathbf{P}(\Pi(A) = k) = \frac{(\Lambda(A))^k}{k!} \exp(-\Lambda(A)).$$

- 2 For every family of disjoint sets A_1, A_2, \dots, A_n from $\mathcal{B}(\mathbb{R}^d)$, the random variables

$$\Pi(A_1), \Pi(A_2), \dots, \Pi(A_n)$$

are independent.

From this definition it follows that $\mathbf{E}\Pi(A) = \Lambda(A)$. Hence, the distribution of a Poisson process is completely defined by its intensity measure. A Poisson process is simple when the measure Λ has no atoms. In the special case when $\Lambda(B) = \lambda|B|$ for any $B \in \mathcal{B}(\mathbb{R}^d)$, the Poisson process Π is called *homogeneous*.

A.2 Voronoi Diagram and Delaunay Graph

The concept of Voronoi diagram is used in a great variety of applications, with the scope ranging from astronomy and physics to biology and social sciences. It is constructed by partitioning the space \mathbb{R}^d into the areas between the points of the nuclei set $\{x_i\}$ so that the area assigned to x_i consists of all points of \mathbb{R}^d that are closer to x_i than to any other point of the nuclei set.

Definition A.2.1 *The Voronoi diagram with the nuclei set $\{x_i\} \in \mathcal{P}'$ is a family of subsets of \mathbb{R}^d defined by*

$$C(x_i) = \{y \in \mathbb{R}^d : \|y - x_i\| \leq \|y - x_j\|, j \neq i\}.$$

The set $C(x_i)$ is called a *Voronoi cell* with the *nucleus* x_i . It can be easily seen that the cells of a Voronoi diagram are all non-empty convex polytopes and that $\mathbb{R}^d = \cup_i C(x_i)$. The boundary and the intersection of any number of Voronoi cells have Lebesgue measure zero.

A Voronoi diagram is unique if all points of the nuclei set are in a general quadratic position: no $k + 1$ points lie on a $(k + 2)$ -dimensional hyperplane, $k = 2, \dots, d$, and no $d + 2$ points lie on the boundary of a sphere.

The boundary of each Voronoi cell consists of convex polytopes, called facets. More specifically, a $(d - k)$ -facet is defined as a non-void intersection of $k + 1$ neighboring cells, $k = 0, 1, \dots, d$. The dimension of a $(d - k)$ -facet equals $d - k$, provided that the points of the nuclei set are in general quadratic position.

Definition A.2.2 *A tessellation Θ of \mathbb{R}^d is a countable collection of closed bounded subsets of \mathbb{R}^d called cells such that*

- (a) *union of all cell is the whole space;*
- (b) *intersection of any different two cells has Lebesgue measure zero;*
- (c) *each bounded set intersects a finite number of cells.*

As follows from the definition, some auxiliary conditions on the nuclei set are needed for a Voronoi diagram to be a tessellation.

The Delaunay graph is a dual object to the Voronoi diagram.

Definition A.2.3 *The Delaunay graph constructed on the vertex set $\{x_i\}$ is the graph connecting all the pairs of points (x_i, x_j) such that the Voronoi cells $C(x_i)$ and $C(x_j)$ share a $(d - 1)$ -facet.*

If the points of the set $\{x_i\}$ are in general quadratic position, then there is a one-to-one correspondence between the Delaunay graph and the Voronoi diagram.

A Voronoi diagram generated by a stationary point process is a tessellation, since all the Voronoi cells are bounded. A Poisson point process thus generates a Poisson-Voronoi tessellation and a Poisson-Delaunay graph. The distributions of this tessellation and this graph are thus themselves stationary and isotropic.

Appendix B

Résumé

Introduction

Les méthodes mathématiques jouent un rôle important pour la conception et l'exploitation des réseaux de télécommunications. Les problèmes de planification, d'évaluation des coûts et des performances, et d'optimisation de ces systèmes nécessitent le développement et l'analyse de modèles qui décrivent l'architecture du réseau, qui prennent en compte les positions et les modes d'interconnexion de ses éléments dans l'espace.

La notion d'objet aléatoire en géométrie stochastique s'est avérée très utile pour ce type de modélisation. L'idée de nouvelle approche, développée dans [4], est de représenter les composants d'un réseau (utilisateurs, nœuds, zones de service) par des familles d'objets aléatoires (processus ponctuels, graphes, pavages), c'est-à-dire, par des réalisations de processus stochastiques. Cette représentation donne des modèles dont les paramètres caractérisent les distributions de ces processus.

L'intérêt de cette approche probabiliste par rapport à une description combinatoire réside dans le fait que pour des grands réseaux, la description combinatoire (l'ensemble des caractéristiques des éléments individuels : types, positions, états) induit un très grand nombre de données qui sont très difficiles à analyser. La distribution des éléments du réseau dans l'espace est un objet plus simple que la collection des coordonnées individuelles, et les modèles peuvent être traités par des méthodes analytiques. En plus, le nombre de paramètres dans les modèles probabilistes ne dépend pas du nombre des éléments dans le réseau.

L'analyse de modèles stochastiques de réseaux dans l'espace est basée sur des méthodes *générales* de la géométrie stochastique, la théorie des processus

ponctuels, la statistique spatiale et la théorie des graphes. Il faut remarquer que les outils développés dans le cadre de cette approche pour l'étude de la géométrie des graphes et des pavages aléatoires ainsi que pour le calcul et l'optimisation des fonctionnelles de processus ponctuels ont d'autres domaines d'application.

La thèse se divise en deux parties. La première partie est inspirée par des problèmes de routage dans les réseaux homogènes. Elle est consacrée à l'étude des propriétés de chemins sur un graphe aléatoire représentant l'infrastructure de ce type de réseaux. Dans la deuxième partie, on s'intéresse à la géométrie des zones de service dans un réseau à plusieurs niveaux hiérarchiques. Pour cela on considère un modèle de partition de l'espace généré par une suite de pavages stationnaires.

Construction de modèles

Réseaux téléphoniques Dans §1.1 nous donnons la description schématique de divers réseaux de communication. Notre but est de décrire leur organisation spatiale, leurs fonctions et les principes d'interconnexion de leurs éléments de façon à mettre en évidence les structures communes à toutes les architectures et de montrer la possibilité de modélisation par une approche géométrique. Une introduction plus complète à l'architecture des réseaux se trouve par exemple dans [32]. Les trois types principaux de réseaux que l'on considère sont :

- Les réseaux téléphoniques fixes, destinés à fournir des services à des utilisateurs fixes. Les nœuds d'un tel réseau s'appellent commutateurs et sont organisés de manière hiérarchique : tous les commutateurs se trouvant dans une zone géographique particulière sont connectés sous forme d'étoile ou de boucle à un commutateur du niveau plus élevé. Le niveau le plus bas de la hiérarchie est composé des terminaux des utilisateurs. Le niveau le plus haut est composé de commutateurs reliés par des liaisons optiques à hauts débits.
- Les réseaux sans fil fixes avec des utilisateurs mobiles (*ad hoc*). Plusieurs stations de base sont déployées dans la région de service. Les utilisateurs possèdent des terminaux mobiles, qui peuvent communiquer avec les stations de base par transmission hertzienne et choisir la station dont le signal reçu a la meilleure qualité. La région de service est donc partitionnée en cellules dont la forme et la taille sont définies par la qualité du signal reçu. Les stations mobiles sont raccordées aux centres de contrôle qui assurent le transfert des données, la recherche

des mobiles, l'acheminement des appels et la commutation avec les réseaux fixes.

- Les réseaux sans fil avec stations mobiles. Dans un tel réseau, les stations sont les utilisateurs du réseau qui se déplacent dans l'espace sans aucun contrôle centralisé. Les stations communiquent par transmission hertzienne. Le transfert d'information se fait par des paquets, un mécanisme de routage (voir ci-dessous) assure que chaque station mobile peut faire le relai des paquets vers leurs destinations.

Les principes de la modélisation La construction des modèles est le thème principal de §1.2. Pour simplifier la terminologie, nous utiliserons par la suite les termes génériques : *station* et *lien* pour décrire les deux principales entités dans un réseau. Selon le cas, *station* désignera donc un commutateur, une station de base, un routeur ou une station mobile. Un *lien* entre deux stations est un moyen de transfert d'information sans référence au type de médium (câble, fibre optique, liaison hertzienne, etc).

Un modèle doit fournir une description simple et synthétique d'un objet. Les descriptions présentées dans §1.2. montrent que les stations sont organisées de manière hiérarchique et que dans chaque niveau de la hiérarchie, les positions de ces stations forment une configuration irrégulière de points. On ne possède souvent que des informations partielles concernant cette configuration : soit parce que la grande taille du système ne permet pas de le décrire complètement, soit parce que l'on s'intéresse aux propriétés d'un réseau hypothétique. Un processus ponctuel stochastique est par conséquent une représentation appropriée de l'ensemble des positions des stations. Le choix de sa distribution dépend des hypothèses que le modèle doit vérifier. Le cas le plus simple est de supposer l'absence d'interactions entre les points, ce qui est la propriété caractéristique de la distribution du processus de Poisson. De manière schématique, les liens dans les réseaux hiérarchiques se divisent en deux classes :

- *Inter-liens*. Les connexions entre des stations de différents niveaux de la hiérarchie. Des exemples sont les boucles locales connectant les postes téléphoniques aux commutateurs et les canaux hertziens lors de la communication des mobiles avec des stations de bases. Les éléments connectés par ce type de lien sont en relation «parent – descendant»,
- *Intra-liens*. Les connexions entre les stations de même niveau. Des exemples sont les liens d'un réseau téléphonique entre les commutateurs du niveau le plus haut ou les canaux radio dans un réseau *ad hoc*.

Quelques hypothèses générales permettent d'affiner la description de la struc-

ture. Une pratique commune est de raccorder les éléments qui sont physiquement proches pour économiser les ressources. Dans les modèles de réseaux hiérarchiques, on peut donc supposer, qu'un inter-lien connecte toujours une station avec la station la plus proche du niveau supérieur et qu'un intra-lien connecte une paire de stations de même niveau si elles sont voisines.

Les pavages et les graphes sont les objets géométriques qui apparaissent naturellement lorsque l'on considère les connections entre les stations du réseau et les zones qu'elles desservent. Nous montrons maintenant comment les principes évoqués ci-dessus peuvent être traduits dans les modèles.

Modèle de base Considérons un réseau générique avec un seul niveau de hiérarchie. Chaque station dessert sa zone et les stations sont interconnectées. Une représentation simple de ce système peut être construite sur le plan (également sur \mathbb{R}^d) avec trois composantes : un processus de Poisson $\Pi = \{x_i\}$, un pavage de Voronoi $\Theta = \{C(x_i)\}$ généré par Π , et le graphe de Delaunay D ayant Π comme ensemble de sommets.

La cellule de Voronoi $C(x_i)$ de noyau x_i est définie comme l'ensemble des points du plan qui sont plus proches de x_i que de n'importe quel autre point $x_j \in \Pi$. Les arêtes du graphe de Delaunay connectent les sommets x_i et x_j si les cellules $C(x_i)$ et $C(x_j)$ ont une face commune de dimension $d-1$. Le modèle tient donc compte des hypothèses de raccordement local.

Ce modèle sert d'élément de base pour construire des modèles de systèmes plus complexes. Il admet plusieurs interprétations :

- Le niveau supérieur (dit *core*) d'un réseau téléphonique fixe. Les points du processus sont les coordonnées des commutateurs. Le pavage de Voronoi représente la division de l'espace entre les régions desservies par chaque commutateur et le graphe de Delaunay représente l'infrastructure des intra-liens.
- La partie fixe d'un réseau sans fil. Le processus Π est une configuration des stations de base, les cellules du pavage Θ sont les cellules radio dans le cas où la propagation est idéale.
- Image instantanée d'un réseau mobile. Le processus Π donne une configuration des stations mobiles, le graphe de Delaunay représente les liaisons radio établies entre les stations.

Modèle hiérarchique Le modèle hiérarchique est une extension du modèle de base avec les mêmes hypothèses. Considérons une suite de processus de Poisson indépendants

$$\Pi_0, \Pi_1, \dots, \Pi_n,$$

où $\Pi_k = \{x_i^k\}$ représente les stations du niveau k . Soit $\Theta^k = \{C^k(x_i^k)\}$ le pavage de Voronoi généré par Π_k . Les stations de Π_{k+1} qui sont plus près de x_i^k que des autres points de Π_k se trouvent donc dans $C^k(x_i^k)$. Les inter-liens connectent chaque station x_i^{k+1} du niveau $k+1$ qui se trouve dans la cellule $C^k(x_i^k)$ au noyau x_i^k de cette cellule. Les liens forment donc une famille d'arbres couvrants (Fig. 1.5, page 22). Les intra-liens connectent chaque paire de stations x_i^0 et x_j^0 du niveau supérieur dont les cellules $C^0(x_i^0)$ et $C^0(x_j^0)$ partagent une face de dimension $d-1$.

Ce modèle représente un réseau téléphonique fixe (avec des utilisateurs considérés comme points du plan ou donnés par le processus ponctuel Π_n) et la partie fixe d'un réseau sans fil.

Notons que les règles d'interconnexion dans ce modèle sont imposées par les pavages Θ_k associés avec Π_k . On peut donc changer la définition de Θ_k et considérer d'autres modes de raccordement que la connexion à la station la plus proche. On peut aussi introduire les connexions entre les stations de niveaux non-adjacents et varier la représentation des intra-liens (par exemple, considérer l'arbre couvrant minimal sur un sous-ensemble fini de Π_0). Finalement, un choix doit être fait pour les mesures d'intensité $\Lambda_k(\cdot)$ des processus Π_k . Le modèle homogène où $\Lambda_k(\cdot) = \lambda_k |\cdot|$ (proportionnelle à la mesure de Lebesgue) permet d'avancer dans l'analyse et sert comme modèle de référence. Il peut être utilisé pour les régions où la densité démographique et la concentration des éléments de réseau sont approximativement constantes.

Modèle d'un réseau sans fil Le modèle d'un réseau sans fil est une superposition de deux composantes : une partie fixe (stations de base, centres de contrôle) et une partie mobile. La première composante peut être décrite comme un modèle de base ou un modèle hiérarchique. La partie mobile est basée sur une représentation des positions et d'états des mobiles sur l'ensemble des routes. Les routes sont données par un processus de Poisson de lignes $\Pi_l = \{D_i\}$, qui est un processus de Poisson dans l'espace des phases $(p, \alpha) \in \mathbb{R} \times [0, \pi)$ (distance de l'origine, inclinaison). Les processus de trafic sur $\{D_i\}$ décrivant les positions et les états de mobiles sur l'ensemble de routes sont définis comme des marques indépendantes des D_i , voir [7].

Analyse des modèles Un survey sur les problèmes qui peuvent être abordés par l'approche de la géométrie stochastique est proposé dans §1.3 (voir aussi [20] et [21]). Nous donnons toutefois une brève description des résultats ayant trait aux modèles décrits ci-dessus.

Plusieurs quantités d'intérêt dans les réseaux se ramènent à des fonction-

nelles des objets géométriques apparaissant dans des modèles générés par des processus ponctuels. Par exemples : le coût de l'infrastructure arborescente rattachée à une station, la surface et autres paramètres des zones desservies par les commutateurs, ou bien le nombre des utilisateurs traversant une cellule de réseau mobile par l'unité de temps. Le premier type de résultats concerne les caractéristiques des distributions (moments, corrélations) de fonctionnelles de ce type [4], [7], [8]. Ces caractéristiques s'expriment au moyen de paramètres des processus stochastiques correspondants. Dans les modèles générés par des processus de Poisson homogènes, elles dépendent des intensités des processus et leurs formes explicites peuvent souvent être calculées. L'optimisation paramétrique devient donc possible. Un exemple d'optimisation de coût d'architecture dans le modèle hiérarchique est donné dans [8]. L'optimisation peut aussi être abordée par l'approche stochastique quand la forme explicite de la relation entre une caractéristique du réseau et les paramètres du modèle ne peut pas être calculée. La méthode des gradients stochastiques permet de construire des estimateurs pour les gradients de fonctionnelles de processus de Poisson homogènes à partir d'une seule réalisation [5], [61].

Chemins Markoviens sur le Graphe de Poisson–Delaunay

Le Chapitre 2 contient des résultats nouveaux concernant une classe de chemins construits par un algorithme simple sur le graphe de Poisson–Delaunay. L'intérêt d'une telle étude est justifié par les deux problèmes pratiques suivants : la recherche d'un algorithme de routage efficace et l'évaluation de coûts d'appel entre les deux stations d'un réseau.

Routage dans les réseaux mobiles Un routage est un mécanisme qui permet à deux utilisateurs du réseau de trouver un chemin de communication les reliant. Dans les réseaux à *commutation de paquets*, ce mécanisme assure qu'une station est capable de faire le relai des paquets vers toutes les destinations avec un coût d'envoi des paquets minimal (par exemple, les paquets suivront le plus court chemin entre la source et la destination).

Le routage peut s'effectuer en absence d'information centralisée sur les positions des stations et l'état des liens entre eux (situation typique pour des réseaux à stations mobiles et notamment les réseaux *ad hoc*). Dans ce cas, on utilise des algorithmes distribués : chaque station construit sa propre

vue de réseau en échangeant des informations avec son voisinage. Les algorithmes distribués se distinguent par le type d'informations échangées : soit ces informations sont les distances d'une station jusqu'à chaque destination (*distance-vector routing*), soit les coûts des liaisons d'une station avec chacun de ses voisins (*link-state routing*).

Les algorithmes distribués nécessitent un certain temps pour que les informations partielles sur l'état du réseau reçues par une station convergent dans une image globale. Si l'image du réseau perçue par une station et l'état actuel du réseau sont très différents, le routage par cette station est impossible.

La topologie d'un réseau mobile change plus fréquemment que celle d'un réseau fixe. Un certain temps est nécessaire pour que l'information sur ces changements se propage dans le réseau. Ce délai est particulièrement grand quand le protocole de routage cherche à construire les chemins les plus courts, parce que cela nécessite la mise à jour de tableaux de routage sur un grand nombre de stations.

Il est donc intéressant d'examiner des algorithmes de construction des chemins qui ne nécessitent pas d'échanges extensifs d'information entre les nœuds du réseau et qui néanmoins produisent des chemins relativement courts. Les modèles de géométrie stochastique représentant l'infrastructure du réseau permettent de tester de tels algorithmes en évaluant les caractéristiques des chemins correspondants.

L'autre intérêt d'étude de tels chemins est l'évaluation des coûts d'appels dans un réseau à commutation de circuits. Cette caractéristique doit prendre en compte le coût d'infrastructure utilisé par les circuits. Il est donc important d'établir une relation entre les coûts des circuits et la distance entre les utilisateurs.

Classe des Chemins Markoviens Dans le Chapitre 2 nous nous plaçons dans le cadre du modèle de base généré par un processus de Poisson homogène $\Pi = \{x_i\}$ et nous étudions des propriétés probabilistes d'une classe de chemins courts construits sur le graphe de Delaunay aléatoire par la méthode suivante. Soit s et t deux points quelconques dans R^d . Soit x_m et x_n les deux sommets du graphe de Delaunay les plus proches de s et t , respectivement. Pour construire un chemin entre les deux sommets x_m et x_n , on utilise la dualité du graphe de Delaunay avec le pavage de Voronoi $\Theta = C(x_i)$ généré par les sommets $\{x_i\}$ du graphe. Les sommets du chemin correspondent à la suite des noyaux de cellules de Voronoi $C(x_m), C(x_{m_0}), \dots, C(x_n)$ traversées par le segment $[s, t]$ (Fig. 2.1, page 43).

On utilise le terme *chemins markoviens* pour cette classe. Cette appellation est justifiée dans §2.3 où on démontre que les segments de ces chemins forment une chaîne de Markov et où on donne les probabilités de transition de cette chaîne. Ensuite, dans §2.4 les résultats d'ergodicité sont démontrés en utilisant l'inclusion des sommets des chemins dans un processus ponctuel ergodique Π . La distribution stationnaire de la chaîne de Markov correspondante est aussi calculée. A partir de cette distribution, on obtient dans §2.5 une expression pour la moyenne et la valeur asymptotique du ratio entre la longueur du chemin et la distance euclidienne entre les points extrêmes. Dans le cas planaire, ce ratio vaut $4/\pi$, pour les dimensions plus grandes nous donnons les résultats des simulation basés sur la forme explicite de la distribution stationnaire de la chaîne. Les implications de ces résultats pour l'estimation de certaines constantes de percolation et de longueurs des chemins les plus courts sont discutées dans §2.7. Dans §2.6 nous démontrons que les conditions du critère de Foster sont remplies pour cette chaîne, et que la distribution de la chaîne converge vers le régime stationnaire avec une vitesse géométrique.

Quelques modifications de la procédure de construction des chemins sont considérées dans §2.7. Finalement, §2.8 est consacré aux applications : on définit un algorithme de routage distribué, basé sur les vues locales de réseau, et on utilise les résultats théoriques pour caractériser ses performances.

Pavages Agrégés et Fractales

Les pavages sont une manière naturelle de représenter les partitions de l'espace entre les éléments du réseau. Un exemple d'une telle partition est la division de la région de service d'un réseau sans fil en cellules desservies par des stations de base. Dans le Chapitre 3 nous étudions les partitions de l'espace en zones associées aux stations d'un réseau hiérarchique.

Partitions de l'espace dans les réseaux hiérarchiques Considérons un modèle hiérarchique dans lequel chaque niveau de stations est représenté par un processus ponctuel stationnaire $\Pi_n = \{x_i^n\}$ d'intensité λ_n et les zones associées aux stations forment les pavages $\Theta^n = \{C^n(x_i^n)\}$, $n = 0, 1, \dots, N$. Les raccordements entre les stations de niveaux adjacents se traduisent comme une opération sur les pavages définie de la manière suivante.

Soit $\Theta^0 = \{C^0(x_i^0)\}$ et $\Theta^1 = \{C^1(x_i^1)\}$ les deux pavages associés à l'ensemble des noyaux, respectivement, $\{x_i^0\}$ et $\{x_i^1\}$. L'opération d'*agrégation*

produit le pavage $\Theta_0^1 = \Theta^0 \circ \Theta^1$ ayant des cellules

$$C_0^1(x_i^0) = \bigcup_{j: x_j^1 \in C^0(x_i^0)} C^1(x_j^1) \quad i \in \mathbb{N}. \quad (\text{B.1})$$

Par récurrence, on construit $\Theta_0^n := \Theta_0^{n-1} \circ \Theta^n$. On appelle Θ_0^n le *pavage agrégé d'ordre n* et on note ses cellules $C_0^n(x_i^0)$. Un cas particulier est la famille des *pavages agrégés de Poisson–Voronoi* (PVAT) générés par une suite Θ^n de pavages de Poisson–Voronoi stationnaires indépendants.

De la relation (B.1) on déduit que la cellule $C_0^n(x_i^0)$ est la réunion des cellules des stations $\{x_i^n\}$ qui sont connectées par des inter-liens à la même station x_i^0 du niveau supérieur. Les propriétés des distributions des cellules agrégées et des pavages associés font l'objet du Chapitre 3.

Voici les résultats analytiques qu'on obtient pour les pavages agrégés. Dans §3.2 nous trouvons l'expression générale pour la probabilité qu'un point quelconque $y \in \mathbb{R}^d$ soit couvert par une cellule agrégée typique d'ordre n (la distribution d'une cellule typique est la distribution de Palm par rapport au processus des noyaux Π_0). Pour les PVAT, on obtient une forme close de cette expression qui s'évalue explicitement dans \mathbb{R}^1 et \mathbb{R}^2 .

Dans §3.3 on s'intéresse à l'évolution de la suite de cellules agrégées des PVAT $\{C_0^n(x_i^0)\}_{n \in \mathbb{N}}$ ayant le noyau commun x_i^0 . On obtient des bornes sur les probabilités pour qu'une suite typique dégénère, ou qu'elle englobe tout l'espace.

Il est clair que si les intensités des processus Π_n croissent suffisamment vite, la différence entre deux pavages successifs Θ_0^n et Θ_0^{n+1} devient de plus en plus petite. Une question se pose : quelles sont les conditions pour que les cellules agrégées se stabilisent quand $n \rightarrow \infty$? On démontre dans §3.4 que si la suite des cellules typiques $\{C_0^n(0)\}_{n \in \mathbb{N}}$ contient p.s. une boule ouverte, les ensembles

$$C_0^\infty(x_i^0) := \liminf_n C_0^n(x_i^0), \quad i \in \mathbb{N}$$

forment un pavage de \mathbb{R}^d (et que les autres définitions possibles de cellules limites sont essentiellement équivalentes). Pour les PVAT auto-similaires on démontre dans §3.3 que la convergence de la série

$$\sum_n \lambda_n^{-1/d+\varepsilon}, \quad 0 < \varepsilon < 1/d$$

est suffisante pour que la condition d'existence du pavage limite soit satisfaite.

Dans le cas des PVAT, l'union des frontières des cellules limites $\Gamma_0^\infty := \cup_i \partial C_0^\infty(x_i^0)$ a une structure auto-similaire, ce qui nous permet de l'appeler une fractale. Pour caractériser son degré d'irrégularité, nous donnons dans §3.6 une borne sur sa dimension de Hausdorff. Cette borne est basée sur l'analyse dans §3.5 de l'asymptotique de la fonction de la distribution de contact $H(r) = \mathbf{P}(rb(0, 1) \cap \Gamma_0^\infty \neq \emptyset)$ quand $r \rightarrow 0$.

Généralisation de modèles cellulaires Les modèles hiérarchiques et les modèles de réseaux sans fil considérés dans [4], [7], [8], utilisent le concept de diagrammes aléatoires de Poisson–Voronoi, où toutes les cellules sont des polytopes convexes. Cette représentation est une approximation du premier ordre pour les zones de service, qui ont toujours une forme plus irrégulière (surtout pour les réseaux sans fil où les formes des cellules dépendent de la propagation du signal). Dans §3.7 on présente les pavages agrégés sous une autre optique comme un modèle plus général de configurations cellulaires qui d'une part tient compte de l'hypothèse de rattachement à la station la plus proche, et qui d'autre part reproduit des fluctuations dans les formes des cellules. Ce modèle possède peu de paramètres et présente une grande ressemblance (Figs. 1.8–1.9, page 38) avec les configurations observées.

Bibliography

- [1] ALBERS, G., GUIBAS, L. J., MITCHELL, J. S. B., AND ROOS, T. (1998). Voronoi diagrams of moving points. *Internat. J. Comput. Geom. Appl.* **8**(3), 365–379.
- [2] BACCELLI, F. AND BRÉMAUD, P. (1993). Virtual customers in sensitivity and light traffic analysis via Campbell’s formula for point processes. *Adv. in Appl. Probab.* **25**(1), 221–234.
- [3] BACCELLI, F. AND BRÉMAUD, P. (1994). *Elements of queueing theory*. Springer-Verlag, Berlin. Palm-martingale calculus and stochastic recurrences.
- [4] BACCELLI, F., KLEIN, M., LEBOURGES, M., AND ZUYEV, S. (1997). Stochastic geometry and architecture of communication networks. *J. Telecommunication Systems* **7**, 209–227.
- [5] BACCELLI, F., KLEIN, M., AND ZUYEV, S. (1995). Perturbation analysis of functionals of random measures. *Adv. in Appl. Probab.* **27**(2), 306–325.
- [6] BACCELLI, F., TCHOUMATCHENKO, K., AND ZUYEV, S. (1998). Markov paths on the Poisson–Delaunay graph, with applications to routing in mobile networks. *Technical Report 3420*, INRIA. To appear in *Adv. in Appl. Probab.*
- [7] BACCELLI, F. AND ZUYEV, S. (1997). Stochastic geometry models of mobile communication networks. In *Frontiers in queueing*, 227–243. CRC, Boca Raton, FL.
- [8] BACCELLI, F. AND ZUYEV, S. (1999). Poisson-Voronoi spanning trees with applications to the optimization of communication networks. *Oper. Res.* **47**(4).

-
- [9] BADDELEY, A. J. (1998). Spatial sampling and censoring. In O. E. Barndorff-Nielsen, W. S. Kendall, and M. N. M. van Lieshout (editors), *Stochastic Geometry: Likelihood and Computation*, chapter 2. Chapman and Hall, London.
- [10] BARBER, C. B., DOBKIN, D. P., AND HUHDANPAA, H. T. (1996). The quickhull algorithm for convex hulls. *ACM Transactions on Mathematical Software* **22**(4), 469–483.
- [11] BELLMAN, R. (1957). *Dynamic programming*. Princeton University Press, Princeton, N. J.
- [12] BOROVKOV, A. A. (1986). *Teoriya veroyatnostei (Russian)*. [Probability Theory]. “Nauka”, Moscow.
- [13] CHENG, C., RELEY, R., KUMAR, S. P. R., AND GARCIA-LUNA-ACEVES, J. J. (1989). A loop-free extended Bellman-Ford routing protocol without bouncing effect. *ACM Computer Communications Review* **19**(4), 224–236.
- [14] CHEW, L. P. (1989). There are planar graphs almost as good as the complete graph. *J. Comput. System Sci.* **39**(2), 205–219. Computational geometry.
- [15] DALEY, D. J. AND VERE-JONES, D. (1988). *An introduction to the theory of point processes*. Springer-Verlag, New York.
- [16] DIJKSTRA, E. W. (1959). A note on two problems in connexion with graphs. *Numer. Math.* **1**, 269–271.
- [17] FALCONER, K. (1997). *Techniques in fractal geometry*. John Wiley & Sons, Chichester.
- [18] FORD, L. R. AND FULKERSON, D. R. (1962). *Flows in networks*. Princeton University Press, Princeton, N.J.
- [19] FOSS, S. G. AND ZUYEV, S. A. (1996). On a Voronoi aggregative process related to a bivariate Poisson process. *Adv. in Appl. Probab.* **28**(4), 965–981.
- [20] FREY, A. AND SCHMIDT, V. (1998). Marked point processes in the plane I – a survey with applications to spatial modeling of communication networks. *Advances in Performance Analysis* **1**, 65–100.

-
- [21] FREY, A. AND SCHMIDT, V. (1998). Marked point processes in the plane II – a survey with applications to spatial modeling of communication networks. *Advances in Performance Analysis* **2**, 171–214.
- [22] GILBERT, E. N. (1962). Random subdivisions of space into crystals. *Ann. Math. Statist.* **33**, 958–972.
- [23] GONDRAN, M. AND MINOUX, M. (1979). *Graphes et Algorithmes*. Editions Eyrolles.
- [24] GUIBAS, L. J., MITCHELL, J. S. B., AND ROOS, T. (1992). Voronoï diagrams of moving points in the plane. In *Graph-theoretic concepts in computer science (Fischbachau, 1991)*, 113–125. Springer, Berlin.
- [25] HEINRICH, L. (1998). Contact and chord length distribution of a stationary Voronoi tessellation. *Adv. in Appl. Probab.* **30**(3), 603–618.
- [26] HEINRICH, L. AND MUCHE, L. (1997). Second-order properties of the point process of nodes in a stationary Voronoi tessellation. Submitted to *Adv. in Appl. Probab.*
- [27] HOWARD, C. D. AND NEWMAN, C. M. (1997). Euclidean models of first-passage percolation. *Probab. Theory Related Fields* **108**(2), 153–170.
- [28] HUITEMA, C. (1999). *Routing in the Internet*. Prentice Hall.
- [29] JOHNSON, D. B. AND MALTZ, D. A. (1996). Dynamic source routing in ad hoc wireless networks. In T. Imielinski and H. F. Korth (editors), *Mobile Computing*, chapter 5. Kluwer Academic Publishers.
- [30] KEIL, J. M. AND GUTWIN, C. A. (1992). Classes of graphs which approximate the complete Euclidean graph. *Discrete Comput. Geom.* **7**(1), 13–28.
- [31] KENDALL, D. G. (1989). A survey of the statistical theory of shape. *Statist. Sci.* **4**(2), 87–120.
- [32] KESHAV, S. (1997). *An Engineering Approach to Computer Networking*. Addison-Wesley.
- [33] KINGMAN, J. F. C. (1973). Subadditive ergodic theory. *Ann. Probability* **1**, 883–909.

- [34] KINGMAN, J. F. C. (1993). *Poisson processes*. The Clarendon Press Oxford University Press, New York. Oxford Science Publications.
- [35] KRICKEBERG, K. (1982). Processus ponctuels en statistique. In *Tenth Saint Flour Probability Summer School—1980 (Saint Flour, 1980)*, 205–313. Springer, Berlin.
- [36] KUTOYANTS, Y. A. (1984). *Parameter estimation for stochastic processes*. Heldermann Verlag, Berlin. Translated from the Russian and edited by B. L. S. Prakasa Rao.
- [37] LEBEDEV, N. N. (1972). *Special functions and their applications*. Dover Publications Inc., New York.
- [38] LEINER, B. (editor) (1987). *Proceedings of IEEE – Special Issue on Packet Radio Networking*, volume 75.
- [39] MACKER, J. P. AND CORSON, M. S. (1998). Mobile ad hoc networking and the IETF. *ACM Mobile Computing and Communications Review* **2**(1-4).
- [40] MATHERON, G. (1975). *Random sets and integral geometry*. John Wiley & Sons, New York-London-Sydney.
- [41] MEYN, S. P. AND TWEEDIE, R. L. (1993). *Markov chains and stochastic stability*. Springer-Verlag London Ltd., London.
- [42] MILES, R. E. (1970). On the homogeneous planar Poisson process. *Math. Biosci.* **6**, 85–127.
- [43] MILES, R. E. (1972). The random division of space. *Suppl. Adv. Appl. Probab.* 243–266.
- [44] MILES, R. E. (1974). A synopsis of “Poisson flats in Euclidean spaces”. In E. F. Harding and D. G. Kendall (editors), *Stochastic geometry*, 202–227.
- [45] MØLLER, J. (1989). Random tessellations in R^d . *Adv. in Appl. Probab.* **21**(1), 37–73.
- [46] MØLLER, J. AND ZUYEV, S. (1996). Gamma-type results and other related properties of Poisson processes. *Adv. in Appl. Probab.* **28**(3), 662–673.

- [47] MOULY, M. AND PAUTET, M.-B. (1992). *The GSM System for Mobile Communications*. Telecom Publishing.
- [48] MUCHE, L. (1996). The Poisson-Voronoi tessellation. II. Edge length distribution functions. *Math. Nachr.* **178**, 271–283.
- [49] MUCHE, L. AND STOYAN, D. (1992). Contact and chord length distributions of the Poisson Voronoi tessellation. *J. Appl. Probab.* **29**(2), 467–471.
- [50] NEVEU, J. (1976). Sur les mesures de Palm de deux processus ponctuels stationnaires. *Z. Wahrscheinlichkeitstheorie und Verw. Gebiete* **34**(3), 199–203.
- [51] OKABE, A., BOOTS, B., SUGIHARA, K., AND CHIU, S. N. (2000). *Spatial tessellations: concepts and applications of Voronoi diagrams*. John Wiley & Sons Ltd., Chichester.
- [52] RATHBUN, S. L. AND CRESSIE, N. (1994). Asymptotic properties of estimators for the parameters of spatial inhomogeneous Poisson point processes. *Adv. in Appl. Probab.* **26**(1), 122–154.
- [53] REDL, S., WEBER, M., AND OLIPHANT, M. (1995). *An Introduction to GSM*. Artech House.
- [54] REIMAN, M. I. AND SIMON, B. (1989). Open queueing systems in light traffic. *Math. Oper. Res.* **14**(1), 26–59.
- [55] RIPLEY, B. D. (1991). *Statistical inference for spatial processes*. Cambridge University Press, Cambridge.
- [56] SCOURIAS, J. (1999). Overview of the global system for mobile communications. URL: <http://ccnga.uwaterloo.ca/~jscouria/GSM/index.html>.
- [57] SEMPERE, J. G. (1998). An overview of the GSM system. URL: <http://www.comms.eee.strath.ac.uk/~gozalvez/gsm/gsm.html>.
- [58] STOYAN, D., KENDALL, W., AND MECKE, J. (1995). *Stochastic Geometry and its Applications*. Wiley, Chichester.
- [59] TCHOUMATCHENKO, K. AND ZUYEV, S. (1999). Aggregate and fractal tessellations. *Technical Report 3699*, INRIA. Submitted to Probab. Theory Related Fields.

- [60] VAHIDI-ASL, M. Q. AND WIERMAN, J. C. (1990). First-passage percolation on the Voronoï tessellation and Delaunay triangulation. In *Random graphs '87 (Poznań, 1987)*, 341–359. Wiley, Chichester.
- [61] ZUYEV, S., DESNOGUES, P., AND RAKOTOARISOA, H. (1997). Simulations of large telecommunication networks based on probabilistic modeling. *J. Electronic Imaging* **6**(1), 68–77.

Résumé

La géométrie stochastique s'est avérée être un outil générique pour la modélisation de réseaux de télécommunications. L'idée de l'approche est de représenter la configuration d'un réseau par une famille d'objets aléatoires (ensembles de points, graphes, pavages). L'analyse des modèles s'effectue par des méthodes générales de la géométrie stochastique, de la théorie des processus ponctuels, de la statistique spatiale et de la théorie des graphes.

La première partie de la thèse est motivée par des problèmes de routage dans les réseaux mobiles décentralisés. Nous étudions une classe de chemins construits par un algorithme simple sur un graphe de Poisson–Delaunay, qui représente l'infrastructure d'un réseau. Les résultats principaux concernent la qualité de l'approximation des chemins les plus courts et de la distance euclidienne par les chemins de cette classe. Un prototype d'algorithme de routage dans les réseaux mobiles est proposé comme application.

Dans la deuxième partie nous introduisons les pavages agrégés, modèle pour les zones de service rattachées aux nœuds d'un réseau hiérarchique. Nous étudions les propriétés de la distribution de tels pavages et la géométrie de leurs cellules. On caractérise leur comportement limite quand le nombre des niveaux dans la hiérarchie tend vers l'infini et on démontre certaines propriétés fractales de l'objet limite. On montre aussi comment les pavages agrégés peuvent servir pour le raffinement des modèles de cellules radio basés sur les pavages de Voronoi.

Mots clés: modélisation spatiale de réseaux, processus ponctuels, pavage de Voronoi, graphe de Delaunay, approximation de la distance euclidienne, chemin le plus court, chemin markovien, routage, réseaux hiérarchiques, pavages agrégés, réseaux sans fil.

Abstract

Stochastic geometry has recently emerged as a framework for spatial modeling of telecommunication networks. The idea of the approach is to represent configurations of large networks as families of random objects (point patterns, graphs, tessellations). The analysis of the models can then be performed using general methods of stochastic geometry, of the theory of point processes, of spatial statistics, and of graph theory.

The first part of the thesis is motivated by routing issues in decentralized mobile networks. We study a class of paths constructed with a simple ray-shoot algorithm on a random Poisson–Delaunay graph representing the network infrastructure. The main results concern the quality of the approximation by such paths of the shortest paths and of the Euclidean distance. A prototype of a distributed routing algorithm for mobile networks is proposed as an application.

In the second part, we investigate aggregate tessellations, which we introduce as a model of service zones assigned to nodes of a hierarchically organized network. We study the distributional properties of such tessellations and the geometry of their cells. We characterize their limit behavior as the number of levels in the hierarchy grows, and study the fractal properties of the limit object. We also show that aggregate tessellations can serve as a refinement of Voronoi-based models of radio cells in wireless networks.

Keywords: spatial network modeling, point processes, Voronoi tessellation, Delaunay graph, approximation of Euclidean distance, shortest path, Markov path, routing, hierarchical networks, aggregate tessellation, wireless networks.